Zebrafish Cx35.1: Cloning, characterization and expression analysis of a retinal gap junction gene

By

Elizabeth McLachlan

A thesis submitted to the Faculty of Graduate Studies, University of Manitoba
In partial fulfillment of the requirements for the degree of

Master's of Science

Department of Zoology

© Copyright by Elizabeth McLachlan 2002

National Library of Canada
Acquisitions and Bibliographic Services
395 Wellington Street
Ottawa ON K1A 0N4
Canada

Bibliothèque nationale du Canada
Acquisitions et services bibliographiques
395, rue Wellington
Ottawa ON K1A 0N4
Canada

Your file Votre référence

Our file Notre référence

The author has granted a non-exclusive licence allowing the National Library of Canada to reproduce, loan, distribute or sell copies of this thesis in microform, paper or electronic formats.

L'auteur a accordé une licence non exclusive permettant à la Bibliothèque nationale du Canada de reproduire, prêter, distribuer ou vendre des copies de cette thèse sous la forme de microfiche/film, de reproduction sur papier ou sur format électronique.

The author retains ownership of the copyright in this thesis. Neither the thesis nor substantial extracts from it may be printed or otherwise reproduced without the author's permission.

L'auteur conserve la propriété du droit d'auteur qui protège cette thèse. Ni la thèse ni des extraits substantiels de celle-ci ne doivent être imprimés ou autrement reproduits sans son autorisation.

0-612-79977-8

Canada

THE UNIVERSITY OF MANITOBA

FACULTY OF GRADUATE STUDIES

*****

COPYRIGHT PERMISSION PAGE

ZEBRAFISH CX35.1: CLONING, CHARACTERIZATION AND EXPRESSION ANALYSIS OF A RETINAL GAP JUNCTION GENE

BY

ELIZABETH MCLACHLAN

A Thesis/Practicum submitted to the Faculty of Graduate Studies of The University of Manitoba in partial fulfillment of the requirements of the degree of

Master of Science

ELIZABETH MCLACHLAN © 2002

Permission has been granted to the Library of The University of Manitoba to lend or sell copies of this thesis/practicum, to the National Library of Canada to microfilm this thesis and to lend or sell copies of the film, and to University Microfilm Inc. to publish an abstract of this thesis/practicum.

The author reserves other publication rights, and neither this thesis/practicum nor extensive extracts from it may be printed or otherwise reproduced without the author's written permission.

ABSTRACT

Members of the vertebrate connexin gene family encode the protein subunits of gap junction channels. Gap junctions provide a route for direct intercellular communication by allowing the passage of small ions, second messengers, and metabolites between cells. As a consequence, they play a vital role in many developmental and homeostatic processes. Aberrant gap junction function is implicated in many human diseases including peripheral neuropathies, cardiac abnormalities, tumorigenesis, and sensory organ defects. In order to elucidate the role of gap junctions in development and disease, each connexin must be studied individually, as they each form gap junctions with unique properties. The connexin35/36 (Cx35/36) orthologues are expressed primarily in nervous tissue and are the predominant connexin in the retina. Zebrafish are an ideal vertebrate model to study development of the visual system as they produce transparent embryos that develop rapidly, thereby facilitating morphological and behavioral testing. In this study, zebrafish connexin35.1 has been cloned from a zebrafish PAC library. Sequence analysis shows a high degree of similarity to the Cx35/36 orthologues from other species. The protein encoded by the gene contains 304 amino acids with a predicted molecular weight of 35.1 kD. Electrophysiological analysis of Cx35.1 channels in the paired *Xenopus* oocyte system, done in collaboration with another lab, showed gating properties similar to those of mouse Cx36. Zebrafish Cx35.1 channels have a large steady state conductance and very weak voltage-sensitivity. In the adult zebrafish, Cx35.1 mRNA is expressed in the brain and retina. In the embryo, it first becomes detectable by Northern analysis and RT-PCR on day two (d2) of development,

coincident with critical points in visual development. Immunohistochemical analysis revealed that the Cx35.1 protein is expressed in two sublaminae of the inner plexiform layer (where interneurons synapse with ganglion cells) of the adult zebrafish retina. A similar pattern was seen in the d4 and d5 embryonic retina. The protein is also expressed in regions of the brain and facial cartilage by d2 and d3 of development, respectively.

ACKNOWLEDGEMENTS

First and foremost, I would like to thank my supervisor, Dr. Gunnar Valdimarsson, for his continual support and guidance throughout this study. I have learned an enormous amount and have truly enjoyed my time in his lab.

I would like to thank Shaohong Cheng and Tara Christie, my labmates, for their support and help over the past years. Without their companionship and laughter the years would have been much more stressful.

I would also like to thank the members of my advisory committee, Dr. Ross McGowan for his counsel on numerous occasions, and Dr. Jim Nagy for his advice and generous donation of Cx36 antibodies.

I would like to thank Dr. McGowan, Dr. Nagy and Dr. Roger Wilson for the use of their cryostats. Plasmid containing the eF-1α cDNA was a gift from Dr. Ross Johnson (University of Minnesota). The anti-perch Cx35 antibody was a gift from Dr. Harris Ripps (Lions of Illinois Eye Research Institute).

This research was funded by an operating grant to Dr. Valdimarsson from the Natural Sciences and Engineering Research Council of Canada (NSERC) and an establishment grant from the Manitoba Health Research Council (MHRC). I was funded by a studentship from MHRC and a post-graduate award (PGSA) from NSERC.

TABLE OF CONTENTS

ABSTRACT I
ACKNOWLEDGEMENTS III
TABLE OF CONTENTS IV
LIST OF FIGURES VI
LIST OF TABLES X
LIST OF TABLES X
CHAPTER 1: INTRODUCTION 1
1.1 Gap Junctions and Connexins 1
1.2 Gap Junctions in Vertebrate Development 7
1.3 Gap Junctions in Neural Development 9
1.4 Neuronal Connexins 11
1.5 Gap Junctions in the Retina 13
1.6 Retinal Connexins 15
1.7 Gap Junctions and Disease 18
1.8 The Cx35/36 Orthologues 19
1.9 Zebrafish as a vertebrate model 22
1.10 Hypothesis and Objectives 25
CHAPTER 2: MATERIALS AND METHODS 26
2.1 Zebrafish Care 26
2.2 Isolation of Genomic Clone 27
2.2.1 Genomic DNA isolation 27
2.2.2 PCR Cloning 27
2.2.3 DNA Probe Synthesis 29
2.2.4 Screening of a zebrafish genomic PAC library 30
2.2.5 PAC DNA Isolation 31
2.2.6 Subcloning 33
2.2.7 Sequencing and Structural Analysis 34
2.3 Isolation of cDNA clone 35
2.3.1 Synthesis of cDNA 35
2.3.2 PCR Cloning 36
2.3.3 Sequencing and Structural Analysis 37
2.4 Electrophysiology 37
2.4.1 Expression Cloning 37
2.4.2 Transcription Verification 38
2.5 mRNA Expression Analysis 40
2.5.1 Northern Analysis 40
2.5.1.1 Poly A+ RNA Isolation and Blot Preparation 40
2.5.1.2 Zebrafish Cx35.1 Probe Synthesis and Hybridization 41
2.5.1.3 eF-1α Probe Synthesis and Hybridization 42
2.5.2 RT-PCR 42
2.6 Protein Expression Analysis 44
CHAPTER 3: RESULTS 47
3.1 Cloning of zebrafish Cx35.1 47
3.2 Electrophysiology 55

3.3 mRNA Expression Analysis 60
3.3.1 Northern analysis 60
3.3.2 RT-PCR Analysis 64
3.4 Protein Expression 69
3.4.1 Immunohistochemistry of Adult Retina 69
3.4.2 Immunohistochemistry of Embryonic Retina 71
CHAPTER 4: DISCUSSION 73
4.1 Zebrafish Cx35.1 belongs to the Cx35/36 group of orthologues 73
4.2 Cx35.1 mRNA is expressed in development and in the adult brain and eye 76
4.3 Cx35.1 protein is expressed in the zebrafish retina 78
4.4 What is the function of the Cx35/36 orthologues? 81
APPENDIX A 83
APPENDIX B 85
LITERATURE CITED 86

LIST OF FIGURES

Figure 1: A) Schematic representation of gap junction channels connecting two cell membranes (Guthrie and Gilula, 1989). A connexon, made of 6 connexin proteins, is formed in the cell membrane. This interacts with a connexon in the adjacent cell membrane and forms a complete channel. Clustering of up to thousands of these channels constitutes a gap junction. B) Schematic representation of a generic connexin protein topology within the plasma membrane. Hydropathy analysis predicts four transmembrane domains (TM1-TM4), two extracellular loops (E1 and E2) with cysteines in conserved positions (C), a central cytoplasmic loop (C-Loop), and cytoplasmic carboxy and amino-terminal tails (CT and NT respectively). The cytoplasmic loop and the carboxy terminus account for most of the inter-connexin variation in molecular weight. 2

Figure 2: A phylogenetic analysis of the connexin gene family in the form of a rectangular cladogram. The analysis was done with the TREEVIEW program (Page, 1996) using the amino acid sequences of the family members identified in chicken (ch), mouse (m), and zebrafish (zf), representing the classes of birds, mammals and fish, respectively. The amino acid sequences both within a species and across a species are highly conserved. 3

Figure 3: Schematic connexin (Cx) protein expression pattern in the layers of the mouse retina (after Güldenagel *et al.*, 2000). PEL = pigment epithelium layer, ONL = outer nuclear layer, OPL = outer plexiform layer, INL = inner nuclear layer, IPL = inner plexiform layer, GCL = ganglion cell layer, NFL = nerve fiber layer, E = epithelial cells of vasculature..... 16

Figure 4: The consensus zebrafish Cx35.1 sequence (4.3 kb) derived from PAC clones. The bold lettering depicts the coding region (912 bp total), while the translation start sequence and the translation stop sequence are italicized. The lettering in between the two sections of coding region represents the 1953 bp intron that interrupts after the first 71 bp of coding sequence. The upstream and downstream non-coding sequences are in regular lettering at the start and the end of the sequence, respectively. 49

Figure 5: Nucleotide and corresponding amino acid sequence of the Cx35.1 coding region. The coding region is 912 bp in length, which translates to 304 amino acids. The predicted molecular weight of the protein is 35.1 kD and so it is named zebrafish Cx35.1. Amino acid codes are found in Appendix B..... 50

Figure 6: A predicted hydrophobicity plot for the Cx35.1 amino acid sequence generated using the TMpred tool from Swiss EMBnet (www.ch.embnet.org/index.html). It shows four highly hydrophobic areas presumably corresponding to the transmembrane domains one through four starting from the left. The remainder of

is considered the hydrophobic range and below 0 is the hydrophilic range. The amino acid position within the protein is depicted on the X axis. 51

Figure 7: Alignment of the zebrafish Cx35.1 amino acid sequence with the Cx35/36 orthologue sequences using Clustal X (Thompson *et al.*, 1997). Amino acid identity between all sequences is designated with (*) and similarity between the amino acids is shown by (:). The four predicted transmembrane segments (TM1-TM4) are designated with a line over them and the conserved cysteines are marked with (+). Potential phosphorylation sites are designated with a (o) above them. The amino acid sequence is highly conserved with the most divergence occurring in the cytoplasmic loop between the second and third transmembrane segments. Amino acid codes are found in Appendix B. 52

Figure 8: A phylogenetic analysis of the Cx35/36 group of connexins in the form of a rectangular cladogram. The analysis was done with the TREEVIEW program (Page, 1996) using the amino acid sequences of the family members. Zebrafish Cx35.1 appears to be most closely related to perch Cx35, followed by chicken Cx36 and skate Cx35. The mammalian orthologues are grouped together on one branch while perch Cx34.7 is the most basal member of the clade. 54

Figure 9: Splice site sequences of Cx35.1. Splice sites that match the conserved eukaryotic splice sequences considerably (donor: CAAG/GTAGAGT; acceptor: TCnNCTAG/G) (Mount, 1982) are shown in larger print, with the splice site denoted by an arrow. The complete upstream coding sequence and a portion of the downstream coding sequence are shown in bold. 56

Figure 10: (A) Time dependent decay of Cx35.1 junctional currents in *Xenopus* oocyte pairs injected with Cx35.1 cRNA induced by applied transjunctional voltage. Voltage steps were applied in 20 mV increments from a resting potential of –40 mV and lasted 10 seconds. (B) Normalized steady state junctional conductance for Cx35.1 channels plotted as a function of applied transjunctional voltage (mV). Data for mouse Cx36 are shown in (C) and (D) for comparison, with the Cx35.1 curve superimposed as a dotted line on the Cx36 curve. In (A) the currents show a voltage-induced closure of the channels at voltage shifts greater than 40 mV from resting. In (B) Cx35.1 shows similar voltage sensitivity to mouse Cx36 (D) with weak initial response, however the Cx35.1 channel is slightly asymmetric. At the most extreme transjunctional voltages applied, Cx35.1 still maintains a normalized conductance of over 40%, where Cx36 maintains a normalized conductance of over 50%..... 59

Figure 11: PolyA+1: Northern Blot analysis of Cx35.1 mRNA expression. PolyA+ RNA was isolated from embryonic stages d4 and d5 and adult brain (B) and eye (E) (lens removed), separated by electrophoresis on a gel, blotted to a membrane, and subsequently hybridized with a zebrafish Cx35.1-specific riboprobe. A 2.7 kb band was detected in all four samples although there was a shift in the d5 sample due to an abnormality in that lane of the gel. Elongation factor 1α (eF-1α) is ubiquitously

expressed throughout development and in all adult tissues and therefore its detection allows the verification of RNA integrity in each sample..... 62

Figure 12: PolyA+2: Northern Blot analysis of Cx35.1 mRNA expression. PolyA+ RNA was isolated from embryonic stages d0, d1, d2, d3, d4, and d5 and adult brain (B), eye (E) (lens removed), liver (L), and ovary (O). The RNA was separated by electrophoresis on a gel, blotted to a membrane, and subsequently hybridized with a zebrafish Cx35.1-specific riboprobe. A 2.7 kb band was detected in the d3, d4, and d5 embryonic stages and in adult brain and eye. No signal was detected with any exposure length at d0, d1, or d2 or in adult liver or ovary. Elongation factor 1α (eF-1α) is ubiquitously expressed throughout development and in all adult tissues and therefore its detection allows the verification of RNA integrity in each sample..... 63

Figure 13: PolyA+3: Northern Blot analysis of Cx35.1 mRNA expression. PolyA+ RNA was isolated from embryonic stages d0, d1, d2, and d3 and adult brain (B), liver (L), and ovary (O). The RNA was separated by electrophoresis on a gel, blotted to a membrane, and subsequently hybridized with a zebrafish Cx35.1-specific riboprobe. A faint 2.7 kb band was detected in d2, and a strong band in d3 at this exposure length and in adult brain. No signal was detected with any exposure length at d0, or d1, or in adult liver or ovary. Elongation factor 1α (eF-1α) is ubiquitously expressed throughout development and in all adult tissues and therefore its detection allows the verification of RNA integrity in each sample..... 65

Figure 14: RT-PCR analysis of Cx35.1 mRNA expression during zebrafish embryonic development. Zebrafish Cx35.1-specific primers were used to PCR amplify products from cDNA prepared from d0, d1, d2, d3, d4, and d5 embryos and the products were separated by electrophoresis on a gel, blotted to a membrane and hybridized with a zebrafish Cx35.1-specific probe. A single band was detected in d2, d3, d4, and d5 embryo samples, but no band was detected in d0 or d1 embryo samples. Elongation factor 1α (eF-1α) is ubiquitously expressed throughout development and so its amplification by PCR allows the verification of the presence of starting template for the PCR reaction. The PCR reaction for eF-1α was run in parallel to that run for Cx35.1, and separated by electrophoresis on the same gel, but was not blotted to a membrane. This is an inverse image of the ethidium bromide stained gel. 67

Figure 15: RT-PCR analysis of Cx35.1 mRNA expression between 24-72 hpf of zebrafish embryonic development. Zebrafish Cx35.1-specific primers were used to PCR amplify cDNA prepared from 24 hpf, 30 hpf, 36 hpf, 40 hpf, 48 hpf, 54 hpf, 60 hpf and 72 hpf embryos and the products were separated by electrophoresis on a gel, blotted to a membrane and hybridized with a zebrafish Cx35.1-specific probe. Numbers above the blot denote hours post fertilization. A single band was detected in 48 hpf, 54 hpf, 60 hpf and 72 hpf embryo samples, but no band was detected in earlier stages of embryo samples. Elongation factor 1α (eF-1α) is ubiquitously expressed throughout development and so its amplification by PCR allows the verification of the presence of starting template for the PCR reaction. The PCR

reaction for eF-1α was run in parallel to that run for Cx35.1, and separated by electrophoresis on a gel, but was not blotted to a membrane. This is an inverse image of the ethidium bromide stained gel..... 68

Figure 16: Protein expression analysis in adult zebrafish retina. Cryosections (10 μm) were probed with an anti-mouse Cx36 primary antibody, Ab298, that recognizes zebrafish Cx35.1 and detected with the fluorescent secondary antibody Alexa 488. Sections were double stained for Cx35.1 (A) and with Hoechst (B) to show the nuclear layers of the retina. Punctate staining, characteristic of gap junctions, is revealed in two rows in the inner plexiform layer (IPL), the synaptic layer between the interneurons and the ganglion cells. The outer plexiform layer (OPL) is also faintly labeled. (C) shows a similar section labeled only with the secondary antibody. (D) shows a section similar to (A) at a higher magnification while (E) shows its Hoechst counter-staining. (F) is the control section lacking primary antibody. GCL = ganglion cell layer, INL = inner nuclear layer, ONL = outer nuclear layer. Scale bar for (A-C) = 50 μm. Scale bar for (D-F) = 25 μm..... 70

Figure 17: Protein expression analysis in embryonic zebrafish retina and head. Cryosections (10 μm) were probed with anti-mouse Cx36 primary antibodies that recognize zebrafish Cx35.1 and detected with the fluorescent secondary antibody Alexa 488. Sections were double stained for Cx35.1 (A-C) and with Hoechst (D-F) to show the nuclear layers. Sections not treated with primary antibody were used as controls (G-I). The upper row shows d5 embryo retina labeled with antibody C. Punctate staining is detected in the inner plexiform layer (IPL) and the outer plexiform layer also fluoresces. In the middle row, showing d3 embryo retina labeled with Ab298, no specific Cx35.1 staining is detected in the retina. The bottom row shows a region of facial cartilage in the d4 embryo labeled with Ab298. Punctate staining is detected around the chondrocytes. Scale bars = 25 μm. GCL = ganglion cell layer, INL = inner nuclear layer..... 72

LIST OF TABLES

Table I: Mean junctional conductance detected after injection of Cx cRNA or water into Xenopus oocyte pairs 57

Table II: Comparison of Boltzmann parameters of gap junction channels composed of zebrafish Cx35.1 or mouse Cx36 expressed in paired *Xenopus* oocytes. 58

CHAPTER 1: INTRODUCTION

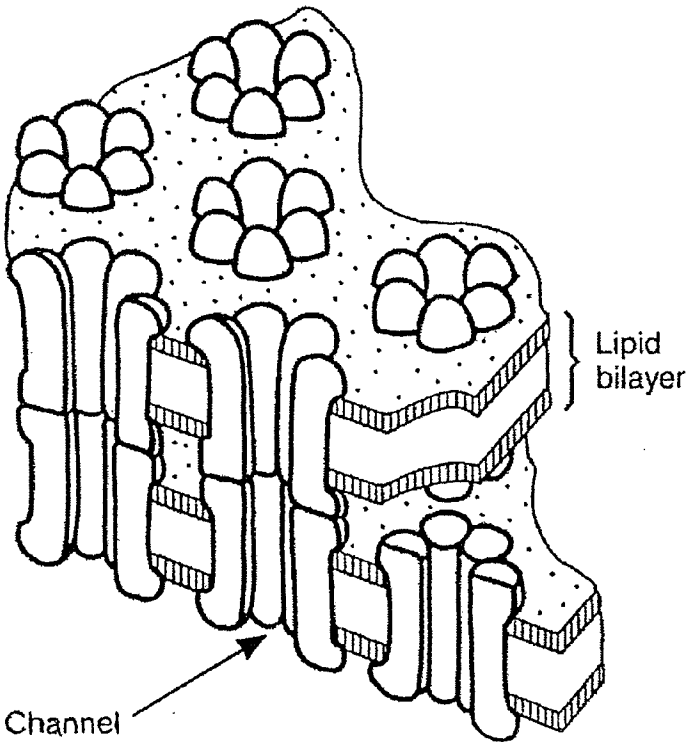
1.1 Gap Junctions and Connexins

Gap junctions are cell membrane specializations that provide a pathway for intercellular communication. They connect adjacent cells and, via intercellular channels, allow the specific and selective exchange of small ions, nutrients, metabolites and signaling molecules under 1 kD in size (White *et al.*, 1995). Gap junctions are important in maintaining tissue homeostasis in response to environmental signals. They play a role in cell growth control and proliferation, as well as differentiation and pattern formation during early development. They also allow the propagation of action potentials at electrical synapses (White *et al.*, 1995; Bruzzone *et al.*, 1996a).

Gap junctions are aggregations (plaques) of intercellular channels, each of which is made of two hemi-channels called connexons (White *et al.*, 1995; Bruzzone *et al.*, 1996a,b). A connexon in each of two cells with apposing plasma membranes will align and lock, forming an aqueous pore to allow cytoplasmic continuity (Fig. 1a). The connexons are hexamers of connexin protein subunits arranged radially around a central pore. Although intercellular junctions are present in all multicellular organisms, connexin proteins are found only among the vertebrates (White and Paul, 1999). Connexin proteins are encoded by a multigene family and all connexin genes within a species and across species share a degree of homology (Fig. 2). To date approximately 21 human connexins have been identified, almost all of which have murine orthologues (Eiberger *et al.*, 2001; Altevogt *et al.*, 2002). The most common connexin nomenclature uses the prefix Cx, followed by the protein's molecular weight in kD based on its amino

Figure 1: A) Schematic representation of gap junction channels connecting two cell membranes (Guthrie and Gilula, 1989). A connexon, made of 6 connexin proteins, is formed in the cell membrane. This interacts with a connexon in the adjacent cell membrane and forms a complete channel. Clustering of up to thousands of these channels constitutes a gap junction. B) Schematic representation of a generic connexin protein topology within the plasma membrane. Hydropathy analysis predicts four transmembrane domains (TM1-TM4), two extracellular loops (E1 and E2) with cysteines in conserved positions (C), a central cytoplasmic loop (C-Loop), and cytoplasmic carboxy and amino-terminal tails (CT and NT respectively). The cytoplasmic loop and the carboxy terminus account for most of the inter-connexin variation in molecular weight.

A)



B)

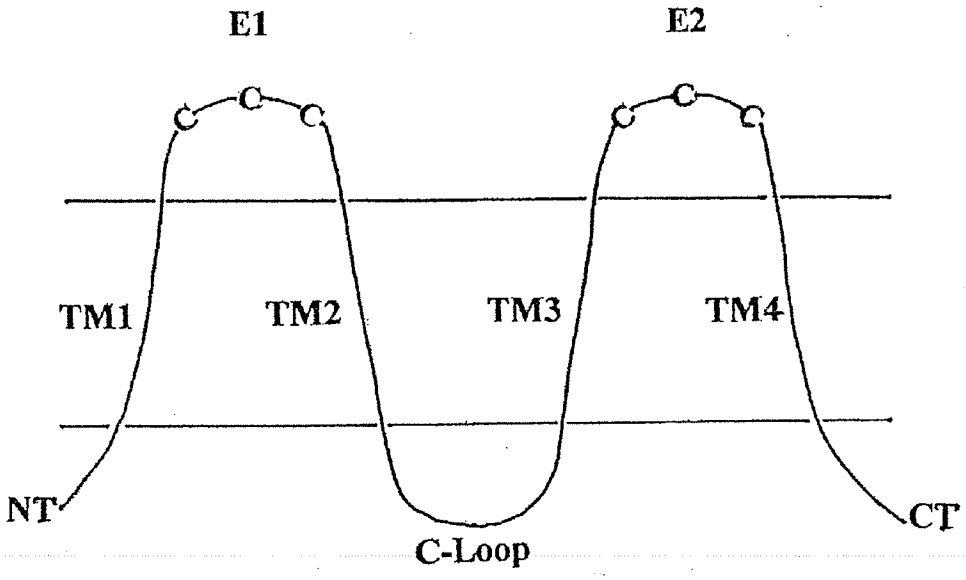
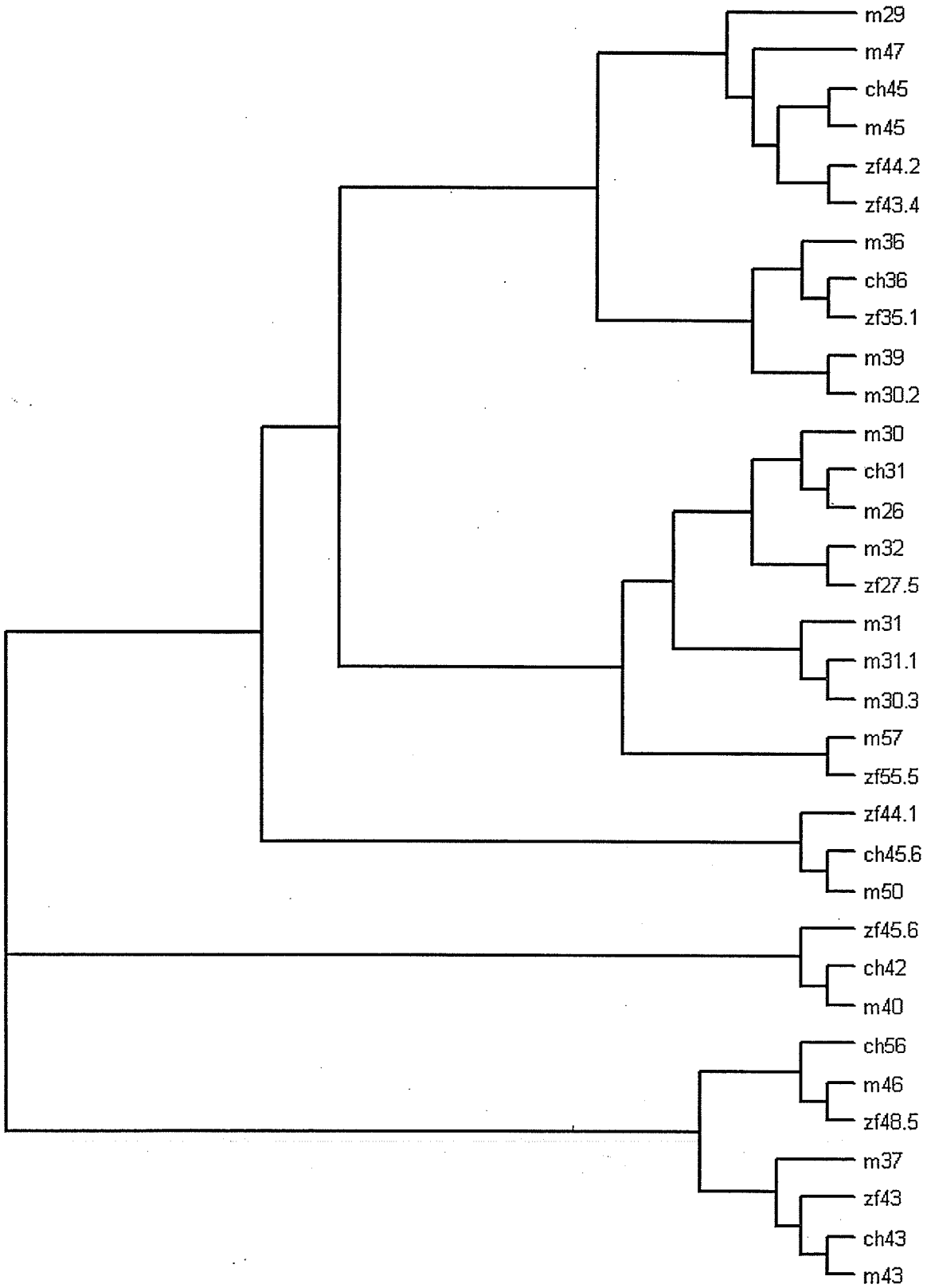


Figure 2: A phylogenetic analysis of the connexin gene family in the form of a rectangular cladogram. The analysis was done with the TREEVIEW program (Page, 1996) using the amino acid sequences of the family members identified in chicken (ch), mouse (m), and zebrafish (zf), representing the classes of birds, mammals and fish, respectively. The amino acid sequences both within a species and across a species are highly conserved.


m29
m47
ch45
m45
zf44.2
zf43.4
m36
ch36
zf35.1
m39
m30.2
m30
ch31
m26
m32
zf27.5
m31
m31.1
m30.3
m57
zf55.5
zf44.1
ch45.6
m50
zf45.6
ch42
m40
ch56
m46
zf48.5
m37
zf43
ch43
m43

acid sequence as predicted from the cDNA (Beyer *et al.*, 1990).

Most connexins have a similar gene structure. Their coding region is contained entirely within one exon, and there is only one intron located in the 5' untranslated region (UTR) (Bruzzone *et al.*, 1996a). There are, however, some exceptions. For example, the coding region of the Cx35/36 orthologues is contained within two exons (O'Brien *et al.*, 1996; Condorelli *et al.*, 1998; O'Brien *et al.*, 1998; Söhl *et al.*, 1998; Belluardo *et al.*, 1999). This group has an intron of variable length that interrupts the coding sequence 71 base pairs (bp) after the translational start site and there is no upstream intron. Rat Cx31 also has an intron within the coding region (Gabriel *et al.*, 2001). The coding region of mouse Cx45 is contained within one exon, but it has two introns in the 5'UTR (Jacob and Beyer, 2001).

The transmembrane structure of several connexins has been examined and they have a common membrane topology and it is hypothesized that all connexins share this topology (Yeager and Gilula, 1992; Zhang and Nicholson, 1994; Bruzzone *et al.*, 1996a). Each connexin has four transmembrane regions, resulting in two extracellular loops and one cytoplasmic loop with both the amino (N) terminus and the carboxy (C) terminus on the cytoplasmic side of the membrane (Fig. 1b). The amino acid sequence of the N-terminus and the hydrophobic transmembrane segments are similar in all connexins, but the most highly conserved regions are the extracellular loops. Each of the extracellular loops has three cysteines in conserved positions presumed to be involved in the connexon-connexon interaction (Foote *et al.*, 1998). The first transmembrane domain is hypothesized to form at least part of the wall of the channel pore, although it may be composed of more than one transmembrane segment (Zhou *et al.*, 1997; Unger *et al.*,

1997, 1999). The cytoplasmic loop and the C-terminus are unique to each connexin in sequence and in length and influence the gating properties of the channels they form.

Each connexin has a unique temporal and spatial expression pattern. Some connexins are expressed widely in an organism, such as Cx43, while others have more restricted expression and are tissue-specific, such as Cx36, which is primarily expressed in nervous tissue (Bruzzone *et al.*, 1996a,b; Condorelli *et al.*, 2000). Connexin expression is also temporally regulated. For example, in the rat cerebral cortex Cx26 is expressed early in development and continues to be highly expressed up to the second week after birth after which its levels diminish, while Cx32 is only expressed in the cerebral cortex post-natally (Nadarajah *et al.*, 1997). Individual connexin expression patterns often overlap. For example, Cx32 and Cx26 are both expressed in acinar cells of lactating mammary glands (Yamanaka *et al.*, 2001).

Connexin expression is regulated by numerous factors, both pre-transcriptionally and post-transcriptionally. For example, as a result of shifts in estrogen and progesterone levels in the plasma, Cx43 mRNA levels dramatically increase in the uterus prior to labour when simultaneous smooth muscle contraction is needed (Chow and Lye, 1994; Lefebvre *et al.*, 1995; Risek *et al.*, 1995; Orsino *et al.*, 1996; Ou *et al.*, 1997). On the other hand, all-trans retinoic acid increases gap junction communication in various cell lines by up-regulating Cx43 at the post-transcriptional level (Bex *et al.*, 1995; Clairmont *et al.*, 1996).

As a consequence of the dynamic expression profiles of connexins, more than one type of connexin may be expressed within the same gap junction plaque and the combinations can form various types of channels (Bruzzone *et al.*, 1996a,b). Homomeric

connexons are those in which a single connexin type makes up the hemi-channel. Heteromeric connexons occur when individual hemi-channels are composed of two or more different connexins. Homotypic channels are formed when the connexins making each connexon in a channel match. Heterotypic channels are formed when the two connexons making the channel are each made from different connexins. Not all connexins can form heterotypic channels. Connexin compatibility appears to depend on the amino acid sequence in the second extracellular loop (White *et al.*, 1994; Haubrich *et al.*, 1996; White and Bruzzone, 1996). Therefore, although gap junctions facilitate intercellular communication, the selective formation of heterotypic channels can limit cell-cell communication when neighboring cells express incompatible connexins. This is significant as each connexin forms channels with specific physiological properties, so a consequence of the diversity of channels is that each has unique permeability characteristics. For example, homomeric, homotypic Cx32 channels allow passage of cAMP and cGMP, while heteromeric channels made of Cx32 and Cx26 are permeable to cGMP but not cAMP (Bevans *et al.*, 1998). When a gap junction is formed between two cells of the same type it is referred to as homologous coupling. When a gap junction connects two different cell types, it is referred to as heterologous coupling (Vaney and Weiler, 2000).

Each connexin that has been tested forms channels with unique properties including size selectivity, ion permeability, conductance and gating (White *et al.*, 1995; Bruzzone *et al.*, 1996a). Ion permeability is dependent on the charge of the amino acids lining the pore wall, which may be determined by the first extracellular domain. Channel conductance is determined by the voltage difference between the coupled cells. Due to

differing ion selectivity and voltage sensitivity between connexins, heterotypic channels can favour unidirectional signaling creating rectifying channels. Channel gating is dependent on voltage, intracellular Ca^{2+} concentration, pH, and phosphorylation. Determinants of voltage gating lie in the first extracellular loop and second transmembrane segment. The cytoplasmic loop and carboxy terminus are pH sensitive and upon decrease of intracellular pH, the channel will close. The coupled state is also sensitive to post-translational modification by phosphorylation on serine, threonine and tyrosine by protein kinases.

1.2 Gap Junctions in Vertebrate Development

Gap junctions appear early in vertebrate development and have been shown to play an essential role in normal development. The role of mouse Cx43 in development has been extensively studied and provides some examples of the importance of gap junctions in this process. The necessity for gap junctions begins even before fertilization, during gametogenesis. Connexin43 gap junctions are the most abundant in the testis and they homologously couple Sertoli cells and Leydig cells, and couple spermatogonia and spermatocytes to Sertoli cells. In the male Cx43 null mutant, the germ cell population does not increase after birth (Roscoe *et al.*, 2001). Similarly, the granulosa cell population in the ovarian follicles of female Cx43 deficient mice fail to develop properly, despite the presence of other Cxs, leading to improper oocyte development (Ackert *et al.*, 2001). In contrast, although gap junctions are present by the eight cell stage in development (McLachlin *et al.,* 1983), they do not seem to play an integral role in preimplantation development, as evidenced by null mutations and pharmacological

inhibitors of gap junctional coupling (De Sousa *et al.*, 1997; Kidder and Winterhager, 2001; Houghton *et al.*, 2002). Instead, the expression of several connexins at this stage may simply be in preparation for the need for post-implantation communication. However, the role of gap junctions in preimplantation is unclear.

Communication compartments, as shown by lucifer yellow transfer, are established post implantation as cells begin to differentiate and gap junctional communication is lost between tissues with different cell fates (Lo and Gilula, 1979). For example mouse and rat Cx43 are expressed in the trophectoderm and inner cell mass at the blastocyst stage but at implantation it becomes restricted to the embryo proper (Dahl *et al.*, 1996; Reuss *et al.*, 1997). The communication domains in developing tissues often correspond to specific developmental compartments and may serve to ensure their stability in order for cellular proliferation, differentiation, and contact-mediated induction to occur (Caveney, 1985).

The regulation of cell growth and differentiation is dependent on gap junctions as evidenced by numerous studies on the tumor suppressor role of connexins (Yamasaki *et al.*, 1999). For example, in human brain glioblastoma tumor cells Cx43 expression is down-regulated, but upon transfection of Cx43 into cell lines, their cell proliferation was dramatically reduced *in vitro* and *in vivo* (Huang *et al.*, 1998b).

Gap junctions are also involved in migrating cells, such as cardiac neural crest cells (Huang *et al.*, 1998a), and in organogenesis. One recent study illustrates the role of Cx43 in both these processes (Li *et al.*, 2002). The Cx43 knockout mouse heart is affected by coronary artery patterning defects and outflow tract obstruction. The patterning defects are attributed to Cx43 loss in proepicardial cells which results in an

increase in cell migration speed and an increase in cell proliferation. This, in turn, leads to aberrant localization of fibroblasts and smooth muscle cells, which are derivatives of proepicardial cells, in the infundibular pouches. The outflow obstruction is due to Cx43 loss in cardiac neural crest cells, which decreases their migration to the outflow tract (Huang *et al.*, 1998a).

1.3 Gap Junctions in Neural Development

The nervous system develops from the embryonic ectoderm and grows at a very high rate throughout development. It is responsible for much of the information integration, processing, and output in an organism and, consequently, it is very complex. In order for the nervous system to develop properly, and to carry out its functions correctly, intercellular communication is essential. This communication comes in many forms including chemical synapses, electrical synapses, and biochemical coupling. The latter two forms are entirely dependent on gap junctions.

Structural analysis, dye coupling, and electrical measurements have documented gap junction function in the central and peripheral nervous systems (Dermietzel and Spray, 1993). There are varying degrees of intercellular communication within functional compartments of the nervous system, and some communication between compartments. The degree of coupling is regulated by developmental and functional factors, such as second messengers and neurotransmitters. A specific connexin expression pattern may be required in the brain for the appropriate signal exchange and electrical coupling that is required for proper development (Dermietzel and Spray, 1993; Spray and Dermietzel, 1995). To date over a dozen connexins have been identified in the

mammalian nervous system both *in vivo* and *in vitro,* under various culture conditions, and at various developmental stages. These include Cx26, Cx30, Cx31, Cx32, Cx33, Cx36, Cx37, Cx40, Cx43, Cx45, Cx46, Cx47 and Cx50 (Dermietzel and Spray, 1993; Bruzzone and Ressot, 1997; Güldenagel *et al.*, 2000; Rozental *et al.*, 2000b; Barnett *et al.*, 2001; Teubner *et al.*, 2001). The role of these connexins in electrical synapses and biochemical signaling has, thus far, been primarily investigated in the neocortex.

In the mammalian neocortex, gap junctional coupling begins very early in development. Neurogenesis and glial cell formation occur prenatally in the mouse and rat, but the first two postnatal weeks are critical in cortical development, as it is at this time that morphological, neurochemical, and functional differentiation are occurring. As well, this is when synapses and the neuronal circuits form (Nadarajah *et al.*, 1997). In order to form the proper circuits in the brain, coordinated activity is essential. As the neocortex develops, neuronal precursors and radial glia in the ventricular zone aggregate into clusters and become coupled by gap junctions. The result is creation of neuronal domains with synchronous biochemical activity. Within the domains, an IP_3 (inositol 1, 4, 5-triphosphate)-induced Ca^{2+} wave is propagated by diffusion of IP_3 through gap junctions to neighboring cells. If gap junctions are artificially blocked, the neuronal domains do not form (Yuste *et al.*, 1992, 1995).

Gap junctions in the developing neocortex are regulated by neurotransmitters (Roerig and Feller, 2000). Dopamine and noradrenaline both induce uncoupling of junctions through a receptor mediated protein kinase A-dependent pathway. Serotonin also reduces gap junctional coupling through a receptor-mediated pathway.

1.4 Neuronal Connexins

Neurons are capable of chemical and electrical excitability and are responsible for relaying and processing of information signals in the nervous system. Gap junctions homologously couple neurons, and heterologously couple neurons to glial cells. The role of neuronal gap junctions is to aid in mediating synchrony, to pass signals from pre-synaptic cells to post-synaptic cells, and in exchange of second messengers (Dermietzel and Spray, 1993). They allow electrical synapses between cells, which are thought to precede the chemical synapses most often seen between mature neurons (Fischbach, 1972). To date, six neuronal connexins have been reported in mammals; Cx26, Cx32, Cx36, Cx43, Cx45 (see section 1.6) and Cx47. However, these reports are controversial due to differences in the reliability of the methodologies used. Studies using freeze-fracture replica immunogold labeling, which claims to have the highest resolution of all methods used to date allowing for identification of gap junctions in ultrastructurally and immunologically identified cell types, have only found Cx36 in neurons (Rash *et al.*, 2000, 2001a,b). Regardless of this, results from studies using various methodologies will be reported here.

Connexin26 is expressed in early development and is present at high levels until two weeks after birth where it is localized to neuronal cells in the neocortex and may play a role in establishing coupling in corticogenesis (Nadarajah *et al.*, 1997). In the adult, Cx26 expression is restricted to non-neuronal cells such as astrocytes, leptomeninges, pinealocytes and ependymal cells (Saez *et al.*, 1991; Spray and Dermietzel, 1993; Nagy *et al.*, 2001).

Connexin 32 has been reported in the both neonatal and adult rat brainstem neurons (Soloman *et al.*, 2001). As well, it has been reported in neurons in the hippocampus and cortex of the adult mouse (Oguro *et al.*, 2001; Priest *et al.*, 2001).

Connexin43 is expressed throughout development in neuroblasts and becomes progressively reduced in those cells that will become neurons, and remains expressed in non-neuronal cells such as astrocytes, pinealocytes, ependymal cells, and leptomeninges (Nadarajah *et al.*, 1997; Rozental *et al.,* 2000a; Nagy *et al.*, 2001; Rash *et al.*, 2001a,b). It is, however, maintained in some neuronal populations. For example, Cx43 is expressed in olfactory neuron precursors and mature olfactory neurons (Zhang *et al.*, 2000), in a sub-population of cortical neurons (Nadarajah *et al.*, 1997) and in motor neurons (Chang and Balice-Gordon, 2000).

Connexin 47 is expressed in alpha motor neurons of the spinal cord as well as some regions of the brain including, brainstem nuclei, cortex, cerebellum, hippocampus and dentate gyrus (Teubner *et al.*, 2001). Its expression often overlaps with that of Cx36.

Connexin 36 is the only undisputed neuronal connexin. As well, the above connexins are also expressed in other tissue types, whereas Cx36 is almost exclusively expressed in neurons, as evidenced by experiments with neurotoxins and neuronal markers (Condorelli *et al.*, 1998; Belluardo *et al.*, 2000). Rodent Cx36 mRNA is first expressed at embryonic day 9.5 (E9.5) in the forebrain and it increases to a maximum at postnatal day seven (P7) (Söhl *et al.*, 1998; Gulisano *et al.*, 2000). This peak in Cx36 expression coincides with circuit formation in the cortex and hippocampus (Rozental *et al.*, 2000b). In the adult brain, Cx36 is highly expressed in the nuclei of the inferior olivary complex, the olfactory bulb, the hippocampus and various brainstem nuclei

(Condorelli *et al.*, 1998; Belluardo *et al.*, 2000; Rash *et al.*, 2000; Teubner *et al.*, 2000). It is also moderately expressed in the granular layer, the molecular layer and the Purkinje cell layer of the cerebellum, the substantia nigra, the hypothalamus, the basal ganglia, the cerebral cortex, the anterior pituitary, the pineal gland and neurons of the spinal cord (Condorelli *et al.*, 2000; Rash *et al.*, 2000). Parenti *et al.* (2000) showed that Cx36 is differentially expressed in neurons in the motor pathway versus those in the sensory pathway, implying that Cx36 may play specific roles within different neuronal systems.

1.5 Gap Junctions in the Retina

The vertebrate retina is considered to be part of the central nervous system because it is derived from the developing forebrain through interactions between the neural tube and cranial ectodermal placodes (Gilbert, 1994). Though the retina is a complicated structure, it is simplified in comparison to the brain and therefore is an excellent model to study the nervous system. It is a highly ordered laminar structure consisting of three compact layers of neurons separated by two synaptic layers. There are many other advantages to using the retina as a model system (Vaney, 1999). Its structure and function have been studied in detail in the past and, therefore, any new discoveries pertaining to the retina can often be related to an established knowledge. The rodent retina can be isolated intact from the animal and, therefore, although the experiments are done *in vitro*, the retina retains some *in vivo* qualities. Its neuronal circuitry remains intact and it is able to respond to natural stimuli. Its *in vitro* benefits include the capability to microscopically identify the many cell types, good electrical recording stability, and the accessibility for controlled application of drugs.

There are five major types of retinal neurons. Photoreceptors, bipolar cells, and ganglion cells form a horizontal pathway through the retina, and horizontal cells and amacrine cells form a lateral pathway. However, there are approximately 100 different cell types in the retina and virtually every type of cell can be coupled by gap junctions, as they are present in all layers of the teleost and mammalian retinas (Deans and Paul, 2001). In development, gap junctions play a role in forming the circuits in the retina that will allow signal flow from photoreceptors to ganglion cells. In the adult, gap junctions are involved in rewiring the circuits that will transmit and code for visual signals under different lighting conditions (Vaney and Weiler, 2000). The range of light the vertebrate eye is exposed to far exceeds the operating range of individual neurons and, as a consequence, dynamic electrical coupling is needed (Weiler *et al.*, 2000). To achieve this numerous types of connexins and coupling are found in the retina, which act in concert with a range of chemical neurotransmitters.

Gap junctions are permeable to numerous second messengers, such as Ca^{2+}, cAMP, cGMP, and IP_3, as well as some small amino acids like glutamate and glycine. The electrical synapses formed by gap junctions in the retina are modulated by these neurotransmitters and also by light. For example, conductance between homotypic channels joining amacrine cells is reduced by cAMP and dopamine (Vaney, 1999), whereas activation of dopamine receptors and retinoic acid reduce coupling between horizontal cells (Weiler *et al.*, 2000).

Heterologous coupling occurs between AII amacrine cells and bipolar cells, rods and cones, various types of bipolar cells, various types of ganglion cells, various glial cells, and between amacrine cells and ganglion cells. These junctions are not affected by

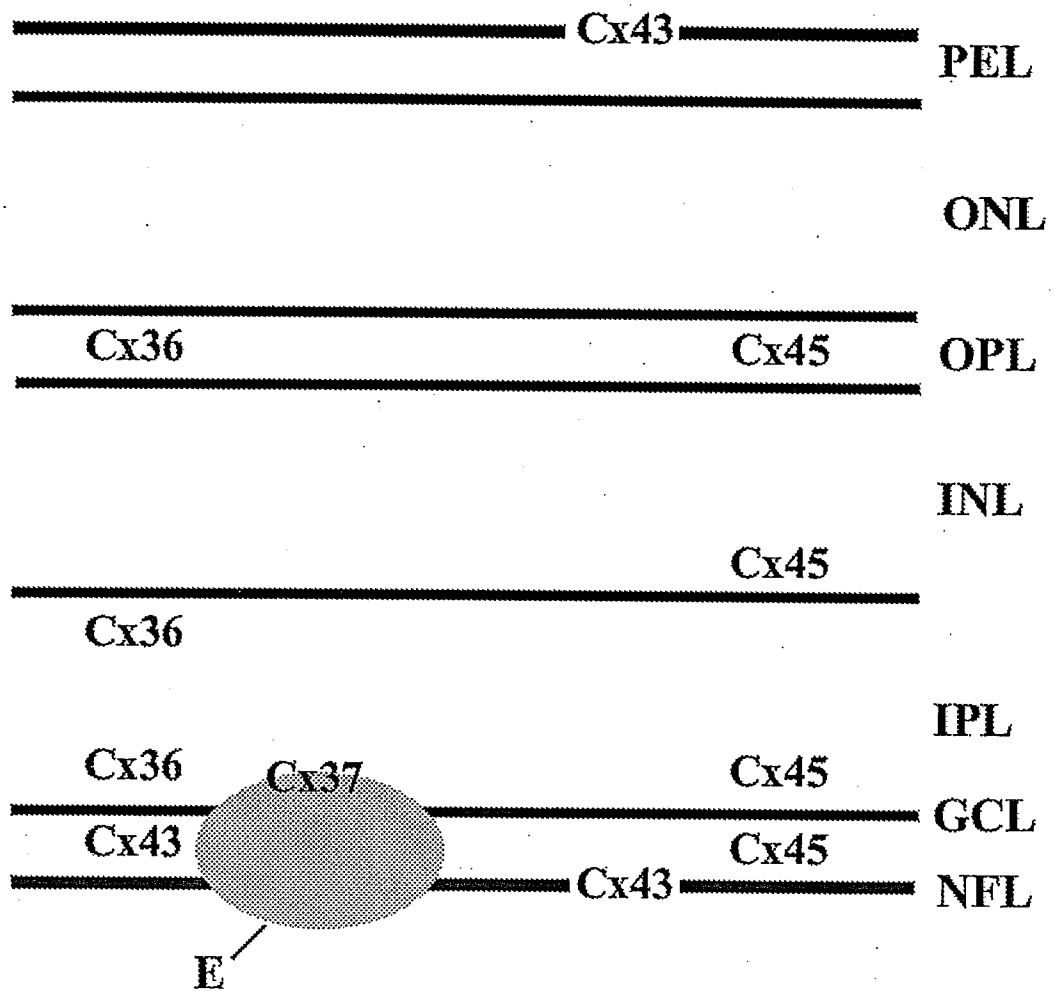
dopamine or cAMP, but coupling is reduced by cGMP, cGMP agonists, and nitric oxide (Vaney, 1999). Most often there is unidirectional conductance through heterologous junctions. For example, dye transfer will occur from astrocytes to Muller cells, or astrocytes to oligodendrocytes cells, but not in the other direction (Söhl *et al.*, 2000). Transfer of the neurotransmitter glycine will occur from amacrine rod cells to cone bipolar cells, but not in the opposite direction. As well, an injection of neurobiotin into amacrine cells travels to the neighboring bipolar cells, but an injection into the bipolar cell will not pass to the amacrine cell (Feigenspan *et al.*, 2001). This phenomenon is referred to as chemical rectification, where there is asymmetric permeability to small ions (Vaney *et al.*, 1998). Chemical rectification also occurs between ganglion cells and amacrine cells.

1.6 Retinal Connexins

To date there have been nine connexins identified in the mammalian retina by RT-PCR techniques: Cx37, Cx40, Cx43, Cx45, Cx50 Cx26, Cx31, Cx32, and Cx36 (Güldenagel *et al.*, 2000). However, only the Cx36, Cx37, Cx43, and Cx45 proteins have been documented in the retina (Fig. 3).

Connexin37 and Cx43 are primarily non-neuronal. Connexin37 is vascular and found in the endothelium of the blood vessels in the ganglion cell layer (GCL) of the inner retina (Güldenagel *et al.*, 2000). Connexin43 is found primarily between glial cells; the endfeet of Muller cells in lower vertebrates, and astrocytes in higher vertebrates. It also heterologously couples astrocytes to Muller cells. Connexin43 expression is widespread in the retina. It is found in the pigment epithelium layer of all species tested

Figure 3: Schematic connexin (Cx) protein expression pattern in the layers of the mouse retina (after Güldenagel *et al.*, 2000). PEL = pigment epithelium layer, ONL = outer nuclear layer, OPL = outer plexiform layer, INL = inner nuclear layer, IPL = inner plexiform layer, GCL = ganglion cell layer, NFL = nerve fiber layer, E = epithelial cells of vasculature.


Cx43
PEL
ONL
Cx36
Cx45
OPL
INL
Cx45
Cx36
IPL
Cx36
Cx37
Cx45
GCL
Cx43
Cx45
Cx43
NFL
E

to date (Janssen-Bienhold *et al.*, 1998). In addition, in the mammal, it is found in the nerve fiber layer, GCL, the stria medullaris, and around blood vessels of the inner retina. In the zebrafish and carp, Cx43 is localized to the outer limiting membrane, outer plexiform layer (OPL), and the inner plexiform layer (IPL). In the zebrafish and carp IPL, Cx43 may be restricted to amacrine cells suggesting it is not only glial, but also neuronal (Janssen-Bienhold *et al.*, 1998; Güldenagel *et al.*, 2000).

The remaining two rodent retinal connexins are strictly neuronal. Cx45 is found in the GCL, IPL, OPL and inner nuclear layer (INL) presumably between amacrine cells and possibly cone bipolar cells (Güldenagel *et al.*, 2000; Söhl *et al.*, 2000). Connexin36 is the most highly expressed connexin in the retina, suggesting it plays a major role there. It has therefore been studied extensively in numerous species. Immunolocalization shows punctate staining in two bands in the mouse IPL, as well as in a faint band in the OPL and GCL (Al-Ubaidi *et al.*, 2000; Söhl *et al.*, 1998). Cx36 is expressed in the dendrites of mammalian AII amacrine cells, however, the amacrine cells form both homologous junctions with other amacrine cells, and heterologous junctions with bipolar cell axons. The bipolar cells do not label for Cx36 though, so these junctions may be heterotypic (Feigenspan *et al.*, 2001; Mills *et al.*, 2001). This is interesting because, up until this time, Cx36 had not been shown to form heterotypic channels with any other connexin.

In addition to the retinal connexins in the rodent, three others have been cloned from the zebrafish retina by RACE (rapid amplification of cDNA ends) strategies from retinal cDNA (Dermietzel *et al.*, 2000). Connexin44.1, which is homologous to rodent Cx50, is expressed at low levels in the retina. By *in situ* RT-PCR, it was localized to the GCL, however this data is somewhat controversial because Cx44.1 could not be detected

by *in situ* hybridization (Dermietzel *et al.*, 2000; Cason *et al.*, 2001). Connexin27.5, which shows homology to both rodent Cx26 and Cx32, was detected in the INL and GCL and is also expressed in the brain. Connexin55.5, which shows homology to rodent Cx57 and Cx50, is found in the GCL and the outer layer of the INL, suggesting it is localized to horizontal cells. All three of these zebrafish connexins can form heterotypic channels with each other.

1.7 Gap Junctions and Disease

Gap junctions have been extensively characterized both structurally and biochemically, however, there is now a shift to studies aimed at determining the normal biological roles of gap junctions, and what role they may play in the development of disease. Impaired connexin expression during development has been implicated in numerous diseases (Donaldson *et al.*, 1997; White and Paul, 1999; Krutovskikh and Yamasaki, 2000; Kelsell *et al.*, 2001). Mutations in Cx43 have been identified in congenital heart abnormalities in mice (Reaume *et al.*, 1995). Certain forms of hearing loss are associated with Cx26 mutations (White, 2000). Connexin46 knockout mice develop cataracts, and Cx50 knockout mice develop cataracts and microphthalmia (White, 2002). Connexins have also been implicated as tumor suppressor genes (Yamasaki *et al.*, 1999).

A specific connexin expression pattern is likely required in the nervous system for proper second messenger exchange and electrical coupling so it is not surprising that connexin mutations have also been associated with nervous tissue diseases (Spray and Dermietzel, 1995). For example, the X-linked dominant form of Charcot-Marie-Tooth

disease (CMTX), a genetic disease affecting the myelin of the peripheral nervous system, has been linked to mutations in Cx32. To date, more than 160 different mutations in Cx32 have been identified in CMTX patients (Scherer *et al.*, 1999; Abrams *et al.*, 2000). Some of the mutations result in loss of functional channels due to accumulation of the protein in the cytoplasm while other mutants produce functional channels but with altered gating properties.

An increase in electrical coupling between neurons and between astrocytes may result in epileptic symptoms, due to continual depolarization of neurons. One evidence for this is that anti-epileptic drugs block gap junctional channels (Spray and Dermietzel, 1995). In contrast, a decrease in gap junction mediated coupling in the nervous system may result in a loss of growth control. For example, connexin43 (Cx43) is down-regulated in several human cancer cell lines, and up-regulation reduces tumorigenicity (Huang *et al.*, 1998b; Krutovskikh *et al.*, 1998; Zhang *et al.*, 1998). The mechanism of the tumor suppressor function of connexins is not yet clear. Given the many neural disorders known, it is important to investigate the role nervous tissue connexins may play in development to elucidate any role they may have in disease.

1.8 The Cx35/36 Orthologues

The novel Cx35/36 group of connexins is almost exclusively expressed in neural tissue, primarily the brain and retina. O'Brien *et al.* (1996) cloned the first member of the subfamily, skate Cx35, and since then eight more members have been defined; mouse Cx36 (Söhl *et al.*, 1998), rat Cx36 (Condorelli *et al.*, 1998), perch Cx35, perch Cx34.7 (O'Brien *et al.*, 1998), human Cx36 (Belluardo *et al.*, 1999), chimp Cx36, gorilla Cx36,

and orangutan Cx36 (GenBank accession numbers; AB037510, AB037511, AB037512). All of the above, except for perch Cx34.7, are orthologues, which are genetic elements in two different species that are derived from a single element in the common ancestor. They share a high degree of overall amino acid conservation, although the sequence of the cytoplasmic loop is quite diverse. This group of connexins is unique in that they are missing the 5' UTR intron that all other connexins have, but instead have an intron located 71 bp after the translation start site. The introns vary in length from 900 bp in perch Cx35 to 20 kb in perch Cx34.7, and all have consensus splice sequences. Other defining characteristics of the Cx35/36 group are unusually long cytoplasmic loops, up to 99 amino acids in mouse Cx36, and fairly short C-terminal tails.

Functional analyses of the perch connexins, skate Cx35 and mouse Cx36 have shown that the gap junctions have a very high voltage sensitivity threshold, being the least voltage sensitive of any connexin tested to date (O'Brien *et al.*, 1998; Srinivas et al., 1999; White *et al.*, 1999; Al-Ubaidi *et al.*, 2000; Teubner *et al.*, 2000). This may be due to the need to keep the channels open, independent of voltage shifts in the nervous system. However, other neuronal connexins have high voltage sensitivity which conflicts with this theory (Dermietzel *et al.*, 2000; Teubner *et al.*, 2001).

The divergence from other connexins may be due to unique forms of channel regulation, as much of the variation occurs in the regions of the sequence responsible for gating properties (O'Brien *et al.*, 1998). Perch Cx34.7 and perch Cx35 are able to form heterotypic channels with each other in *Xenopus* oocytes (O'Brien *et al.*, 1998). Skate Cx35 was also tested for heterotypic channel formation with Cx46, Cx32, Cx26 and Cx50, which most readily interact with other connexins, but were unable to form

functional channels. It did show hemi-channel activity however, in *Xenopus* oocytes (White *et al.*, 1999).

Although skate Cx35 is expressed only in retina, its orthologues are expressed in both retina and regions of the brain. Perch Cx34.7 has also been detected at extremely low levels in the gut (O'Brien *et al.*, 1998). The mammalian orthologues are expressed in the central nervous system in a complex and widespread pattern. In the brain they are most intensely expressed in the inferior olive complex, but are expressed at moderate levels in the olfactory bulb, hippocampus, pineal glands, brain stem nuclei, and cerebellar cortex (Condorelli *et al.*, 1998; Belluardo *et al.*, 1999; Teubner *et al.*, 2000). Human Cx36 is also found in all layers of the spinal cord gray matter (Belluardo *et al.*, 1999). Mouse Cx36 expression was analyzed during development and it increased in abundance to a maximum at seven days post-partum and then began decreasing to only 8% of this in the adult brain (Söhl *et al.*, 1998). The regulatory mechanism responsible for the developmental modulation is unknown and the maximum expression is still lower than in adult retina. Mouse Cx36 is expressed 18 times higher in the retina than in the adult brain. The mammalian orthologues have a unique 18 amino acid glycine-rich tract in their cytoplasmic loop. The function of this has not yet been determined.

Although little is known about neuronal gap junctions, they may be involved in genetic disease. Human Cx36 has been mapped to chromosome 15q14. A form of juvenile epilepsy and an abnormality in response to sensory stimuli have also been linked to this locus (Belluardo *et al.*, 1999). More studies must be done to verify any connection between these diseases and Cx36 mutations.

1.9 Zebrafish as a vertebrate model

Development of most organisms, from worm to human, is controlled by a similar set of genes (Mullins and Nusslein-Volhard, 1993). Therefore, researchers have been able to use many organisms as models to study developmental processes. Traditionally, genes involved in developmental processes have been examined in *Drosophila melanogaster* or *Caenorhabditis elegans* using large-scale mutational approaches. However, a vertebrate model must be used to address vertebrate-specific biology. The chick and *Xenopus* are used but they too have limitations, including relatively long generation time and low number of offspring. Since the goal of many developmental studies is to apply the results to human development and disease, many researchers use the mouse as a closely related mammalian model. It is an established biological model and many genetic mutations have been produced by homologous recombination of cloned genes in embryonic stem cell lines to create knockout mice. However, it is difficult to assess early developmental events because mouse development occurs *in utero* and, due to its large genome size, large-scale mutagenesis is laborious. As well, mice are costly to maintain, financially, and in time and space required.

In comparison, the zebrafish, *Danio rerio*, has many attributes that favour its use as a model for genetic analysis. Though not a mammal, the zebrafish is a vertebrate and so it shares a great deal of similarity with higher organisms, therefore, its gene sequences can be used to isolate the homologous gene sequences of other vertebrates. The embryology of this fish is almost perfect for mutational studies (Driever and Fishman, 1996). Zebrafish are very prolific breeders as each female can yield up to 250 eggs weekly. Fertilization is external and so the embryos are easily accessible, being

harvested from the bottom of the fish tank. The embryos are large and transparent so development can be observed under a regular dissecting microscope in the live animal. Embryonic development occurs quickly. By 24 hours post fertilization (hpf), the fish has developed all of its primordial organs and by three days post fertilization (dpf) they are functional. Also, the fish need little space and cost relatively little to maintain.

As the number of research labs working on zebrafish grows, rapid progress is being made in zebrafish genetics and genomics and many resources have been established (Dooley and Zon, 2000). Wolfgang Driever's lab, at that time in Boston, and now in Freiberg, and Christiane Nusslein-Volhard's lab in Tübingen undertook saturation screens of zebrafish mutations. As a result more than 1500 mutations involved in embryonic development, representing about 400 genes and over 500 phenotypes, were isolated and identified (Driever *et al.*, 1996; Granato and Nusslein-Volhard, 1996; Haffter *et al.*, 1996). There are various genomic libraries available for positional cloning, as well as expressed sequence tagged (EST) cDNA libraries (Dooley and Zon, 2000). Radiation hybrid panels are available and can be used to map cloned genes and there are also meiotic maps available with over 2000 microsatellite repeat markers. Transgenic fish can be generated using microinjection techniques and retroviruses have recently been successfully used for insertional mutagenesis. The US National Institutes of Health and the Sanger Centre at Cambridge University are currently heading the zebrafish genome initiative and zebrafish sequence is being compared to that of humans to identify regions of synteny for candidate gene identification in disease. Many of the zebrafish phenotypes identified show resemblance to human diseases so the zebrafish is an excellent model to study not only vertebrate development, but also human disease.

Zebrafish have been recognized as an excellent model for the development of the vertebrate visual system (Bilotta and Saszik, 2001). Along with morphological and physiological observations, behavioral assays have been developed that allow the identification of single-gene mutations that affect vision (Baier, 2000; Li, 2001). These include testing the optokinetic (OKR) and optomotor (OMR) responses of the fish, as well as their phototactic and visual startle responses. For example, Neuhauss *et al.* (1999) screened 450 developmental mutants recovered in the 1996 Tübingen saturation screen by testing OKR and OMR and revealed that over 25 of these mutants showed abnormal responses to visual stimuli. This study and many others have led to the identification of many zebrafish genes that play a role in development of the visual system. Further characterization of the mutants, as well as the continuing development of behavioral and physiological assays to test visual development makes the zebrafish a fundamental model to provide insights into the molecular genetics of vertebrate vision.

1.10 Hypothesis and Objectives

This thesis project is based on the hypothesis that the zebrafish genome contains a Cx35/36 orthologue and that it is expressed in neurons of the retina and brain during embryonic development and in the adult, and that it is essential to proper embryonic development and function. The specific objectives of this project are

- **isolation, cloning and sequencing of the full coding sequence of the zebrafish Cx35/36 orthologue for structural analysis**
- **analysis of its biophysical properties**
- **temporal expression analysis at the RNA and protein levels**
- **spatial expression analysis at the RNA and protein levels**

CHAPTER 2: MATERIALS AND METHODS

Composition of common buffers and media are found in Appendix A.

2.1 Zebrafish Care

The zebrafish were maintained by the animal holding staff at The University of Manitoba. The fish were kept in water at 28.5°C in 20-gallon tanks. They were maintained on a constant light/dark cycle of 14 hours of light and 10 hours of darkness per day. They were fed flaked tropical fish food and trout pellets twice a day and frozen brine shrimp once a week. One quarter of the tank water was replaced weekly. To breed, the fish were brought to 10-gallon tanks in Z314 Duff Roblin and held within the tank in a plastic enclosure with a netted bottom at 28.5°C. Upon breeding, the embryos fell through the netting and were siphoned from the bottom of the tank. The embryos were incubated in batches of 50 in 250 ml beakers in egg water (60 μg/ml Instant Ocean® sea salts) in a 28.5°C water bath. The embryos were cleaned and placed in fresh egg water daily. Embryos were reared to a maximum of five days post fertilization, a time period in which they do not need to be fed as their yolk sac provides nutrition. Adult fish were sacrificed by decapitation after being anesthetized in Tricaine (Sigma, Mississauga, ON) solution according to The Zebrafish Book (Westerfield *et al.*, 1995). Embryos beyond hatching were also anesthetized before being frozen or fixed.

2.2 Isolation of Genomic Clone

2.2.1 Genomic DNA isolation

Total zebrafish genomic DNA was isolated according to The Zebrafish Book (Westerfield, 1995). One adult zebrafish was sacrificed and ground to a fine powder in liquid nitrogen. The powder was suspended in 10 ml of digestion buffer (10 mM Tris-HCl pH 8.0, 1% SDS, 5 mM EDTA, 100 μg/ml of proteinase K (Boehringer Mannheim, Laval, QC)) and digested for five hours at 37°C. The suspension was extracted with equal volume of phenol, followed by two extractions with equal volume of phenol:chloroform:isoamyl alcohol (25:24:1). Sodium chloride was added to the extract to a concentration of 0.3 M and the DNA was precipitated with 2.5 volumes of ethanol at -20°C overnight. The DNA was pelleted by centrifugation at 3,000 x g for 10 minutes and then washed with 70% ethanol. It was then resuspended in 1 ml of TE buffer (10 mM Tris-HCl, pH 8.0, 1 mM EDTA) and NaCl was added to a concentration of 100 mM. The DNA was treated with 100 μg/ml of ribonuclease A (Sigma, Oakville, ON) at 37°C for three hours. SDS was added to a concentration of 0.2% and the mixture was extracted twice with phenol:chloroform:isoamyl alcohol and precipitated with ethanol as above. Finally, the DNA pellet was dissolved in TE buffer.

2.2.2 PCR Cloning

A PCR generated putative Cx35/36 fragment was cloned from genomic DNA as part of a previous project (Elizabeth McLachlan, Honours Thesis, University of Manitoba), but was used in this project as a probe to isolate the full genomic clones.

Primers identical to those originally used to amplify and clone the mouse Cx36 sequence (Söhl *et al.*, 1998), were used to PCR amplify zebrafish genomic DNA. They are each 32 nucleotides long and anneal inside the second exon in the coding region. The primers were custom manufactured by Invitrogen: Life Technologies (Burlington, ON). They were used with the following program on a PTC-100™ thermocycler (MJ Research, Inc., Watertown, MA); 94°C, 3 minutes; 94°C, 45 seconds (denature); 60°C, 45 seconds (anneal); 72°C, 1 minute 15 seconds (extend); repeat last three steps 35X; extend at 72°C, 10 minutes. PCR reactions contained 0.5 μg of genomic DNA, 0.5 μM of each primer, 200 μM of each dNTP, 1.5 mM $MgCl_2$, 1X PCR buffer (20 mM Tris-HCl pH 8.4, 50 mM KCl; Invitrogen) and 2.5 units of Taq polymerase (Invitrogen) in a 50 μl total volume. Controls for all PCR attempts were reactions with no template. To verify amplification and determine the size of the amplified fragment, all PCR products were separated by electrophoresis, with 1X DNA loading buffer, on a 1.2% agarose gel in 0.5X TBE buffer with a 1 kb Plus DNA marker (Invitrogen).

An approximately 750 base pair (bp) fragment was cloned into the pCR® 2.1 vector using the Original TA Cloning Kit (Invitrogen) with INVαF' One Shot™ cells. The plasmid vector has a single deoxythymidine overhang on the 3' end of each strand that complements the single deoxyadenosine that *Taq* polymerase automatically adds to all PCR products. This allows ligation of the PCR product into the vector. Competent bacterial cells were then transformed with these plasmids and plated on LB agar plates containing X-gal (5-bromo-4-chloro-3-indolyl-B-D-galactosid; Invitrogen) and 50 μg/ml of ampicillin. White colonies were picked from the agar plates for overnight cultures and plasmid minipreps were prepared with the High Pure Plasmid Isolation Kit (Boerhinger

Mannheim). To verify insertion and size, samples of the minipreps were digested with five units of the restriction enzyme EcoR I (Invitrogen) at 37°C for several hours to release the insert. The digested sample was separated by electrophoresis on a 0.8% agarose gel in 0.5X TBE buffer.

2.2.3 DNA Probe Synthesis

Ten micrograms of plasmid containing the partial sequence of the zebrafish Cx35/36 orthologue was digested with 25 units of EcoR I to release the fragment. The digest was separated by electrophoresis on a 1% low-melt agarose gel in 1X TAE buffer. The band corresponding to the insert was cut out of the gel and boiled for approximately five to 10 minutes to melt the agarose and denature the DNA. Approximately 50 ng of the purified, denatured DNA was used as a template for each random priming reaction. The DNA was incubated at 37°C for two hours with 5 μg BSA (bovine serum albumin), 10 μl OLB, 5 μl of α^{32}P-dCTP (3000 Ci/mmol, 10 mCi/ml) (NEN^{TM}), 4.65 units of Klenow enzyme (Invitrogen), and ddH_2O (double distilled water) to a final volume of 50 μl. To remove non-incorporated α^{32}P-dCTP, the reaction was then diluted to 100 μl with ddH_2O, loaded onto a NICK^{TM} Column (Pharmacia Biotech, Baie d'Urfe, QC), and eluted with 400 μl of 10 mM Tris-HCL, pH7.5, 1 mM EDTA. Incorporation of α^{32}P-dCTP into the DNA was determined by scintillation counting and the probe was alkali-denatured by addition of 40 μl of 3 M NaOH followed by neutralized with 40 μl of 3 M HCL.

2.2.4 Screening of a zebrafish genomic PAC library

A zebrafish genomic PAC (P1 artificial chromosome) library from the Resource Center for the German Human Genome Project (www.RZPD.DE) was screened with the above DNA probe to isolate a genomic clone. The library was generated from erythrocyte genomic DNA which was partially digested with the restriction enzyme Mbo I into approximately 120 kb fragments (Amemiya *et al.*, 1999; Amemiya and Zon, 1999). The fragments were ligated into the vector pCYPAC-6, which were then grown in *E.coli* DH10B. A total of 104,064 clones were then spotted in duplicate on four membrane filters. The filters were prehybridized in tubes with hybridization solution 1 for two hours at 65°C in a hybridization incubator (Robbins Scientific, model 1000). The DNA probe from section 2.2.3 was then diluted to approximately three to five million counts per minute (cpm) per ml in hybridization solution 1 and incubated with the filters overnight at 65°C. The following day the filters were washed three times for one hour each in 40 mM phosphate buffer, pH 7.2, 0.1% SDS and then rinsed in 4X SSC. Positive signals were detected by autoradiography on Kodak X-Omat film. Positive signals on the film were matched to their x and y coordinates on the template of the filters and the corresponding clones were ordered from RZPD.

To verify that these clones were indeed positive, they were streaked on LB agar plates containing 50 μg/ml of kanamycin and grown for 16 hours at 37°C. A region of the densely grown colonies was then picked, diluted in LB liquid medium to reduce the density, spread on kanamycin plates and grown overnight. The resulting individual clones were picked and streaked on duplicate nitrocellulose filers that were placed on kanamycin plates and left to grow overnight. One of the duplicate membranes was stored

at 4°C to isolate DNA from after the positive clones were identified. To identify the positive clones, the other membrane was processed for screening by placing it on a filter wet with lysozyme solution (1.5 mg/ml lysozyme, 25% sucrose, 50 mM Tris-HCL, pH7.5) for one minute and then blotting it on a dry filter for one minute. This was repeated two more times for a total of three cycles with the purpose of lysing the bacteria. This three step procedure was repeated with the following solutions; 0.2% Triton X-100, 0.5 M NaOH (denature); 0.5 M NaOH (denature); 1.5 M Tris-HCl, pH7.5 (neutralize); 0.15 M NaCl, 0.1 M Tris-HCl, pH 7.5 (neutralize). The membrane was then baked at 80°C for one hour and stored at room temperature until hybridization. The membrane was prehybridized in hybridization solution 2 at 42°C for two hours. It was then incubated overnight at 42°C with the probe. The probe was prepared as in 2.2.4 and diluted to three to five million cpm per ml in hybridization solution 2. The following day the membrane was washed three times in 0.2% SDS, 0.2X SSC. The first two washes were for 30 minutes at 42°C and the third was at 65°C for one hour. The membrane was subjected to autoradiography. Positive signals were then associated with a position on the membrane and the complimentary clone from the duplicate membrane stored at 4°C was used for DNA isolation.

2.2.5 PAC DNA Isolation

The DNA was isolated, using two different protocols, from two independent PAC clones sent from RZPD. PAC DNA was isolated from one clone with the QIAGEN Large Construct Kit, according to the manufacturer's protocol. Briefly, three ml of LB medium, containing 50 μg/ml kanamycin, was inoculated with one of the final positive

clones from 2.2.4 and grown at 37°C for eight hours. The starter culture was then added to 500 ml of LB medium and grown overnight at 37°C. The cells were pelleted by centrifugation at 6,000 x g for 15 minutes and then resuspended in lysis buffers. The DNA was precipitated with isopropanol and washed with ethanol. It was then treated with ATP-dependent exonuclease to digest any contaminating genomic DNA and any nicked PAC DNA, leaving only supercoiled PAC DNA. The DNA was bound to QIAGEN Resin under the appropriate buffer conditions and the RNA, proteins, and remaining impurities were washed away. The DNA was then eluted from the resin, precipitated with isopropanol, and washed with ethanol. It was dissolved in Tris-HCl, pH 8.5 and the yield was determined by spectrophotometry.

PAC DNA was isolated from the second clone as follows. A sterile toothpick was used to pick an isolated colony of cells and it was then dropped in 2 ml of LB medium with 25 μg/ml of kanamycin. The culture was grown overnight at 37°C. The cells were pelleted by centrifugation at 16,000 x g for 30 seconds and then resuspended in 0.3 ml of buffer P1 (15 mM Tris, pH 8.0, 10 mM EDTA, 100 μg/ml RNase A). Next, 0.3 ml of buffer P2 (0.2 N NaOH, 1% SDS) was added followed by addition of 0.3 ml of buffer P3 (3 M KOAc, pH5.5). The suspension was incubated on ice for five minutes and then centrifuged at 16,000 x g for 10 minutes. The supernatant was precipitated with an equal volume of isopropanol at -80°C for two to three hours and then the DNA was pelleted by centrifugation. It was washed twice in 70% ethanol and redissolved in TE buffer for yield determination by spectrophotometry.

2.2.6 Subcloning

PAC clones are very large and, therefore, difficult to work with. To generate clones of more manageable size, the positive PAC clones were digested with a restriction enzyme and the resulting smaller fragments were subcloned into the vector pBluescript (Stratagene, La Jolla, CA). Five micrograms of the DNA, isolated by either method in 2.2.5, and 5 μg of the vector were each digested with 15 units of EcoR I at 37°C for several hours. The vector reaction was then heat inactivated at 65°C for 10 minutes and alkaline phosphatase treated, to prevent the ends from reannealing, by addition of one unit of CIAP (calf intestinal alkaline phosphatase; Invitrogen) and incubation at 37°C for 20 minutes. The reaction was stopped with 0.5 M EDTA and heat inactivation. This reaction and the PAC DNA digests were then phenol-chloroform extracted. First the samples were extracted with an equal volume of phenol:chloroform:isoamyl alcohol (25:24:1) and centrifuged at 10,000 x g for 5 minutes at 4°C, followed by extraction with only chloroform. The DNA was then precipitated by addition of 1/10 the volume of 3 M NaOAc and 2.5 volumes of 100% ethanol and placed at –80°C for several hours. The DNA was then pelleted by centrifugation at 16,000 x g for 15 minutes and washed with 75% ethanol. The pellets were air-dried and dissolved in water. The PAC DNA fragments were ligated into the vector by incubating 20 ng of the vector with 100-1000 ng of fragments and 400 units of T4 ligase (Invitrogen) with 1X ligation buffer (50 mM Tris-HCL, pH7.6, 10 mM $MgCl_2$, 1 mM ATP, 1 mM DTT, 5% w/v polyethylene glycol) at 14°C overnight. The control ligation did not receive any insert.

SoloPack® Gold Competent Cells (Stratagene) were transformed with the ligated plasmid according to protocol. The cells were treated with β-mercaptoethanol to

puncture their membrane, and 50-100 ng of either the plasmid containing the insert or the control plasmid were incubated with the cells for 30 minutes on ice. The cells were heat-pulsed at 42°C and then incubated with growth broth for one hour at 37°C. The cells were spread on LB-ampicillin (50 μg/ml) agar plates coated with X-Gal for colour selection, and grown overnight at 37°C.

White colonies were picked from the plates of the experimental transformation and streaked onto duplicate filters as in 2.2.4 and grown on ampicillin plates. One membrane was processed, probed, and subjected to autoradiography as before. Positive clones were streaked onto ampicillin plates and grown as usual and then isolated colonies were grown in overnight cultures. Miniprep DNA was isolated and digested with EcoR I to verify the presence of the insert.

2.2.7 Sequencing and Structural Analysis

Sequencing reactions were carried out at the DNA Sequencing Laboratory at the University of Calgary on ABI PRISM 377 sequencers. Each reaction contained 0.05 - 0.1 μg of DNA template per 1000 bases and 3.2 pmol of primer. Initially, the primers used in the PCR reaction in 2.2.2 were used, and then primers were designed from the recovered sequences for the subsequent sequencing reactions. Both strands of both PAC subclones were fully sequenced in the region surrounding and including the coding region. The recovered sequences were then assembled into a consensus sequence using the software program Xesee 3.2 (Eric Cabot) and conceptually translated into the corresponding amino acid sequence. Both the nucleotide and amino acid sequences were subjected to a BLAST similarity search of GenBank to reveal the most closely related

sequences previously identified. Open reading frames were found within the amino acid sequence with NCBI's ORF Finder program (www.ncbi.nlm.nih.gov/gorf/). These were used in conjunction with the known consensus sequences of splice sites to predict the intron-exon boundaries. The putative amino acid sequence of the coding region was then used to predict the protein's molecular weight with the ProtParam Tool from ExPASy (www.expasy.ch/cgi-bin/protparam). The hydrophobicity profile of the protein was predicted with the TMpred tool from Swiss EMBnet (www.ch.embnet.org/index.html). Potential phosphorylation sites were identified with the ScanProsite tool from ExPASy. The amino acid sequence was then aligned with the Cx35/36 orthologous group members' sequences using the Clustal X program (Thompson *et al.*, 1997). A phylogenetic analysis was then done with the amino acid sequences of the Cx35/36 orthologous group members using the program TREEVIEW (Page, 1996).

2.3 Isolation of cDNA clone

2.3.1 Synthesis of cDNA

Total RNA was isolated from adult zebrafish brain using TRIzol reagent (Invitrogen). The tissue was homogenized in one ml of reagent, extracted with 0.2 ml chloroform and centrifuged at 12,000 x g for 15 minutes at 4°C. The RNA was precipitated with 0.5 ml isopropyl alcohol at room temperature for 10 minutes and pelleted at 12,000 x g for 10 minutes at 4°C. The pellet was washed in one ml of 75% ethanol, and then air-dried and dissolved in DEPC (diethyl pyrocarbonate) treated water.

To degrade any remaining genomic DNA, equal amounts of the RNA samples were treated with one unit of RQ1 RNase-free DNase (Promega, Madison, WI) per microgram of total RNA at 37°C for 30 minutes. The reaction was inactivated with stop solution (20 mM EGTA, pH8.0) and incubated at 65°C for 10 minutes. The samples were then phenol-chloroform extracted, precipitated and re-dissolved in DEPC-treated ddH_2O.

The RNA samples were divided equally and each half was used as template for cDNA synthesis, following the SUPERSCRIPT II reverse transcriptase (Invitrogen) protocol for RT-PCR (reverse transcriptase polymerase chain reaction). One hundred nanograms of oligo dT was added to the RNA to complement the RNA poly A tail and serve as a primer for the reverse transcriptase. The samples were incubated at 70°C for 10 minutes and then chilled quickly on ice. Next, 4 μl of 5X buffer (25 mM Tris-HCl, pH8.3, 375 mM KCl, 15 mM $MgCl_2$), 2 μl of 0.1 mM DTT (dithiothreitol), 1 μl of 10 mM dNTPs and water were added to a total volume of 19 μl and the mixture incubated at 42°C for two minutes. Then 1 μl (200 units) of SUPERSCRIPT II reverse transcriptase was added for a total volume of 20 μl. The enzyme was only added to one of the two divided samples while the remaining sample served as a negative control for the PCR reaction. The samples were incubated for another 50 minutes at 42°C and then for 15 minutes at 70°C to inactivate the enzyme.

2.3.2 PCR Cloning

PCR cloning was done as in section 2.2.2 with the following differences. Primers were designed, based on the genomic sequence, to amplify the full coding region. They

anneal just upstream of the translation start site and just downstream of the stop codon (Forward: 5'-CTGTGTTACATTCGCCTCC-3', Reverse:5'-GCAACCTGTGCTCTTTC-TG-3'). These were used with 10% of the above cDNA as template. Negative controls for the PCR attempts used 10% of the control reverse transcription reactions as template. Positive controls were reactions with 100 ng of zebrafish genomic DNA as template.

2.3.3 Sequencing and Structural Analysis

Both strands of the cDNA clone were fully sequenced as in 2.2.7. The resulting, assembled sequence was then compared with the genomic sequence to verify intron-exon boundaries. The cDNA sequence was subjected to the same software-based structural analyses as the genomic sequence for corroboration.

2.4 Electrophysiology

This section was done in collaboration with T.W. White at SUNY, Stony Brook. The portion I did at the University of Manitoba, the cloning and transcription tests, will be described here.

2.4.1 Expression Cloning

PCR was done with brain cDNA as template and the same primers as in 2.3.2, however, this time a proofreading polymerase Pwo (Roche, Laval, QC) was used with the following PCR thermocycler program: 94°C, 2 minutes; 94°C, 15 seconds (denature); 60°C, 30 seconds (anneal); 72°C, 1 minute (extend); repeat last three steps 14X; 94°C, 15

seconds; 60°C, 30 seconds; 72°C, 1 minute + 5 seconds/cycle; repeat last three steps 19X; extend at 72°C, 7 minutes. PCR cloning was done as in 2.3.2 and minipreps were made from overnight cultures of Cx35.1-positive clones in the pCR® 2.1 vector.

The insert was then subcloned into an expression vector, pCS2+ (Turner and Weintraub, 1994) that contains the SP6 promotor for RNA transcription. The pCR® 2.1 plasmid was digested with EcoR I to release the insert, and at the same time, pCS2+ was cut with EcoR I. The pCS2+ digestion was phenol-chloroform extracted to remove the restriction enzyme and buffer and treated with alkaline phosphatase as in 2.2.6. The pCR® 2.1 digestion was separated by electrophoresis on a 1% TAE agarose gel. The band corresponding to the insert was cut out of the gel and purified from it with GENECLEAN SPIN Kit (BIO101®, Quantum Biotechnologies, Carlsbad, CA). The gel fragment was melted and suspended with a solution containing silica beads to bind the DNA. The solution was centrifuged through a filter, which binds the silica beads. The filter was then washed with buffer to remove the agarose, and the purified DNA was eluted with a low-salt buffer, which disrupts its binding to the silica. Ligation and transformation were done as in 2.2.6. Since the pCS2+ vector does not allow colour selection, minipreps were isolated and screened by restriction enzyme digestion to verify both insert presence and orientation. The insert was also sequenced to verify that it did not include any base pair mutations.

2.4.2 Transcription Verification

To transcribe the sense strand, five to 10 μg of miniprep DNA with the insert in the 5'-3' orientation were linearized with the restriction enzyme Not I. The sample was

then phenol:chloroform extracted to remove the restriction enzyme and buffer. One microgram of the DNA was used for *in vitro* transcription following the mMessage mMachine™ protocol (Ambion, Austin, TX). This kit includes a cap analog to allow transcription of capped RNAs, which are ideal for oocyte microinjection and *in vitro* translation. The reaction was carried out with SP6 polymerase at 37°C for two hours. To verify transcription of the approximately 1 kb fragment, a portion of the reaction was separated by electrophoresis on a 1% agarose-formaldehyde gel (1% agarose, 1X MOPS/EDTA buffer, 1.1% formaldehyde).

Once the sequence of the construct and its ability to be transcribed successfully were verified, 10 μg of the original miniprep was dried down by spinning for 30 minutes in a speedvac. This was then shipped to T.W. White and he tested the ability of Cx35.1 to form intercellular channels, and assessed the channels' conductance and voltage gating properties in the well-characterized paired *Xenopus* oocyte expression system (see Cason *et al.*, 2001 for a description of similar electrophysiology work by T.W. White). Generally, single oocytes are injected with zebrafish Cx35.1-specific mRNA and cell-cell channels form upon pairing of two oocytes. Intercellular communication is measured by double voltage clamp recordings to assess the junctional currents and voltage gating (Spray *et al.*, 1981).

2.5 mRNA Expression Analysis

2.5.1 Northern Analysis

2.5.1.1 Poly A+ RNA Isolation and Blot Preparation

Northern analysis of mRNA expression was initially attempted with total RNA, but these attempts failed, presumably due to the low level of Cx35.1 message. Instead, to reduce the amount of tRNA and rRNA and enrich for mRNA, poly A+ RNA was isolated. Total RNA was isolated as in 2.3.1 from adult brain, eye (lens removed), liver and ovary, and embryonic stages d0 (Day 0: the day the embryos were fertilized), d1, d2, d3, d4, and d5. All tissues were flash frozen in microcentrifuge tubes by immersion in a dry ice and methanol bath.

Poly A+ RNA was purified from the total RNA using the Oligotex mRNA Spin-Column Kit (QIAGEN). Briefly, 100-200 μg of total RNA was heated to denature any secondary structure and hybridized with Oligotex Suspension containing polystyrene-latex particles covalently linked to oligodT. Polyadenylated mRNA molecules bind the Oligotex via their polyA+ tail and are pelleted by centrifugation. Since tRNA and rRNA are not polyadenylated, they do not bind to the Oligotex and are subsequently washed away with buffer. The dT:A bond is only stable in high-salt conditions, so the mRNA was eluted from the particles with low-salt buffer. Two micrograms of each sample was precipitated with glycogen and NaOAc in absolute ethanol. The RNA samples, as well as an RNA ladder (Invitrogen), were denatured at 65°C for five minutes. They were then separated by electrophoresis, with 1X RNA loading buffer, on a 1.0% agarose-formaldehyde gel for approximately four hours at 100 V. The gel was rinsed in 10X SSC

and then blotted by capillary transfer overnight to a MAGNACHARGE nylon membrane (Osmonics, Minnetonka, MN) using 10X SSC as transfer buffer. The blot was rinsed in 2X SSC at 65°C for five minutes, then air-dried and UV-irradiated.

In total, three blots were produced. PolyA+1 had only d4, d5, adult brain and adult eye samples on it. PolyA+2 had d0-d5 and adult brain, eye, liver and ovary samples on it. PolyA+3 had d0-d3, and adult brain, liver and ovary samples on it. The total RNA samples were independently isolated for each of the blots, except for the adult liver and ovary samples. For the adult liver and ovary samples, the polyA+ RNA for the two blots was isolated separately, but they were both derived from the same initial total RNA sample.

2.5.1.2 Zebrafish Cx35.1 Probe Synthesis and Hybridization

Each blot was hybridized with an anti-Cx35.1 riboprobe for increased sensitivity. The template for the probe transcription was the construct from 2.4.1. The template plasmid was digested with the restriction enzyme BamH I. This restriction enzyme cuts the insert approximately 87 bp from its 5' end, in addition to a site in the vector 13 bp beyond the 5' end of the insert. Therefore a 100 bp fragment is removed. The linearized plasmid was not purified from the 100 bp band, as such a small fragment was unlikely to hinder *in vitro* transcription. The reaction was phenol-chloroform extracted to remove the restriction enzyme and buffer.

In vitro transcription was set up as follows: 1.0 μg DNA, 0.5 mM dNTPs (A,C,G), 1X transcription buffer (25 mM Tris-HCl, 375 mM KCl, 15 mM $MgCl_2$), 20 units RNaseOUT (Invitrogen), 5.0 μl ^{32}P-dUTP (NEN^{TM}), 0.01 M DTT, 50 units of T7

RNA polymerase (Invitrogen), and ddH_2O to give a total volume of 20 µl. The reaction was left at 37°C for 30 minutes and then treated with RQ1 DNase (Invitrogen) for 15 minutes at 37°C. The probe was then purified through a mini Quick Spin™ RNA Column (Boehringer Mannheim). Scintillation counting assessed success of the radiolabeling. The probe was heat-denatured at 65°C for five minutes and used at a concentration of three to five million cpm per ml of hybridization solution.

Hybridization was done as in 2.2.4 with the following differences. Prehybridization of the membrane was for two hours at 55°C with hybridization solution 2. Hybridization was overnight at 55°C and the membrane was washed three times for 30 minutes with 0.1% SDS/0.1X SSC at 68°C. The membrane was then subjected to autoradiography.

2.5.1.3 eF-1α Probe Synthesis and Hybridization

Subsequent to the above probing, all Northern blots were hybridized with a zebrafish elongation factor 1α (eF-1α) probe. This gene is ubiquitously expressed throughout development and adult tissues and, therefore, can be used in Northern analysis to assess RNA integrity for all samples on the blot (Essner *et al.*, 1996). It was linearized with EcoR I and phenol-chloroform extracted by Gunnar Valdimarsson. *In vitro* transcription and hybridization were done as in 4.3.1.2. except T3 polymerase (Invitrogen) was used.

2.5.2 RT-PCR

RT-PCR was performed to confirm the Northern analysis results as well as to

narrow down the time at which expression begins. RNA was isolated and cDNA prepared as in 2.3.1 from zebrafish embryonic stages d0 through d5 for one experiment and a series of embryonic stages four to eight hours apart from 24 hpf-72 hpf for another experiment. The cDNA was used as template for PCR as in 2.2.2 with a forward primer (5'-GAGGGCATTCTCCAGGTTTTAC-3') that anneals in the second exon and a reverse primer (5'-TCACTTACGGTGCTCAGC-3') that anneals in the 3' UTR. The product was an approximately 1.2 kb fragment. In order to assess the equality of the cDNA template amounts in each sample, PCR reactions designed to amplify eF-1α cDNA were set up concurrently with the above ones. The product of this reaction was an approximately 550 bp fragment.

To verify that the product was indeed Cx35.1, 20% of the PCR reactions were separated by electrophoresis on a 1.0% agarose TBE gel and then processed and blotted to a 0.45 μm MAGNACHARGE nylon membrane (OSMONICS) following Sambrook *et al.*, 1989. This was only performed for the PCR samples that were amplified with the Cx35.1 primers and not the eF-1α control reactions. The gel was soaked in 0.25 M HCl for 15 minutes to fragment the DNA, then in 1 M NaCl/0.5 M NaOH for 30 minutes to denature the DNA. It was neutralized by soaking in 0.5 M Tris-HCl, pH 8.0/0.5 M NaCl for 30 minutes. The gel was then blotted by capillary transfer to a membrane overnight using 10X SSC as transfer buffer. The following day, the membrane was air-dried and UV-irradiated to bind the DNA to the membrane. The membrane was hybridized with a DNA probe prepared as in 2.2.3. Prehybridization of the membrane was for two hours at 42°C with hybridization solution 2. Hybridization, in solution 2, was overnight at 42°C and the membrane was washed three times for 30 minutes with 0.1% SDS/0.1X SSC at

55°C. The membrane was then subjected to autoradiography.

2.6 Protein Expression Analysis

In order to reveal Cx35.1 expression in the zebrafish retina immunohistochemistry was employed. Freshly dissected adult zebrafish eyes and d2, d3, d4, and d5 embryos were fixed by immersion for 15-30 minutes in Real Lana's fixative (4% paraformaldehyde, 0.17% picric acid, 0.05 M PO_4 buffer, pH 7.1). The tissue was then infiltrated with two changes of 10% sucrose/0.04% sodium azide and stored at 4°C overnight. The tissue was then embedded in blocks of 5% acrylamide. The embryos were embedded in pairs. The blocks were infiltrated overnight in 1:1 10% sucrose solution:OCT embedding medium (Mirivac Limited, Halifax, NS) at 4°C. They were then infiltrated overnight at 4°C in OCT alone. The blocks were positioned in tinfoil moulds with a drop of OCT and snap-frozen in liquid nitrogen. The tissue was stored at –80°C until sectioned. For sectioning, the blocks were adhered to the chuck with OCT and sectioned on a Damon-IEC Division Minotome cryostat. All sections were 10 μm thick. The sections were attached to Superfrost®/Plus (Fisher Scientific, Nepean, ON) microscope slides and stored at –80°C.

For antibody staining, sections were outlined on the slide with a hydrophobic pen and all solutions were placed directly onto the slide. Slides were brought to room temperature and rinsed in PBS, pH 7.4 (phosphate buffered saline: 140 mM NaCl, 2.7 mM KCl, 4 mM Na_2HPO_4, 1.8 mM KH_2PO_4) three times for 10 minutes each at room temperature. They were then incubated with blocking solution (3% skim milk powder,

0.03% Triton-X 100 in PBS (PBS-T), pH 7.4) for one hour at room temperature. The sections were then incubated in primary antibody, appropriately diluted in blocking solution, at 4°C overnight in a humidity chamber. Control sections were incubated without primary antibody. The following day, the sections were washed three times for 10 minutes each in PBS-T at room temperature before incubation with secondary antibody diluted 1:500 in blocking solution for one hour at room temperature. The sections were washed two times in PBS-T for 10 minutes at room temperature. The second wash included Hoechst (0.5 μg/ml). They were then washed twice for five minutes each in PBS before they were mounted in Prolong antifade solution (Molecular Probes, Eugene, OR). Staining was detected with UV light using a Zeiss Axioskop FS microscope and the appropriate filter set. Images were captured with a Sony DXC-950 CCD video camera and Northern Eclipse imaging software (Empix, Mississauga, ON).

Several antibody combinations were used. Four different primary antibodies were tested. All antibodies are affinity-purified polyclonals. Ab51-6300 is directed against mouse Cx36 in the carboxy tail region (Zymed Laboratories Inc., South San Fransisco, CA). The zebrafish sequence in this region matches 88%. It was tested at dilutions ranging from 1:500 to 1:50. Antibody 298 (Ab298) is directed against mouse Cx36 in the region from amino acid 298-318 (Rash *et al.*, 2000) and the corresponding zebrafish sequence matches 90%. It was used at a dilution of 1:500. Antibody C is directed against a different region in the carboxy tail of the mouse Cx36 sequence and the zebrafish sequence matches 100% in this region. It was used at a dilution of 1:100. Anti-perch Cx35 targets a region 76 amino acid long in the cytoplasmic loop of perch Cx35 and the corresponding zebrafish sequence matches 82%. It was used at a dilution of 1:20.

Each of these primary antibodies was used with either Alexa 488 or Alexa 546 (Molecular Probes) secondary antibodies and fluorescein or rhodamine filter sets, respectively.

CHAPTER 3: RESULTS

3.1 Cloning of zebrafish Cx35.1

Ten positive signals, representing five positive clones, were detected on the zebrafish genomic DNA PAC library filters. The corresponding clones were ordered from RZPD and rescreened because the clone is picked from a microtiter plate rather than a single colony, and it is possible that there are contaminating clones in the microtiter plate well. A sample of the clone was diluted and grown on agar plates and the resulting individual clones, 10 to 75 for each original clone received, were hybridized with the same probe initially used to screen the library. Four of the five clones received were 100% positive while the fifth was only 17% positive. PAC DNA was isolated from two individual positive clones using two independent methods, as the first method attempted was laborious and inconvenient. PAC DNA has a low yield and can be relatively impure after its isolation so, in order to sequence the clones, they had to be subcloned and cultured in conventional plasmid vectors. The subclones were screened and a positive subclone from each original clone was sequenced. The subclones were both approximately 6 kb in length. For the first subclone, sequencing was initiated from the vector on both sides. However, once the coding sequence was located, only that portion of the subclone, including the intron, was sequenced on both strands. The same primers used to sequence the gene from the first subclone were then used to sequence the coding region in the second subclone, rather than sequencing in from the vector, to save time. Approximately 4.3 kb of consensus sequence was obtained from the two subclones.

The sequence revealed a single open reading frame, interrupted 71 bp after the

translation start site by a 1953 bp intron, which comprises a coding region of 912 bp (Fig. 4). The sequence translates into a 304 amino acid protein (Fig. 5). The protein sequence shows all the characteristic connexin features, including four putative hydrophobic transmembrane regions (Fig. 6, 7) and the three conserved cysteines in each extracellular loop (Fig. 7). The predicted molecular weight of the protein is 35,059 Daltons (35.1 kD), therefore, the putative connexin will be named zebrafish Cx35.1.

Eleven potential phosphorylation sites were identified by ScanProsite (http://ca.expasy.org/tools/scanprosite/) in the Cx35.1 cytoplasmic loop and carboxy tail, and four of these are conserved in all the Cx35/36 amino acid sequences (Fig. 7). There is one potential protein kinase C phosphorylation site (consensus: S/T-x-R/K) at serine 101 (**S**aK). There is one potential tyrosine phosphorylation site (consensus: R/K-xx-D/E-xxx-Y or R/K-xxx-D/E-xx-Y) at tyrosine 109 (KqkErr**Y**). There is one potential cAMP and cGMP-dependent protein kinase site (consensus: R/K(2)-x-S/T) at serine 276 (RRk**S**) and there is also a potential casein kinase II phosphorylation site (consensus: S/T-xx-D/E) at serine 276 (**S**iyE). Two of these potential sites had been previously identified in the skate (O'Brien *et al.*, 1996) but were not experimentally examined. Recently, Zoidl *et al.*, (2002) identified various potential phosphorylation sites in mouse Cx36 and tested their function in the regulation of transport to the cell surface. Using site-directed mutagenesis they induced point mutations at potential phosphorylation sites, including serine 293 (S293A) in mouse Cx36, which is equivalent to the serine 276 in zebrafish Cx35.1. However, the mutagenesis did not alter the Cx subcellular localization, indicating no role for phosphorylation at this site in the transport regulation mechanism. The equivalent positions to serine 101 and tyrosine 109 in zebrafish Cx35.1 were not

Figure 4: The consensus zebrafish Cx35.1 sequence (4.3 kb) derived from PAC clones. The bold lettering depicts the coding region (912 bp total), while the translation start sequence and the translation stop sequence are italicized. The lettering in between the two sections of coding region represents the 1953 bp intron that interrupts after the first 71 bp of coding sequence. The upstream and downstream non-coding sequences are in regular lettering at the start and the end of the sequence, respectively.

ZfCx35.1

CCGTTTGACTCCTTTCTTTCATTTCAGGGGGTTTAAGCCTTAATTACCCCCCATGATTTGCGCCTTGTTTGCTATCGC
GCGCCCACCCAAACGCTAAACTCTAATCTGCTTCCTGTCTCGCTTATGGGTGTGTGTTGCAAACATCCCCGGCGATTT
GACTTGATCGCCAATGATTTTATTACGGATTAATCAGCGCATCTCTGGCATATTCGGGGAATAATGAAACGGAGAAAT
CCTGCTGTTCTGATTTCTCTCCAACAACCTGTGTGCGCGTGACGCAAGGGGAGGAGGGAGCCAGAGTCTACTTAAAGC
GGGATTAGCACGAGCCAAACATTACACTCCCCTCCGTTTAGACTCAGAGCGACCTGTCGTCCTGCGCGCGAGACAGAA
AATAGGAGGGCTTTAGACTAATCAGGACTTCAGACGAGCGCGCGCTCCGGAGCGAGGCGTGGACGGCAAGGTGGACAG
CAGCGACTAAATCAATGCATTCGCCCGACACTACGCTCGCCTTCAGACGCGAAACAGTTGCTCGCATTTGATTTCACA
CGGTTCTCTGTGTTACATTCGCCTCCGAATGAACAGCC***ATG***GGGGAATGGACAATTCTCGAGCGTCTCCTGGAG
GCGGCTGTCCAACAGCACTCTACTATGATTGGGAGGTGAGGGGAAAAAGTGTTGTGGAAAATGTTTATTGATAA
AGTAGTACATTAAACAAAACACTGAGGTCATTACGCATTGACCCTTCTGACTAAGGGCGATTGGCTTCTGGAGCCTAA
TGTGTGCTTTGCACAGGAGACGAAAGTGTTCGACGATTTAAGTTAACGCGTTTGTTGTTGCTGTTTGAACATTTAAAA
AAAAAAACAAAGAGGTTATGGTTTGTCTGGTTTGAGCCATCTGTAAGATTGCTGTTTTATGTCAGATCTGGTTTGCTT
TCAAAGAAATGCCGTGCGCGCACTGTCTGGAAGCGCGCGTTTGACTGTAGAGAGAGTTTCAGCACTGGACAGCTCCCC
GCGTCAGGCTGCAATCTCCAACGCACAAACGTTAAGAGTTAAAATGTGTATCGATTAGCTGTAAGTTATTAGTTTATT
TATATTATTAGCTATATTATATTTTACTGTGAAATACATATTGAGTTATATGTTGTATAAATCAACAGTAATTTAATT
ATAATATAGATAATATAATTATTAAAGTAAAAAATAACTCTTAAGTCACCTTTTAATTCACTTTCAAAATAGTTATCA
AACCTTGAAAAGTCACATTTCATTGCGTTTATTTCATTAATTCGTTATTTTAACGTGTCAACATATCAGAAAATATTC
ACGTTGAATATAATGTATGTTTTTGAGTGATGAATGACTGGTGCGTGCTGTTATATTGATTTGATTATTCGGTTGTAT
TAAAGCCACCTCATAAATTATGTTGAAAAATCCCAGACATTCTCAGATATTACACATCTCATTTGCTTATATTTGATT
AAAATACAGTGCTCAGCATAAATGTCTACACCCCATTTGATAATTAAAAATTTTACTAATTCTCAGTAAATATGGGTA
TATATACTGGTGCATTTGAACAAAACCGATTTATTACACAGATATATTTTTATTAAAATAATATTGTAGTCACAAAAT
ATCTTTTGAAATAGAAAGATAATACAATTAAATTTAAGCAAAAGTTACAAAATTTTATATATATTTTTTGTTTCTCTT
GATTTTTGCTATTTTTGAAAATTATATTTAACAATTTTCCCTACAAATACATTTGGGCTACTCATTTTTAAACCATTA
TATTGTGTTAGATGAGCTCTTCAATGCTGACTGATCTAATGTATATGCACACATATAATATTGTAAAGCATCTTATAG
AAAATATTAATTTAAATGAATGATCTGGTTGGGGTGGCTGACAGAGCACTGTACATAACTTTCTTTAATTTTTAACCT
AATGTGACATGTACATTCACAAGTGTTTAATTATGCATTTTATGTACATTAATGACTTCACTTTGCACAATTTCAGTG
CCGTGTGTATTTTGATAGTGTTTTACAAGTGTAAACATACACTATAATATTCATCGCACACTTATATTTTGTACACAT
GTATTGCTTATGACTTTAGGAGTGTCAGATTATATGAAATTCAATTCATCATGAGCTCTCCTGTTTCAAAAAGTGTAT
TATGTGTCAGCACACTGCATGGCAGTCACTGGAATAATAATGTTCCCAGATAACAGAATGGACCATTAACATTATATT
TGTTCATGTAATAGACTTATGACTTGCAATCCCATGAAGCCTAATATATGTTACTATGTTTTATTAATGTATCCCTAG
CAAACACAGCCACCTGATTTTAACAGGTTTAGAGCTGATCTATTTTGTGTTCTTCAAAGAACCATTTGTACAGAACAT
TTTGTAGTCTAATAGAATGCTTTTGCTACATTAAAACAACAAAATTAAATCTAATACAAAGGTTTTTTTATGGACCAT
TAATGACAAATAATAATAATAATAATAATTAATAGTGAAGTGTTTAATCTTTCATTTATAGTCTTGATTTACTGGAGC
AGATGTTCTTTGAGCTTAAAATGTTCCTTTCCTCTCCTGTAG**GATCCTGCTAACTGTTGTGGTGATCTTCCGGA**
TTCTAATTGTGGCGATTGTTGGAGAGACCGTGTACGACGACGAGCAGTCAATGTTTGTGTGTAACACTCT
GCAGCCAGGCTGTAACCAAGCTTGCTATGACAAAGCGTTCCCTATATCTCACATCAGATACTGGGTTTTC
CAGATCATCATGGTTTGCACACCCAGTCTCTGCTTCATCACATACTCTGTGCATCAGTCGGCCAAACAGA
AGGAGCGGAGGTATTCTACCATCTACCTGTCCCTCGACAAAGACCCCGATACGATGAGGCGAGACGACAG
CAAAAAGATCAAAAACACCATTGTGAACGGAGTACTTCAAAACACGGAGAACTCCACCAAAGAGTCCGAG
CCTGACTGTCTAGAGGTCAAAGAGATCCCCAATTCAGCCATGAGAACTACCAAATCTAAAATGAGAAGAC
AAGAGGGCATCTCCAGGTTTTACATCATTCAGGTGGTGTTCAGAAACGCGTTGGAAATTGGCTTCCTGGT
GGGCCAGTATTTCTTGTACGGATTCAACGTGCCCGCCGTGTACGAGTGCGACCGCTATCCTTGCATCAAA
GACGTCGAATGCTATGTATCAAGACCTACAGAGAAAACTGTGTTCCTCGTCTTCATGTTTGCTGTCAGTG
GGATTTGCGTAGTGCTCAACCTGGCTGAACTCAATCACCTGGGCTGGAGGAAAATTAAAACAGCGGTGAG
GGGGGTTCAGGCCAGGAGGAAGTCCATCTATGAGATCAGAAACAAGGACTTACCGAGGATGAGCATGCCG
AATTTCGGAAGAACCCAGTCCAGTGACTCTGCCTACGTT*TAA*TGCTTTCTTCGTGTAGATTATTAGAGTGGTG
GTCCTCAATTCTGGTTCAGAAAGAGCACAGGTTGCACATTTTGGATATGTTCACCCCACCTTATGTAGCTTATTCTGC
AATACGGAAGTAAGCCTTTTTTTGTGATTGTTTTGGAACTTCCGATTCATTTGCTATATGGGAAATGACTAGGAACAA
TAAACAACAGTAAATGATCACAATACTTGCTCTACAAGCAATGTTTAAACAAAATGTTTAAAAAAAAAATTAATAAGA
AAATAGTTTGCAAACATCAAGTTTGCAACATCAAGTAGCATAATAAGCTATTTTCTATGGCTAAAAACAATGGAAGTG
AATAGGACTGGAAGTCTCGTGCCTATAAGGTTCTAATGGCTGGGCCCACATTTACAGCGCTCAGCATAATTAAGTACA
CCTTTATTAAGTTTCTTCTATTAAGCACCTCTACTATTATTAAGTACACTTCATTTTAGAAAATGAATATTTGTATCC
ATTTCTCAGTGAATATAGGCAATGTATTTTGATGCATTTAAACAAAACAGATTTATTAAACAGACATATTTATTAAAA
TATTTTTTCAGTCACCAAACATATTAGAAATTGAATGATAAAACAATTCAGATAAAATATTGCAAAAATAACTTACAA
CCTACAAAATTTGTACATTTTTTTGCTGCTCTTGATTTTTCCTCCTTGATTTTGACTGTTATCGTAGGTTATTGTGAT
AGATTGGCTCCAGATTTAGCTTCAGTATTGACTAATCTAATGTATATGCACAAATGTAATATTGTAAAATTTGATTTA
AATTTTATTTTATATTAATTTAAAAGATAGATTTGGAGGGGTA

Figure 5: Nucleotide and corresponding amino acid sequence of the Cx35.1 coding region. The coding region is 912 bp in length, which translates to 304 amino acids. The predicted molecular weight of the protein is 35.1 kD and so it is named zebrafish Cx35.1. Amino acid codes are found in Appendix B.

```
  1 ATGGGGGAATGGACAATTCTCGAGCGTCTCCTGGAGGCGGCTGTCCAACAGCACTCTACT  60
  0  M  G  E  W  T  I  L  E  R  L  L  E  A  A  V  Q  Q  H  S  T   20

 61 ATGATTGGGAGGATCCTGCTAACTGTTGTGGTGATCTTCCGGATTCTAATTGTGGCGATT 120
 20  M  I  G  R  I  L  L  T  V  V  V  I  F  R  I  L  I  V  A  I   40

121 GTTGGAGAGACCGTGTACGACGACGAGCAGTCAATGTTTGTGTGTAACACTCTGCAGCCA 180
 40  V  G  E  T  V  Y  D  D  E  Q  S  M  F  V  C  N  T  L  Q  P   60

181 GGCTGTAACCAAGCTTGCTATGACAAAGCGTTCCCTATATCTCACATCAGATACTGGGTT 240
 60  G  C  N  Q  A  C  Y  D  K  A  F  P  I  S  H  I  R  Y  W  V   80

241 TTCCAGATCATCATGGTTTGCACACCCAGTCTCTGCTTCATCACATACTCTGTGCATCAG 300
 80  F  Q  I  I  M  V  C  T  P  S  L  C  F  I  T  Y  S  V  H  Q  100

301 TCGGCCAAACAGAAGGAGCGGAGGTATTCTACCATCTACCTGTCCCTCGACAAAGACCCC 360
100  S  A  K  Q  K  E  R  R  Y  S  T  I  Y  L  S  L  D  K  D  P  120

361 GATACGATGAGGCGAGACGACAGCAAAAAGATCAAAAACACCATTGTGAACGGAGTACTT 420
120  D  T  M  R  R  D  D  S  K  K  I  K  N  T  I  V  N  G  V  L  140

421 CAAAACACGGAGAACTCCACCAAAGAGTCCGAGCCTGACTGTCTAGAGGTCAAAGAGATC 480
140  Q  N  T  E  N  S  T  K  E  S  E  P  D  C  L  E  V  K  E  I  160

481 CCCAATTCAGCCATGAGAACTACCAAATCTAAAATGAGAAGACAAGAGGGCATCTCCAGG 540
160  P  N  S  A  M  R  T  T  K  S  K  M  R  R  Q  E  G  I  S  R  180

541 TTTTACATCATTCAGGTGGTGTTCAGAAACGCGTTGGAAATTGGCTTCCTGGTGGGCCAG 600
180  F  Y  I  I  Q  V  V  F  R  N  A  L  E  I  G  F  L  V  G  Q  200

601 TATTTCTTGTACGGATTCAACGTGCCCGCCGTGTACGAGTGCGACCGCTATCCTTGCATC 660
200  Y  F  L  Y  G  F  N  V  P  A  V  Y  E  C  D  R  Y  P  C  I  220

661 AAAGACGTCGAATGCTATGTATCAAGACCTACAGAGAAAACTGTGTTCCTCGTCTTCATG 720
220  K  D  V  E  C  Y  V  S  R  P  T  E  K  T  V  F  L  V  F  M  240

721 TTTGCTGTCAGTGGGATTTGCGTAGTGCTCAACCTGGCTGAACTCAATCACCTGGGCTGG 780
240  F  A  V  S  G  I  C  V  V  L  N  L  A  E  L  N  H  L  G  W  260

781 AGGAAAATTAAAACAGCGGTGAGGGGGGTTCAGGCCAGGAGGAAGTCCATCTATGAGATC 840
260  R  K  I  K  T  A  V  R  G  V  Q  A  R  R  K  S  I  Y  E  I  280

841 AGAAACAAGGACTTACCGAGGATGAGCATGCCGAATTTCGGAAGAACCCAGTCCAGTGAC 900
280  R  N  K  D  L  P  R  M  S  M  P  N  F  G  R  T  Q  S  S  D  300

901 TCTGCCTACGTT                                                  912
300  S  A  Y  V                                                    304
```

Figure 6: A predicted hydrophobicity plot for the Cx35.1 amino acid sequence generated using the TMpred tool from Swiss EMBnet (www.ch.embnet.org/index.html). It shows four highly hydrophobic areas presumably corresponding to the transmembrane domains one through four starting from the left. The remainder of the protein sequence is hydrophilic. The score is on the Y axis, and a score above 0 is considered the hydrophobic range and below 0 is the hydrophilic range. The amino acid position within the protein is depicted on the X axis.

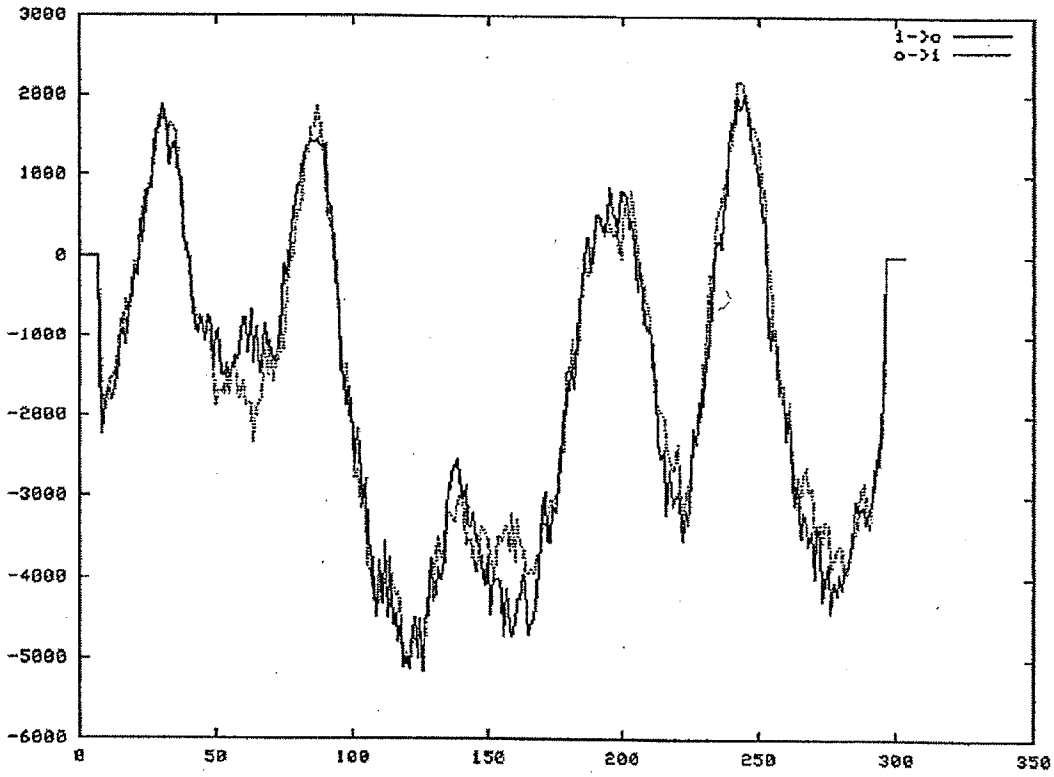

3000
2000
1000
0
-1000
-2000
-3000
-4000
-5000
-6000
0
50
100
150
200
250
300
350
1->0
0->1

Figure 7: Alignment of the zebrafish Cx35.1 amino acid sequence with the Cx35/36 orthologue sequences using Clustal X (Thompson *et al.*, 1997). Amino acid identity between all sequences is designated with (*) and similarity between the amino acids is shown by (:). The four predicted transmembrane segments (TM1-TM4) are designated with a line over them and the conserved cysteines are marked with (+). Potential phosphorylation sites are designated with a (o) above them. The amino acid sequence is highly conserved with the most divergence occurring in the cytoplasmic loop between the second and third transmembrane segments. Amino acid codes are found in Appendix B.

```
pCx35       MGEWTILERLLEAAVQQHSTMIGRILLTVVVIFRILIVAIVGETVYDDEQTMFVCNTLQP
zfCx35.1    MGEWTILERLLEAAVQQHSTMIGRILLTVVVIFRILIVAIVGETVYDDEQSMFVCNTLQP
chCx36      MGEWTILERLLEAAVQQHSTMIGRILLTVVVIFRILIVAIVGETVYDDEQTMFVCNTLQP
mCx36       MGEWTILERLLEAAVQQHSTMIGRILLTVVVIFRILIVAIVGETVYDDEQTMFVCNTLQP
huCx36      MGEWTILERLLEAAVQQHSTMIGRILLTVVVIFRILIVAIVGETVYDDEQTMFVCNTLQP
skCx35      MGEWTILERLLEAAVQQHSTMIGRILLTVVVIFRILVVAIVGETVYDDEQTMFVCNTLQP
            ************************************:************:*********

pCx35       GCNQACYDKAFPISHIRYWVFQIIMVCTPSLCFITYSVHQSAKQKERRYSTVYLTLDKDQ
zfCx35.1    GCNQACYDKAFPISHIRYWVFQIIMVCTPSLCFITYSVHQSAKQKERRYSTIYLSLDKDP
chCx36      GCNQACYDQAFPISHIRYWVFQIIMVCTPSLCFITYSVHQSAKQRERRYSTVFLTLERDQ
mCx36       GCNQACYDRAFPISHVRYWVFQIIMVCTPSLCFITYSVHQSAKQRERRYSTVFLALDRDP
huCx36      GCNQACYDRAFPISHIRYWVFQIIMVCTPSLCFITYSVHQSAKQRERRYSTVFLALDRDP
skCx35      GCNQACYDKAFPISHIRYWVFQIIMVCTPSLCFITYSVHQSSKQRERQYSTVFITLDKDK
            ********:******:*************************:**:**:***::::*::*

pCx35       -DSLK--------------RDESKKIKNTIVNGVLQNTENSTKEAEPDCLEVKEIP--NS
zfCx35.1    -DTMR--------------RDDSKKIKNTIVNGVLQNTENSTKESEPDCLEVKEIP--NS
chCx36      -DSMK--------------REDSKKIKNTIVNGVLQNTENSTKEAEPDCLEVKEIP--NP
mCx36       AESIGGPGGTGGGGSGGSKRED-KKLQNAMVNGVLQNTETTSKETEPDCLEVKEIP--NP
huCx36      PESIGGPGGTGGGGSGGGKRED-KKLQNAIVNGVLQNTENTSKETEPDCLEVKELTPHPS
skCx35      ----K--------------RED-NKIKNTTVNGVLQNSEFFTKEMQSDFLEVKEMQ--NS
                              *:: :*::*: *******:*  :** :.* *****:    .

pCx35       AMRTT-KSKMRRQEGISRFYIIQVVFRNALEIGFLVGQYFLYGFNVPSVYECDRYPCIKD
zfCx35.1    AMRTT-KSKMRRQEGISRFYIIQVVFRNALEIGFLVGQYFLYGFNVPAVYECDRYPCIKD
chCx36      AIRTT-KSKMRRQEGISRFYIIQVVFRNALEIGFLVGQYFLYGFNVPAVYECDRYPCIKD
mCx36       GLRTAARSKLRRQEGISRFYIIQVVFRNALEIGFLVGQYFLYGFNVPSMYECDRYPCIKE
huCx36      GLRTASKSKLRRQEGISRFYIIQVVFRNALEIGFLVGQYFLYGFSVPGLYECNRYPCIKE
skCx35      AARNSKMSKIRRQEGISRFYIIQVVFRNALEIGFLMGQYFLYGFKVPSMYECNRYPCVKM
            . *.:  **:*************************:********.**.:***:****:*

pCx35       VECYVSRPTEKTVFLVFMFAVSGFCVVLNLAELNHLGWRKIKTAVRGVQARRKSIYEIRN
zfCx35.1    VECYVSRPTEKTVFLVFMFAVSGICVVLNLAELNHLGWRKIKTAVRGVQARRKSIYEIRN
chCx36      VECYVSRPTEKTVFLVFMFAVSGICVVLNLAELNHLGWRKIKTAVRGVQARRKSIYEIRN
mCx36       VECYVSRPTEKTVFLVFMFAVSGICVVLNLAELNHLGWRKIKMAVRGVQAKRKSIYEIRN
huCx36      VECYVSRPTEKTVFLVFMFAVSGICVVLNLAELNHLGWRKIKLAVRGAQAKRKSVYEIRN
skCx35      VECYVSRPTEKTVFLVFMFAVSGICVVLNLAELNHLGWRKIKLAVRGAQAKRKSIYEIRN
            VECYVSRPTEKTVFLVFMFAVSGLCVILNLAELNHLGWRKIKTAVRGAQERRKSIYEIRN
            ************************:**:*************** ****.* :***:*****

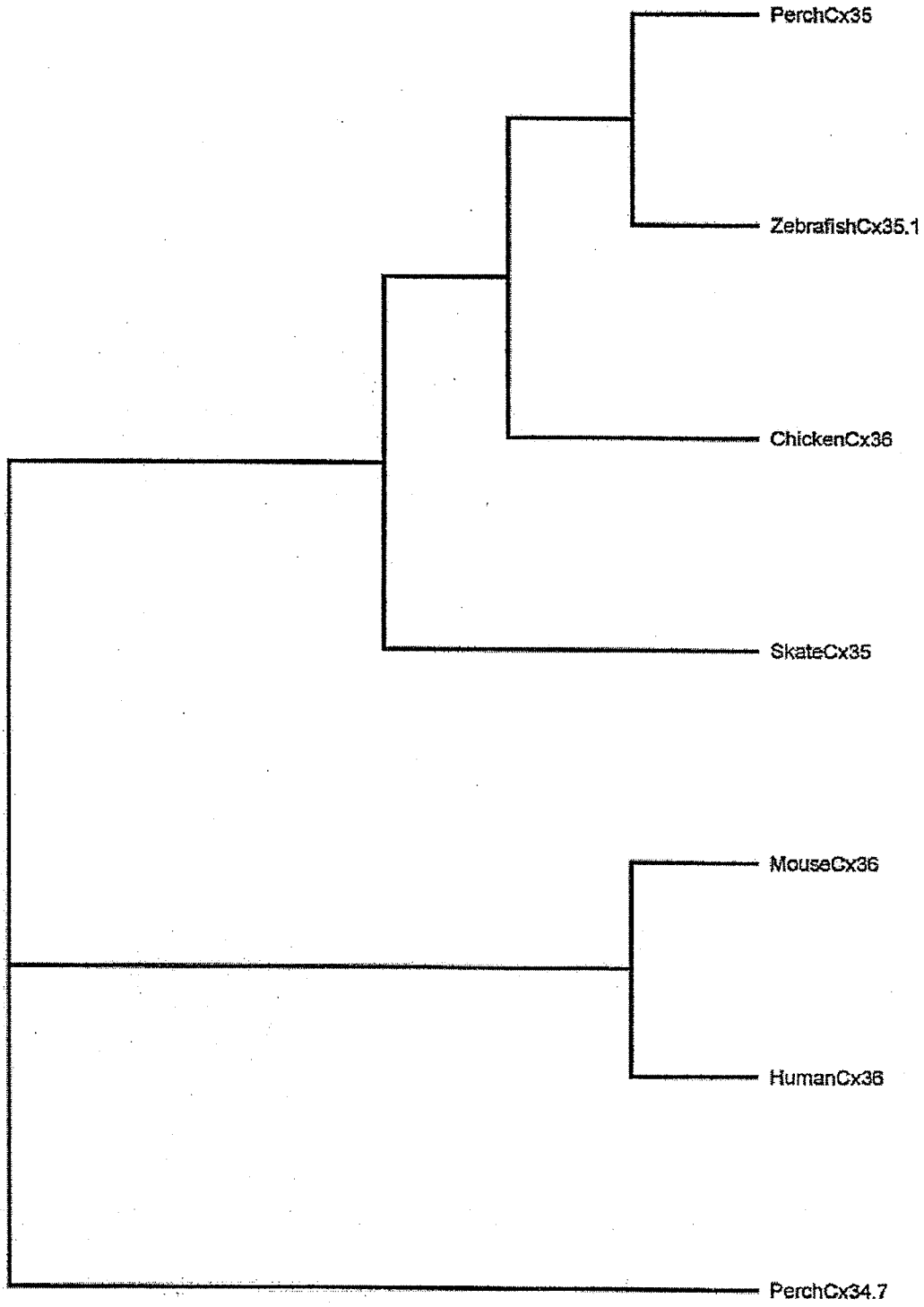
pCx35       KDLP-RMSVPNFGRTQSSDSAYV
zfCx35.1    KDLP-RMSMPNFGRTQSSDSAYV
chCx36      KDLP-RMSMPNFGRTQSSDSAYV
mCx36       KDLP-RVSVPNFGRTQSSDSAYV
huCx36      KDLP-RVSVPNFGRTQSSDSAYV
skCx35      KDSPHRIGVPNFGRTQSSDSAYV
            ** * *:.:**************
```

tested in mouse Cx36.

When compared with the Cx35/36 orthologues, the zebrafish Cx35.1 sequence shows a high degree of similarity and identity (Fig. 7). As expected the cytoplasmic loop is the least conserved region, with 42% identity, however, the C-tail is very highly conserved, with 88% identity. As with the Cx35/36 orthologues, the cytoplasmic loop is relatively long in comparison with other connexin groups, approximately 80 amino acids, while the C-tail is relatively short at approximately 50 amino acids. The mammalian orthologues also have a G-rich region in the cytoplasmic loop that is lacking in the other orthologous sequences. The function of the G-rich region is unknown. Pairwise comparisons using the Emboss global Pairwise Alignment Algorithm at the European Bioinformatics website (www.ebi.ac.uk/emboss/align/) revealed perch Cx35 as having the highest identity, 96.1%, with the zebrafish sequence. Chicken Cx36 has the next highest similarity, 93.4%, followed by skate Cx35, 84.3%, and then the mammalian orthologues, 81.1% (mouse Cx36). A BLAST nucleotide similarity search showed the same pattern. A phylogenetic tree constructed on the basis of the similarity of amino acid sequences illustrates the relationship of the group (Fig. 8). The tree also includes perch Cx34.7 for comparison, which is not considered to be orthologous but has a very similar gene structure (O'Brien *et al.*, 1998) and an amino acid identity of 78.4% with zebrafish Cx35.1.

The cDNA clone includes only the coding region with a small amount of upstream and downstream sequence. The cDNA sequence matches the corresponding region of the PAC sequence perfectly and gives the same software-based results upon analysis. As the cDNA clone does not contain intron sequence, it was used in comparison

Figure 8: A phylogenetic analysis of the Cx35/36 group of connexins in the form of a rectangular cladogram. The analysis was done with the TREEVIEW program (Page, 1996) using the amino acid sequences of the family members. Zebrafish Cx35.1 appears to be most closely related to perch Cx35, followed by chicken Cx36 and skate Cx35. The mammalian orthologues are grouped together on one branch while perch Cx34.7 is the most basal member of the clade.


PerchCx35
ZebrafishCx35.1
ChickenCx36
SkateCx35
MouseCx36
HumanCx36
PerchCx34.7

with the PAC sequence to identify the donor and acceptor splice sites (Fig. 9). The splice sites were confirmed by comparison with consensus splice sequences compiled from numerous nuclear and viral intron-exon and exon-intron boundary sequences (donor: CAAG/GTAG AGT; acceptor: TCnNCTAG/G) (Mount, 1982).

3.2 Electrophysiology

The following electrophysiology results were generated by T.W. White. Table I shows that Cx35.1 forms functional gap junctions with average conductance values of 3.13 μS (μSiemens) which is over 100-fold larger than the background conductance of 0.03 μS from water-injected oocytes. Table II summarizes the Boltzmann parameters of the channel (Spray *et al.*, 1981). The estimated minimum conductance value of the channel (G_{jmin}) at positive and negative transjunctional voltages (V_j) are 0.32 and 0.28, respectively. V_o is the voltage applied that is necessary to reduce the conductance to 50% of maximum and is 90mV for a positive voltage shift and 84mV for a voltage shift of the opposite polarity. Along with the cooperativity constant (A), which is a measure of voltage sensitivity, the G_{jmin} and V_o values demonstrate that Cx35.1 channels are slightly asymmetric. Both tables include mouse Cx36 (mCx36) data for comparison.

Figure 10A shows the recording of Cx35.1 homotypic junctional currents in response to +/-20 mV shifts in transjunctional potential from a resting potential of –40 mV. The voltage steps were 10 seconds in duration. It shows that junctional current varies linearly with voltage but, at higher potentials the current decays with time back down to a residual steady state level. In figure 10B the normalized steady state junctional

Figure 9: Splice site sequences of Cx35.1. Splice sites that match the conserved eukaryotic splice sequences considerably (donor: CAAG/GTAGAGT; acceptor: TCnNCTAG/G) (Mount, 1982) are shown in larger print, with the splice site denoted by an arrow. The complete upstream coding sequence and a portion of the downstream coding sequence are shown in bold.

ATGGGGGAATGGACAATTCTCGAGCGTCTCCTGGA

GGCGGCTGTCCAACAGCACTCTACTATGATTGGG

AG$^{\downarrow}$*GTGAG*...1953bpINTRON...*TGTAG*$^{\downarrow}$***G*ATCCT**

GCTAACTGTTGTGGTGATCTTCCGGATTCTAATTG

TGGCGATTGTTGGAGAGACCGTGTACGACGACGAG

CAGTCAA.....

Table I: Mean junctional conductance detected after injection of Cx cRNA or water into Xenopus oocyte pairs

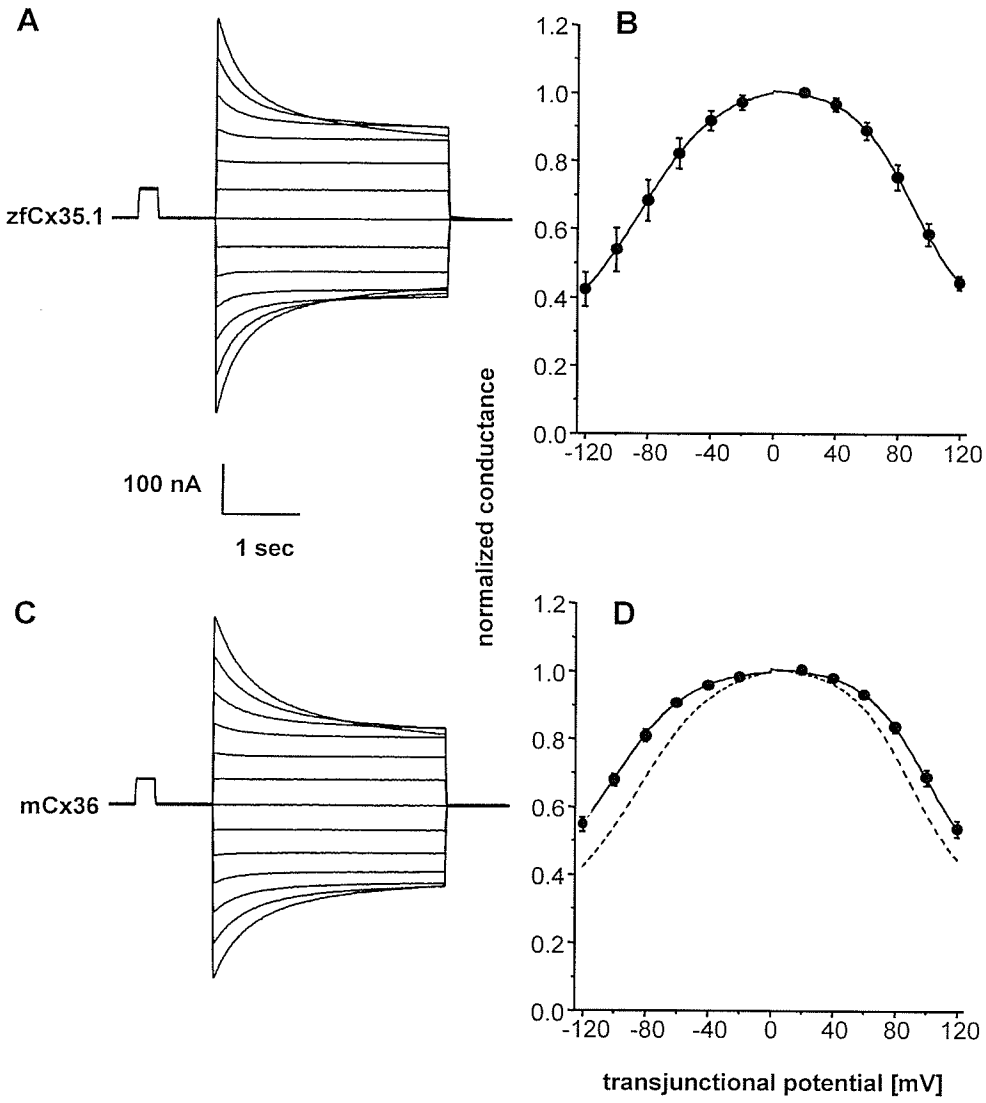
RNA injection	Junctional conductance (μS)	Number of pairs
water	0.03 ± 0.01	17
Cx36	5.80 ± 0.75	15
Cx35.1	3.13 ± 0.97	15

Table II: Comparison of Boltzmann parameters of gap junction channels composed of zebrafish Cx35.1 or mouse Cx36 expressed in paired *Xenopus* oocytes.

channel	V_j	V_0	G_{jmin}	A
Cx35.1	+	90	0.32	0.05
Cx35.1	-	-84	0.28	0.04
Cx36	+	100	0.36	0.05
Cx36	-	-100	0.34	0.04

+/- V_j refers to the polarity of the voltage steps. V_o is the voltage at which half maximal conductance is detected. G_{jmin} is the minimum estimated conductance value according to the Boltzmann equation. A is a measure of the voltage sensitivity of the channel.

Figure 10: (A) Time dependent decay of Cx35.1 junctional currents in *Xenopus* oocyte pairs injected with Cx35.1 cRNA induced by applied transjunctional voltage. Voltage steps were applied in 20 mV increments from a resting potential of –40 mV and lasted 10 seconds. (B) Normalized steady state junctional conductance for Cx35.1 channels plotted as a function of applied transjunctional voltage (mV). Data for mouse Cx36 are shown in (C) and (D) for comparison, with the Cx35.1 curve superimposed as a dotted line on the Cx36 curve. In (A) the currents show a voltage-induced closure of the channels at voltage shifts greater than 40 mV from resting. In (B) Cx35.1 shows similar voltage sensitivity to mouse Cx36 (D) with weak initial response, however the Cx35.1 channel is slightly asymmetric. At the most extreme transjunctional voltages applied, Cx35.1 still maintains a normalized conductance of over 40%, where Cx36 maintains a normalized conductance of over 50%.


A
zfCx35.1
100 nA
1 sec
B
1.2
1.0
0.8
0.6
0.4
0.2
0.0
-120
-80
-40
0
40
80
120
normalized conductance
C
mCx36
D
transjunctional potential [mV]

current is plotted as a function of transjunctional potential. This illustrates the asymmetric junctional current decay through Cx35.1 channels. The rate of decline is slightly greater for negative transjunctional potentials. It also illustrates the V_0 values stated in Table II, and demonstrates that even at maximum shifts of 120 mV in transjunctional potential, conductance never falls below 40% of maximum. Figures 10C and D show the corresponding data for mCx36. The Cx35.1 values are plotted as a dotted line on the curve for mCx36 in 10D.

3.3 mRNA Expression Analysis

3.3.1 Northern analysis

Total RNA Northern analysis was not successful as the Cx35.1 signal was very low so the probe only hybridized to the overwhelming amount of 28S and 18S rRNA. In order to get around this problem, polyA+ RNA was isolated from the total RNA in attempts to enrich the RNA pool for low-level RNA messages while decreasing the overall amount of rRNA and tRNA. As a test for this method, the first poly A+ blot only included d4 embryo, d5 embryo, adult brain, and adult eye samples. It was known from previous work that the protein is present in d4 and d5 embryos and adult brain (Elizabeth McLachlan, Honours thesis, University of Manitoba), so it was likely that the mRNA was expressed in these samples as well. Adult eye was chosen as a likely tissue to express Cx35.1 mRNA based on the literature for the other Cx35/36 orthologues. The lanes of the gel containing the d5 and adult brain samples ran slightly slower due to gel

abnormalities but, as this would not affect signal detection, it was nevertheless blotted for analysis. Hybridization was successful in that neither the 28S or 18S rRNA bands were detected. A single 2.7 kb band was detected in all four samples indicating that all four tissues express Cx35.1 mRNA (Fig. 11).

In order to assess RNA integrity, the blot was then hybridized with a zebrafish elongation factor 1α (eF-1α) probe. This served as a polyA+ RNA loading control because, although an even loading of two μg per sample was attempted, due to variation in precipitation success and accuracy of optical density reading of the samples, it may not have been accurate. This showed that intact RNA was present on the blot for all samples.

After concluding that polyA+ RNA Northern analysis is sensitive enough to detect Cx35.1 despite its low level of expression, a complete analysis of embryonic developmental stages and adult tissues was undertaken. The second polyA+ blot contained samples from d0 through d5 of development as well as adult brain, eye, liver and ovary samples. No signal was detected in embryos after any exposure length until d3 of development (Fig. 12). Expression was detected in d4, d5, adult brain and eye as before, but no signal was present in adult liver and ovary, although there is a background smear over those two lanes of the blot.

Again, by hybridizing the blot with the eF-1α probe, the integrity of the RNA on the blot could be verified. A band was detected in all of the samples so it can be concluded that the lack of signal in the d0, d1, d2, adult liver and adult ovary samples is not simply due to RNA degradation or a lack of RNA on the blot.

To verify the negative results above, a third polyA+ RNA blot was made from new d0 through d3 embryonic RNA, new adult brain RNA, and the same samples of liver

Figure 11: PolyA+1: Northern Blot analysis of Cx35.1 mRNA expression. PolyA+ RNA was isolated from embryonic stages d4 and d5 and adult brain (B) and eye (E) (lens removed), separated by electrophoresis on a gel, blotted to a membrane, and subsequently hybridized with a zebrafish Cx35.1-specific riboprobe. A 2.7 kb band was detected in all four samples although there was a shift in the d5 sample due to an abnormality in that lane of the gel. Elongation factor 1α (eF-1α) is ubiquitously expressed throughout development and in all adult tissues and therefore its detection allows the verification of RNA integrity in each sample.

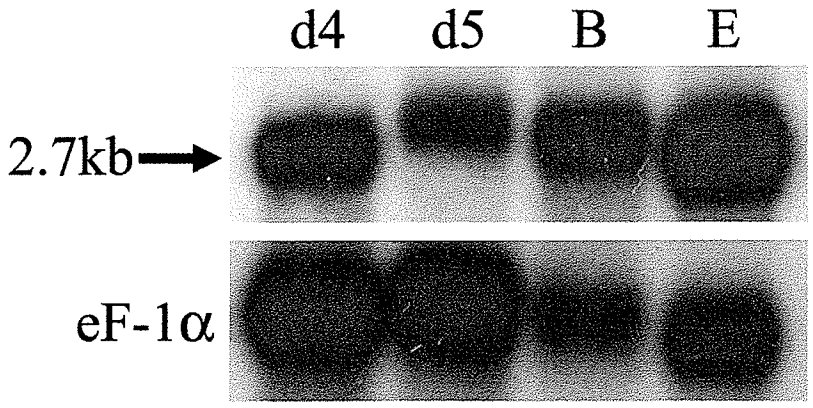
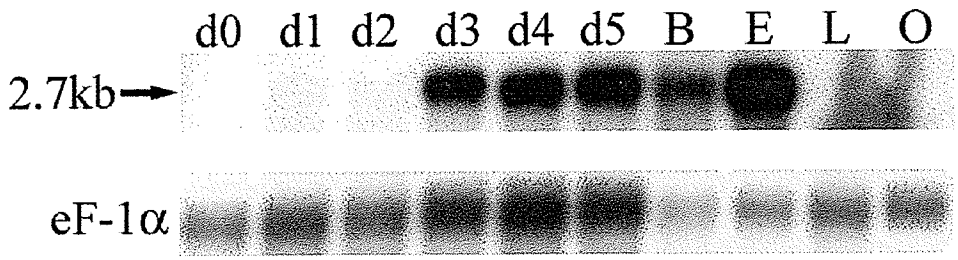

d4
d5
B
E
2.7kb
eF-1α

Figure 12: PolyA+2: Northern Blot analysis of Cx35.1 mRNA expression. PolyA+ RNA was isolated from embryonic stages d0, d1, d2, d3, d4, and d5 and adult brain (B), eye (E) (lens removed), liver (L), and ovary (O). The RNA was separated by electrophoresis on a gel, blotted to a membrane, and subsequently hybridized with a zebrafish Cx35.1-specific riboprobe. A 2.7 kb band was detected in the d3, d4, and d5 embryonic stages and in adult brain and eye. No signal was detected with any exposure length at d0, d1, or d2 or in adult liver or ovary. Elongation factor 1α (eF-1α) is ubiquitously expressed throughout development and in all adult tissues and therefore its detection allows the verification of RNA integrity in each sample.


d0
d1
d2
d3
d4
d5
B
E
L
O
2.7kb
eF-1α

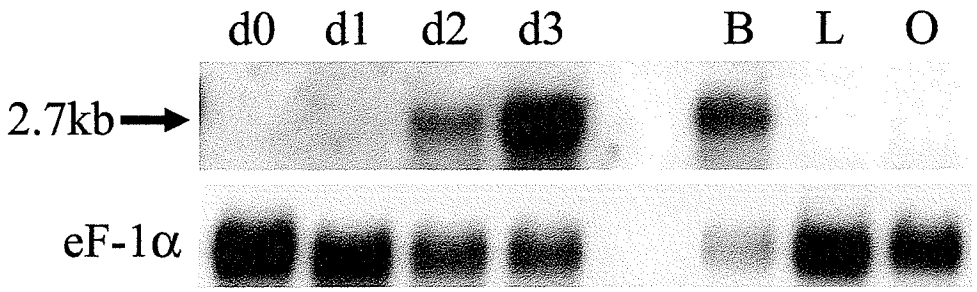
and ovary total RNA as described in the blot above. New polyA+ RNA was isolated from the liver and ovary total RNA, however. With this blot there was still no signal on d0 and d1, however, a faint signal was detected on d2 (Fig. 13). The discrepancy in the signal presence on d2 between the second and third blots could be explained by the fact that embryos were not always collected for RNA isolation at the same time of day. Therefore, the embryos used for RNA isolation for the third blot may have been collected later in the day than those used for the second blot and expression of Cx35.1 begins at a point on d2 between those two collection times. There was once again no Cx35.1 signal from the adult liver and ovary samples but the eF-1α signal shows that the lack of signal from the d0, d1, d2, liver and ovary samples is not due to an absence of intact RNA on the membrane.

From analysis of the above three northern blots, it can be concluded that zebrafish Cx35.1 mRNA expression begins at some point on d2 of development and continues to be expressed through d5 of development. In the adult, it is expressed in the brain and in the eye, but not in the liver or ovary. No conclusions can be drawn about the expression levels of Cx35.1 in the various samples as this method is not quantitative due to signal saturation and because the expression levels of eF-1α in each sample is not known so signal strength comparisons cannot be made.

3.3.2 RT-PCR Analysis

To confirm the results of the northern blots, with regards to the expression of Cx35.1 during embryonic development, the more sensitive method of RT-PCR was employed. The RT-PCR confirmed the Northern analysis results in that no Cx35.1

Figure 13: PolyA+3: Northern Blot analysis of Cx35.1 mRNA expression. PolyA+ RNA was isolated from embryonic stages d0, d1, d2, and d3 and adult brain (B), liver (L), and ovary (O). The RNA was separated by electrophoresis on a gel, blotted to a membrane, and subsequently hybridized with a zebrafish Cx35.1-specific riboprobe. A faint 2.7 kb band was detected in d2, and a strong band in d3 at this exposure length and in adult brain. No signal was detected with any exposure length at d0, or d1, or in adult liver or ovary. Elongation factor 1α (eF-1α) is ubiquitously expressed throughout development and in all adult tissues and therefore its detection allows the verification of RNA integrity in each sample.


d0
d1
d2
d3
B
L
O
2.7kb
eF-1α

amplification occurred from the d0 or d1 cDNA, but an approximately 1200 bp band was amplified from d2, d3, d4, and d5 cDNA. An agarose gel with the amplification products was blotted and hybridized with the zebrafish Cx35.1 probe to confirm that the amplification product was in fact Cx35.1 (Fig. 14).

Another PCR was carried out in parallel, using the same template as above but with primers that amplify eF-1α. This assay was performed as a means of verifying the presence of template in each reaction because after the reverse transcriptase reaction the resulting cDNA was not quantified. Amplification of an approximately 550 bp band occurred from all samples. This RT-PCR is not quantitative because the amount of Cx35.1 signal cannot be assessed by simply comparing the signal strength of the bands as PCR amplification reaches a plateau stage at which product accumulation no longer occurs at an exponential rate (Cha and Thilly, 1995). This may be due to reactant degradation or depletion, or competition for reactants from non-specific products.

To narrow down the time that mRNA expression begins, an RT-PCR was performed with a series of embryonic stages four to eight hours apart, from 24 hpf-72 hpf. The blot shows a band at 48 hpf and later, but not at 40 hpf, or earlier (Fig. 15). Again, a PCR was carried out in parallel, using the same template as above but with primers that amplify eF-1α in order to verify the presence of template in each reaction.

Figure 14: RT-PCR analysis of Cx35.1 mRNA expression during zebrafish embryonic development. Zebrafish Cx35.1-specific primers were used to PCR amplify products from cDNA prepared from d0, d1, d2, d3, d4, and d5 embryos and the products were separated by electrophoresis on a gel, blotted to a membrane and hybridized with a zebrafish Cx35.1-specific probe. A single band was detected in d2, d3, d4, and d5 embryo samples, but no band was detected in d0 or d1 embryo samples. Elongation factor 1α (eF-1α) is ubiquitously expressed throughout development and so its amplification by PCR allows the verification of the presence of starting template for the PCR reaction. The PCR reaction for eF-1α was run in parallel to that run for Cx35.1, and separated by electrophoresis on the same gel, but was not blotted to a membrane. This is an inverse image of the ethidium bromide stained gel.

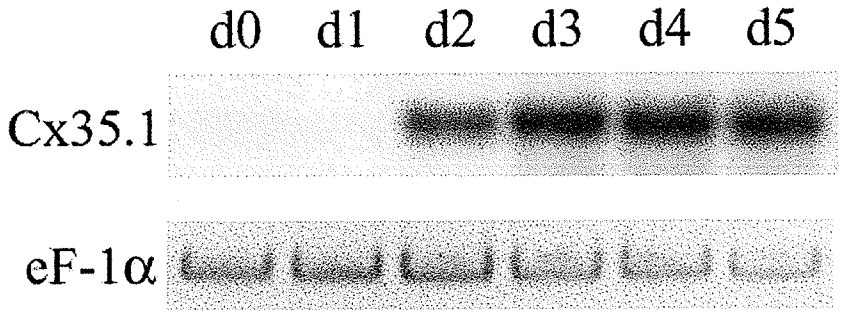
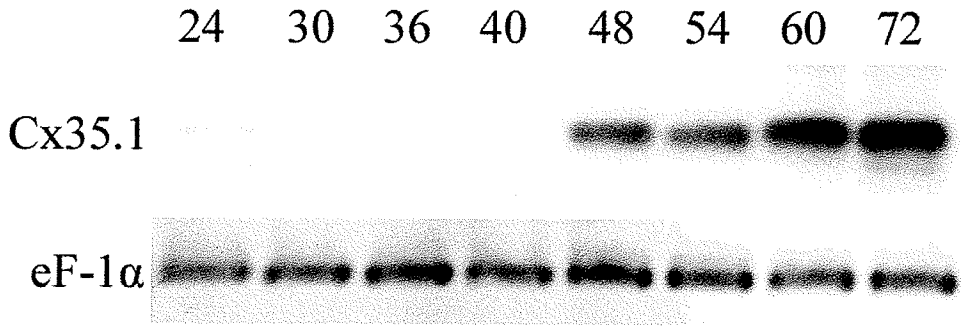

d0
d1
d2
d3
d4
d5
Cx35.1
eF-1α

Figure 15: RT-PCR analysis of Cx35.1 mRNA expression between 24-72 hpf of zebrafish embryonic development. Zebrafish Cx35.1-specific primers were used to PCR amplify cDNA prepared from 24 hpf, 30 hpf, 36 hpf, 40 hpf, 48 hpf, 54 hpf, 60 hpf and 72 hpf embryos and the products were separated by electrophoresis on a gel, blotted to a membrane and hybridized with a zebrafish Cx35.1-specific probe. Numbers above the blot denote hours post fertilization. A single band was detected in 48 hpf, 54 hpf, 60 hpf and 72 hpf embryo samples, but no band was detected in earlier stages of embryo samples. Elongation factor 1α (eF-1α) is ubiquitously expressed throughout development and so its amplification by PCR allows the verification of the presence of starting template for the PCR reaction. The PCR reaction for eF-1α was run in parallel to that run for Cx35.1, and separated by electrophoresis on a gel, but was not blotted to a membrane. This is an inverse image of the ethidium bromide stained gel.


24
30
36
40
48
54
60
72
Cx35.1
eF-1α

3.4 Protein Expression

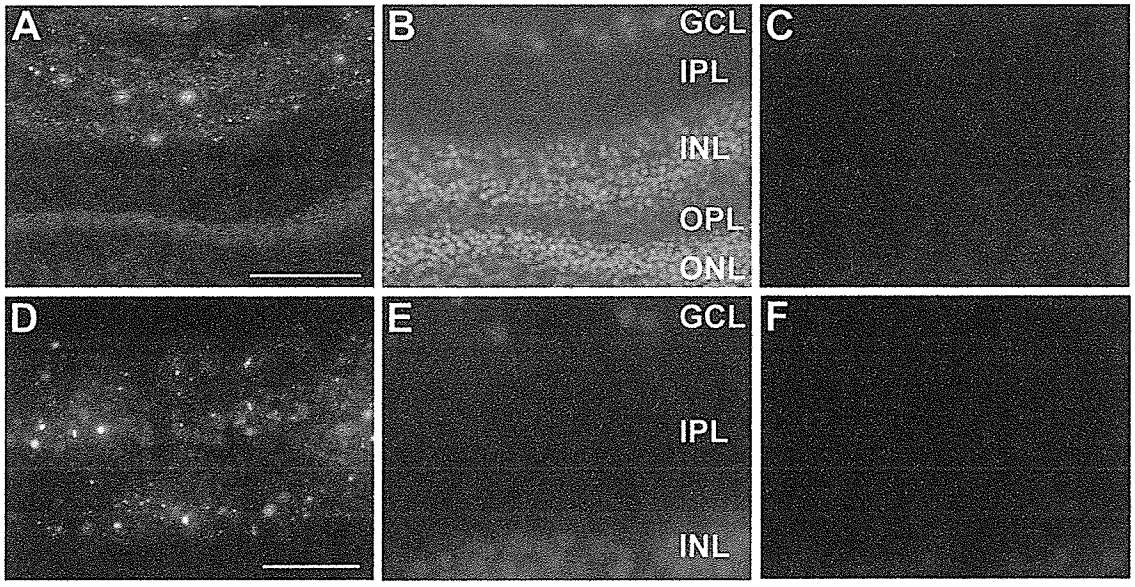
3.4.1 Immunohistochemistry of Adult Retina

Four different primary antibodies directed against either the mouse or perch Cx35/36 orthologues were tested in combination with two different fluorescent secondary antibodies. Regardless of the primary antibody, both secondary antibodies produced the same staining pattern, however, the green fluorescence of Alexa 488 was clearer and more intense. Once this was determined, Alexa 488 was used exclusively as the secondary antibody.

Three of the four primary antibodies, Ab298, antibody C, and anti-perch Cx35, showed similar staining patterns. They all revealed punctate staining, which is the characteristic staining pattern of gap junctions, in the inner plexiform layer (IPL) of the retina (Fig. 16). Specifically the staining was often seen in two rows toward the edges of the IPL. As well, staining was seen in the outer plexiform layer (OPL), although not as consistently and not as clearly punctate. Controls, not receiving primary antibody, did not show this punctate staining. There was at times a general fluorescence seen in the nuclear layers because the Hoechst emission spectrum is broad (approximately 400-600 nm with the peak at 450 nm) and, therefore, overlaps with the Alexa 488 excitation and emission wavelengths (peaks at approximately 475 nm and 525 nm, respectively).

The forth primary antibody, Ab51-6300, showed a similar staining pattern to those above, but at times, it also revealed large punctate staining at the boundary between the outer nuclear layer and the photoreceptor layer. There was also sporadic staining in other layers of the retina, but not consistently. The staining pattern was not seen with any

Figure 16: Protein expression analysis in adult zebrafish retina. Cryosections (10 μm) were probed with an anti-mouse Cx36 primary antibody, Ab298, which recognizes zebrafish Cx35.1 and detected with the fluorescent secondary antibody Alexa 488. Sections were double stained for Cx35.1 (A) and with Hoechst (B) to show the nuclear layers of the retina. Punctate staining, characteristic of gap junctions, is revealed in two rows in the inner plexiform layer (IPL), the synaptic layer between the interneurons and the ganglion cells. The outer plexiform layer (OPL) is also faintly labeled. (C) shows a similar section labeled only with the secondary antibody. (D) shows a section similar to (A) at a higher magnification while (E) shows its Hoechst counter-staining. (F) is the control section lacking primary antibody. GCL = ganglion cell layer, INL = inner nuclear layer, ONL = outer nuclear layer. Scale bar for (A-C) = 50 μm. Scale bar for (D-F) = 25 μm.


A
B
GCL
IPL
INL
OPL
ONL
C
D
E
GCL
IPL
INL
F

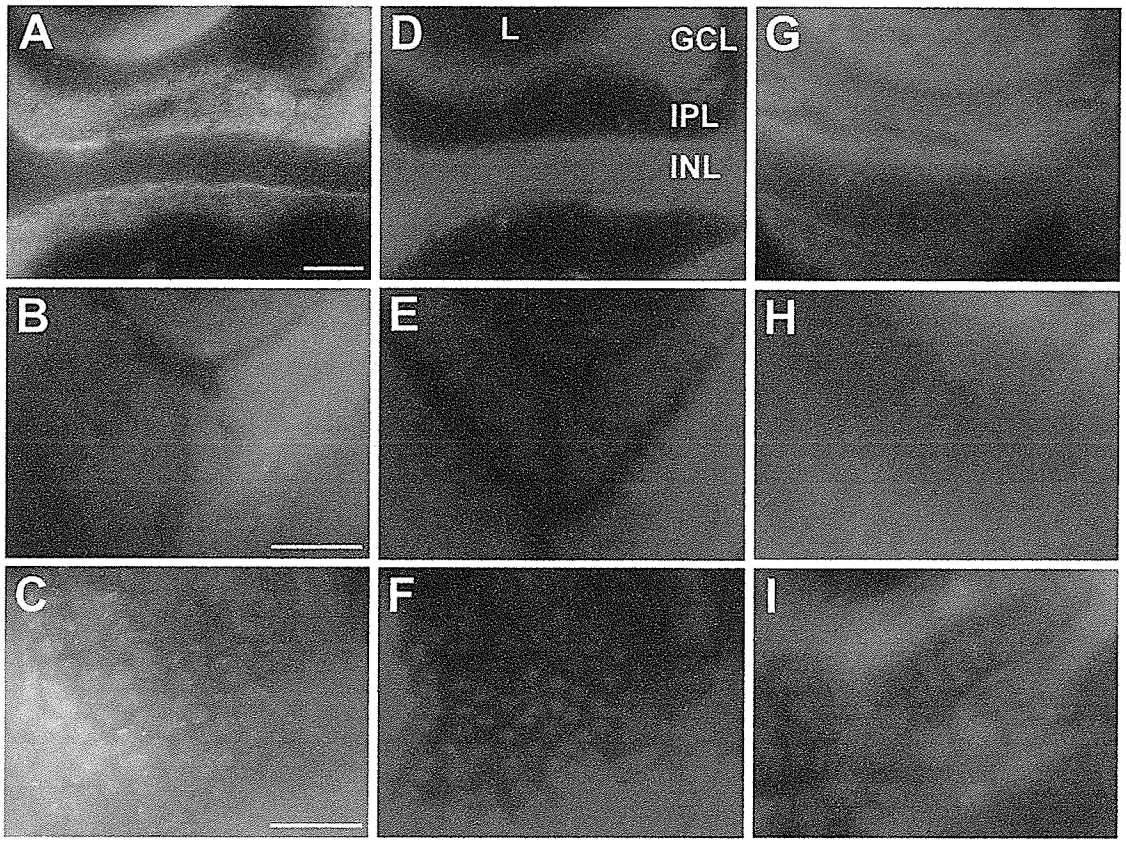
of the other primary antibodies and, therefore, was deemed to be non-specific. Controls lacking primary antibody did not show this staining but only the background fluorescence of the nuclear layers.

3.4.2 Immunohistochemistry of Embryonic Retina

Sections through d2, d3, d4, and d5 embryo heads were stained with the three antibodies that showed identical staining patterns in the adult retina, Ab298, antibody C, and anti-perch Cx35. The secondary antibody used was Alexa 488.

In d5 embryos, the three primary antibodies used for the adult sections showed a matching staining pattern. Retina sections showed punctate staining in the IPL and staining in the OPL, though it was too difficult to confirm whether it was punctate or not (Fig. 17). Staining in the IPL and OPL was also seen with two of the three antibodies in d4 embryos. In the earlier embryo stages, d2 and d3, sections through the head of the embryos did not show any specific staining within the retina (Fig. 17). However, some regions of the brain revealed punctate staining in the d2 and d3 embryos. As well, there was punctate staining surrounding portions of the facial cartilage of the d3 and d4 embryos (Fig. 17). There was not much cartilage left on the d5 embryo sections so cartilage staining cannot be confirmed for this stage.

Figure 17: Protein expression analysis in embryonic zebrafish retina and head. Cryosections (10 μm) were probed with anti-mouse Cx36 primary antibodies that recognize zebrafish Cx35.1 and detected with the fluorescent secondary antibody Alexa 488. Sections were double stained for Cx35.1 (A-C) and with Hoechst (D-F) to show the nuclear layers. Sections not treated with primary antibody were used as controls (G-I). The upper row shows d5 embryo retina labeled with antibody C. Punctate staining is detected in the inner plexiform layer (IPL) and the outer plexiform layer also fluoresces. In the middle row, showing d3 embryo retina labeled with Ab298, no specific Cx35.1 staining is detected in the retina. The bottom row shows a region of facial cartilage in the d4 embryo labeled with Ab298. Punctate staining is detected around the chondrocytes. Scale bars = 25 μm. GCL = ganglion cell layer, INL = inner nuclear layer.


A
D
L
GCL
IPL
INL
G
B
E
H
C
F
I

CHAPTER 4: DISCUSSION

4.1 Zebrafish Cx35.1 belongs to the Cx35/36 group of orthologues

This study was intended to provide a basis for further in depth research on the development of vertebrate vision. The zebrafish provides a unique model in which the structure and function of the eye can be monitored in the live animal throughout development using morphological and physiological observations and behavioral assays. This provides the opportunity to correlate defects with single gene mutations. In order to study the function of a specific gene suspected to be involved in vertebrate visual function, the gene must first be characterized in terms of structure, expression profile and physiological characteristics.

In this study a novel zebrafish connexin gene has been cloned from a genomic PAC library. The 912 bp coding region of the gene encodes a 304 amino acid protein with a predicted molecular weight of 35,059 Daltons. In keeping with the current nomenclature of the connexin gene family, this gene will be called zebrafish connexin35.1 (Cx35.1).

Through structural analysis of both the gene and the protein, it is apparent that zebrafish Cx35.1 belongs to the Cx35/36 group of orthologous genes. The gene is structured such that the coding region is not contained within a single exon, as is true for most other connexins outside of the Cx35/36 group. Instead the coding region is split into two exons by an intron that interrupts 71 bp after the translation initiation site. This corresponds to the division between the amino-terminal domain and the first transmembrane segment in the protein and is the location of the intron in all the Cx35/36

group members cloned to date. However, the size of the intron is variable. It is 1953 bp in the zebrafish, 950 bp in skate (O'Brien *et al.*, 1996), 900 bp in perch Cx35, 20 kb in perch Cx34.7 (O'Brien *et al.*, 1998), 1.14 kb in mouse (Söhl *et al.*, 1998), and 1.05 kb in human (Belluardo *et al.*, 1999).

The sequence of the coding region is highly conserved among the group and zebrafish Cx35.1 maintains that similarity with an amino acid identity and similarity of 96% and 99% respectively with perch Cx35. When the amino acid sequences of the orthologues are compared in a phylogenetic tree, we see that zebrafish Cx35.1 is placed on a branch closest to perch Cx35 and then chicken Cx36 (Fig. 8). The mammalian orthologues are grouped together and the skate Cx35 branches between the others more or less on its own, not surprisingly as it is the basal vertebrate species in the clade. Although, based on sequence and structure similarities perch Cx34.7 could belong to the Cx35/36 group, as it has the same genetic structure, it is not thought to be orthologous to the others. It is a novel gene and has a different expression pattern than perch Cx35 (J. O'Brien, University of Texas Medical School, personal communication) and is the most basal member of the clade.

The biophysical properties, including conductance and voltage-gating, of the Cx35/36 orthologues characterized so far are also remarkably conserved and zebrafish Cx35.1 channels are not significantly different (O'Brien *et al.*, 1996; O'Brien *et al.*, 1998; Srinivas *et al.*, 1999; White *et al.*, 1999; Al Ubaidi *et al.*, 2000). Zebrafish Cx35.1 can form functional gap junctions with conductance values over 100-fold larger than background conductance, but do not have conductance values as high as mouse Cx36. Zebrafish Cx35.1 channels are very weakly voltage sensitive. The Cx35/36 group in fact

has the lowest voltage dependence of all connexins, perhaps to prevent continual uncoupling due to hyperpolarization or depolarization in the electrically active neurons. This also suggests that retinal neurons expressing Cx35.1 could remain coupled despite membrane potential shifts that occur during visual activity (White *et al.*, 1999). As well, although unitary conductance has not been examined yet for Cx35.1, the Cx35/36 group has much lower unitary conductance than any other connexins. It has been suggested this may be a mechanism to have more precise control of the extent of electrical coupling by simply varying the channel number, in comparison to channels with higher unitary conductance (Srinivas *et al.*, 1999; Al-Ubaidi *et al.*, 2000).

Post-translational phosphorylation of connexin proteins is involved in the regulation of many connexin and gap junction properties (Lampe and Lau, 2000), including channel gating. Although phosphorylation has not been investigated in depth with regards to the Cx35/36 group, it may play a role in channel gating or other processes since potential phosphorylation sites seem to be conserved.

What remains to be answered with regards to Cx35.1 channel properties is whether or not Cx35.1 can form hemichannels and whether or not they can form heterotypic channels with other connexins. While skate Cx35, perch Cx35 and perch Cx34.7 are able to form functional hemichannels, no currents were detected for mouse Cx36 hemichannels. As a result of this inconsistency, it is hypothesized that there are discreet mechanisms governing hemichannel versus complete intercellular channel gating (Al-Ubaidi *et al.*, 2000). Both mouse Cx36 and skate Cx35 fail to form heterotypic channels with connexins that are able to form heterotypic channels with a number of different connexins. Nine different connexins were tested with mouse Cx36 including

Cx26, Cx32 and Cx50, which were also tested with skate Cx35 along with Cx46 (Teubner *et al.*, 1999; White *et al.*, 1999; Al-Ubaidi *et al.*, 2000). Perch Cx35 and Cx34.7 are able to form heterotypic channels between each other (O'Brien *et al.*, 1998), however, they have not been tested with other connexins yet. The fact that this group of connexins is restricted as to which connexins it will form channels with, suggests that, in accordance with their sequence divergence from the remaining groups of connexins, they have very distinct functional regulation properties.

4.2 Cx35.1 mRNA is expressed in development and in the adult brain and eye

Analysis of the transcriptional expression profile of zebrafish Cx35.1 transcripts during embryonic development revealed that Cx35.1 mRNA first becomes detectable between 40 hpf and 48 hpf and then is present until at least d5, the last stage that was assayed. Northern analysis revealed intense labeling in d3-d5 samples along with fainter labeling in d2 upon repetition of the experiment. Northern analysis is limited in its sensitivity to detect transcripts expressed at low levels, so RT-PCR, which is a more sensitive method, was employed to further evaluate expression. A more detailed time frame of four to eight hour intervals surrounding d2 of development was analyzed for Cx35.1 expression by RT-PCR. This revealed that Cx35.1 mRNA expression is detectable by this method by 48hpf but not by 40hpf or any earlier stage of development.

Temporal mRNA expression of the Cx35/36 orthologues in development has previously only been analyzed in the mouse and rat brain. These analyses revealed that expression is differentially regulated. Murine Cx36 expression is first detectable in the developing brain by RT-PCR at embryonic day (E) 7.5 (Gulisano *et al.*, 2000). Northern

analysis revealed that its expression increases from E11.5 to a maximum at post-natal day (P) 7 after which expression continually decreases to its adult level of 8% of maximum (Söhl *et al.*, 1998; Gulisano *et al.*, 2000; Rozental *et al.*, 2000b). In the rat, expression was only analyzed postnatally (Belluardo *et al.*, 2000; Prime *et al.*, 2000). During the first two weeks after birth Cx36 mRNA expression is up-regulated in the brain, but then declines markedly after that. The basis for the dynamic expression of Cx36 is yet to be determined although the expression profile does correlate with some major neurogenesis events in the developing brain (Gulisano *et al.*, 2000). While the zebrafish mRNA profiling presented here is not quantitative, Cx35.1 is clearly not expressed at d0 or d1 but then levels do not change drastically from when it is initially expressed at d2 to when the analysis stopped at d5. The onset of expression coincides with a period of rapid neurogenesis in the brain when the scaffold of tracts and commissures is being set up (Wulliman *et al.*, 1996).

Transcript expression analysis was also performed on select adult tissues. This showed that Cx35.1 mRNA is expressed in brain and eye (lens removed) but not in liver or ovary. Since the retina could not be dissected from the rest of the eye other than the lens, which of the remaining tissues express the message cannot be resolved by this method. However, the lens was negative for Cx35.1 transcripts when tested by RT-PCR (not shown). Al-Ubaidi *et al.* (2000) performed Northern analysis on mouse eye after separating it into three components, the lens, the retina, and a combination of the pigment epithelium, choroid and sclera (PECS). This analysis revealed no labeling in the lens, strong labeling in the retina, and very weak labeling in the PECS indicating the potential expression of mRNA in one or more of the PECS tissues. The Northern analysis of the

adult tissues is therefore consistent with the finding that the Cx35/36 orthologues are primarily expressed in the nervous system. In the skate it is only expressed in the retina and in the perch and mammals it is expressed in the retina as well as certain regions of the brain and peripheral nervous system (see sections 1.4 and 1.8). The one known exception is that it is also expressed in rat pancreatic islet cells (Serre-Beinier *et al.*, 2000; Calabrese *et al.*, 2001).

4.3 Cx35.1 protein is expressed in the zebrafish retina

Immunohistochemistry revealed a punctate staining pattern, characteristic of gap junctions, in the inner plexiform layer (IPL) of the zebrafish retina with all anti Cx35/36 antibodies tested. The staining was restricted to two distinct rows within the IPL, close to its borders, and the size of the puncta were heterogeneous. The IPL is subdivided into structurally and functionally discreet sublaminae, a and b, where the OFF and ON bipolar cell terminals lie, respectively (for examples see Nelson et al., 1978; Ammermuller and Kolb, 1995). ON and OFF refer to neuronal pathways that depolarize in response to increases or decreases in light, respectively. The sublamina a (OFF) is outermost and sublamina b (ON) is innermost within the IPL. The zebrafish IPL is divided into two distinct layers that house ON or OFF bipolar cell terminals, but there are also multistratified bipolar cells with termini in both layers and whether they function as ON or OFF is controversial (Connaughton and Nelson, 2000; Connaughton, 2001). The double-row staining pattern seen here suggests that Cx35.1 containing gap junctions are present in both sublaminae. Further experiments, including double labeling with cell-specific markers and EM immunochemistry, will be needed to identify the specific cell

type that is labeled within the IPL of the zebrafish.

In the perch and mammal, Cx35/36 protein has been localized to the IPL as well (O'Brien *et al.*, 1998; Güldenagel *et al.*, 2000; Feigenspan *et al.*, 2001; Mills *et al.*, 2001) and the staining was often distributed with more dense and broad staining in the inner layers of the IPL and less staining closer to the inner nuclear layer. In the zebrafish, however, there appears to be no real difference in distribution. Al-Ubaidi *et al.* (2000) reported localization of the protein to the inner nuclear layer and the ganglion cell layer of the mouse retina with an anti-perch Cx35 antibody. However, Meier *et al.*, (2002) tested various anti-Cx36 antibodies on the retina and compared these results to staining in the Cx36 knockout retina and determined that only staining in the IPL and OPL is specific. In the mouse, rat, and rabbit IPL, the specific cell type labeled has been identified as AII amacrine cells (Feigenspan *et al.*, 2001; Mills *et al.*, 2001). AII amacrine cells, or rod amacrines, are interneurons in the rod pathway that receive output from rod bipolar cells and feed into the cone pathway via chemical and electrical synapses with OFF cone bipolar cells and ON cone bipolar cells, respectively. Therefore, they form homologous gap junctions with other AII amacrine cells and heterologous junctions with ON cone bipolar cells. Cx36 has been localized through immunolabeling and light microscopy methods to both these types of junctions. Since Cx36 cannot be found in ON cone bipolar cells using these methods, this may be a heterotypic junction, but the other participating connexin has yet to be identified. Further evidence of heterotypic coupling between AII amacrine cells and ON cone bipolars is that these channels have different permeability characteristics than homologous, homotypic channels between AII amacrines (Mills and Massey, 1995, 2000).

Labeling was also detected in the OPL of the zebrafish where dendrites of horizontal cells and bipolar cells synapse with photoreceptors. However, the nature of the staining is different from that in the IPL. The puncta are not as large and the staining does not appear to be as strong, presumably due to smaller plaque size. This pattern is consistent with other studies showing a fainter degree of Cx36 labeling in the OPL of the mammalian retina (Güldenagel *et al.*, 2000; Teubner *et al.*, 2000; Feigenspan *et al.*, 2001; Mills *et al.*, 2001). The cell type expressing the protein in this layer has not been identified in any species yet.

This same expression pattern, labeling in the IPL and OPL, is seen in embryonic zebrafish retinas beginning on d4 of development. Before this time, although labeling is detected in regions of the brain and in facial cartilage, it is not seen in the retina. Neurogenesis is complete in the zebrafish retina by approximately d2.5 and the major layers of the retina are distinguishable (Malicki, 1999). Differentiation of the various retinal cell types occurs over approximately the next 36 hours, and is complete by d4. The zebrafish Cx35.1 protein embryonic expression profile supports the hypothesis of Al-Ubaidi *et al.* (2000) that Cx36 orthologues are not expressed, or that functional Cx35/36 channels are not assembled, in the retinal cells until their differentiation is complete. In the mouse, although Cx36 mRNA is detected in the brain as early as E7.5 (Gulisano *et al.*, 2000), Al-Ubaidi *et al.* reported it is not detected in the retina until some time between P1 and P5. Assuming that Cx36 protein expression and the assembly of functional channels follow shortly afterwards, the development of intercellular communication would coincide with the completion of differentiation of amacrine cells and other retinal neuron types in the mouse.

4.4 What is the function of the Cx35/36 orthologues?

With such strong expression in the retina, Cx35.1 likely plays a significant role in vision. Disruption of its expression by antisense morpholino knock-down, or other technologies being developed, will be useful in determining its function. A Cx36 knockout mouse has been constructed and its retinal structure and function have been investigated (Güldenagel *et al.*, 2001). The Cx36 knockout mouse, as a whole, seems to develop normally and does not have any apparent abnormalities. As well, the structure of the retina is completely normal. The coupling between AII amacrine cells and ON bipolars is, however, disabled. As a result, some of the electrical activity normally produced by the ON pathway is disrupted. Therefore it was concluded that one role of Cx36 is in electrical synapses in visual transmission, without which light perception is impaired. Other evidence of its role in light perception is a study in which levels of Cx36 were assessed under various lighting conditions (Al-Ubaidi *et al.*, 2000). Mice reared in constant light or constant darkness expressed Cx36 mRNA at only 40% of the level expressed in mice reared under a typical light/dark cycle.

The Cx35/36 orthologues are also expressed in the brain, and a possible function here is in neuronal network synchronization and epileptic behavior. Connexin36 is predominantly expressed in interneurons, which are capable of producing synchronous activity due to their numerous contacts. This synchronization is functionally important for information processing in the cortex and hippocampus. In the Cx36 knockout there is loss of electrical synapses between mouse cortical interneurons and reduced synchrony of the inhibitory potentials normally produced by them (Deans *et al.*, 2001). A similar study investigating synchronization in the mouse hippocampus showed that Cx36 is involved in

generating sharp wave-ripple complexes and its loss led to reduction of pathological, hypersynchronous epileptiform discharges (Maier *et al.*, 2002). Loss of Cx36 also results in the absence of coupling between inhibitory neurons in the thalamic reticular nucleus in the forebrain, which normally generate synchronous activity during sleep, and seizures (Landisman *et al.*, 2002).

Interestingly, the human orthologue of Cx36 has been cloned and mapped to chromosomal band 15q14 (Belluardo *et al.*, 1999). One of two syndromes linked to this location is juvenile myoclonic epilepsy. In addition, patients with an inverted duplication on chromosome 15 frequently have a rearrangement at 15q14 and are affected with mental retardation and epileptic symptoms.

Since the Cx35/36 orthologues are primarily expressed in neurons, epilepsy is only one of many nervous system disorders that the Cx35/36 orthologues may be involved in. With its predominant expression in the retina, and its recent identification in oligodendrocytes (Parenti *et al.*, 2002), Schwann cells (Nicholson *et al.*, 2001), and insulin-producing β–cells of the pancreatic islets (Serre-Beinier *et al.*, 2000; Calabrese *et al.*, 2001), Cx36 likely has many important functions and could play a role in many human diseases. The exploitation of the advantages of the zebrafish as a model system should prove fruitful to understanding these functions and roles.

APPENDIX A

Buffers and Media

LB (Luria Bertani) solid medium for plates

Bacto-Tryptone	10 g
Bacto-yeast extract	5 g
NaCl	10 g
Bacto-agar	15 g
ddH_20	Up to 1L, autoclaved

LB liquid medium

Bacto-Tryptone	10 g
Bacto-yeast extract	5 g
NaCl	10 g
ddH_20	Up to 1L, autoclaved

10X MTBE

Tris base	162 g
Boric acid	27.5 g
Na_2EDTA	9.3 g
ddH_20	Up to 1L

20X TAE

Tris base	96.9 g
$NaOAc\text{-}3H_20$	32.8 g
Na_2EDTA	14.9 g
Glacial acetic acid	To pH 8.3
ddH_20	Up to 1L

6X DNA loading buffer

0.25% bromophenol blue
30% glycerol in water

5X RNA loading buffer

Saturated bromophenol blue	16 µl
0.5 M EDTA, pH 8.0	80 µl
37% Formaldehyde	720 µl
100% Glycerol	2 ml
Formamide	3084 µl
10X MOPS	4 ml
DEPC H_20	Up to 10ml

OLB

50 A_{260} units of random primer hexanucleotides (Pharmacia) dissolved in 555µl double distilled water, followed by addition of 375µl of Buffer A and 925µl of 2M Hepes (pH Hepes to 6.6 with NaOH)

Buffer A= 1ml 0.125M Tris-HCl pH 8.0, 1ml 0.125M $MgCl_2$, 18µl β-mercaptoethanol, 5µl dNTPs (100mM each, except for dCTP)

50X Denhardt's solution

Ficoll	5 g
Polyvinylpyrrolidone	5 g
Bovine Serum Albumin (BSA)	5 g
ddH_20	Up to 500ml

20X SSC

NaCl	175.3g
Sodium citrate	88.2g
ddH_2O	Up to 1L
NaOH	pH to 7.0

20X SSPE

NaCl	175.3g
NaH_2PO_4-H_2O	27.6g
EDTA	7.4g
NaOH	pH to 7.4
ddH_2O	Up to 1L

Hybridization buffer 1

7% SDS
0.5 M NaPhosphate, pH 7.2
1 mM EDTA

Hybridization buffer 2 (final concentrations)

50% Formamide
5X SSPE
0.1% SDS (sodium dodecyl sulfate)
5X Denhardt's solution
100 µg/ml sheared salmon sperm DNA
ddH_20 (Up to desired total volume)

10X MOPS (3-(N-morpholino) propanesulfonic acid)/EDTA buffer

MOPS	41.9g
NaOAc	6.8g
EDTA	3.7g
ddH_20	Up to 1L

APPENDIX B

Single letter codes of the naturally occurring amino acids

Alanine	A	Methionine	M
Cysteine	C	Asparagine	N
Aspartic Acid	D	Proline	P
Glutamic Acid	E	Glutamine	Q
Phenylalanine	F	Arginine	R
Glycine	G	Serine	S
Histidine	H	Threonine	T
Isoleucine	I	Valine	V
Lysine	K	Tryptophan	W
Leucine	L	Tyrosine	Y

LITERATURE CITED

Abrams CK, Oh S, Ri Y, Bargiello TA. 2000. Mutations in connexin 32: the molecular and biophysical bases for the X-linked form of Charcot-Marie-Tooth disease. Brain Res Brain Res Rev. 32: 203-14.

Ackert CL, Gittens JE, O'Brien MJ, Eppig JJ and Kidder GM. 2001. Intercellular communication via connexin43 gap junctions is required for ovarian folliculogenesis in the mouse. Dev Biol. 233: 258-70.

Altevogt BM, Kleopa KA, Postma FR, Scherer SS, Paul DL. 2002. Connexin29 is uniquely distributed within myelinating glial cells of the central and peripheral nervous systems. J Neurosci. 22: 6458-70.

Al-Ubaidi MR, White TW, Ripps H, Poras I, Avner P, Gomes D, Bruzzone R. 2000. Functional properties, developmental regulation, and chromosomal localization of murine connexin36, a gap junctional protein expressed preferentially in retina and brain. J. Neurosci. Res. 59: 813-26.

Amemiya CT, Zon LI. 1999. Generation of a zebrafish P1 artificial chromosome library. Genomics. 58: 211-3.

Amemiya CT, Zhong TP, Silverman GA, Fishman MC, Zon LI. 1999. Zebrafish YAC, BAC, and PAC genomic libraries. Methods Cell Biol. 60: 235-58.

Ammermuller J, Kolb H. 1995. The organization of the turtle inner retina. I. ON- and OFF-center pathways. J Comp Neurol. 358: 1-34.

Baier, H. 2000. Zebrafish on the move: towards a behavior-genetic analysis of vertebrate vision. Curr Opin Neurobiol. 10: 451-55.

Barnett SC, Thompson RJ, Lakatos A, Pitts J. 2001. Gap junctional communication and connexin expression in cultured olfactory ensheathing cells. J Neurosci Res. 65: 520-8.

Belluardo N, Mudo G, Trovato-Salinaro A, Le Gurun S, Charollais A, Serre-Beinier V, Amato G, Haefliger JA, Meda P, Condorelli DF. 2000. Expression of Cx36 in the adult and developing rat brain. Brain Res. 865: 121-38.

Belluardo N, Trovato-Salinaro A, Mudo G, Hurd YL, Condorelli DF. 1999. Structure, chromosomal location, and brain expression of human Cx36 gene. J. Neurosci. Res. 57: 740-52.

Bevans CG, Kordel M, Rhee SK. Harris AL. 1998. Isoform composition of connexin channels determines selectivity among second messengers and uncharged molecules. J Biol Chem. 273: 2808-16.

Beyer EC, Paul DL, Goodenough DA. 1990. Connexin family of gap junction proteins. J. Membrane Biol. 116: 187-94.

Bex V, Mercier T, Chaumontet C, Gaillard-Sanchez I, Flechon B, Mazet F, Traub O, Martel P. 1995. Retinoic acid enhances connexin43 expression at the post-transcriptional level in rat liver epithelial cells. Cell Biochem Funct. 13: 69-77.

Bilotta J, Saszik S. 2001. The zebrafish as a model visual system. Int J Dev Neurosci. 19: 621-9.

Bruzzone R, Ressot C. 1997. Connexins, gap junctions and cell-cell signalling in the nervous system. Eur J Neurosci. 9: 1-6.

Bruzzone R, White TW, Goodenough DA. 1996a. The cellular internet: On-line with connexins. BioEssays 18: 709-18.

Bruzzone R, White TW, Paul DL. 1996b. Connections with connexins: The molecular basis of direct intercellular signaling. Eur. J. Biochem. 238: 1-27.

Calabrese A, Güldenagel M, Charollais A, Mas C, Caton D, Bauquis J, Serre-Beinier V, Caille D, Söhl G, Teubner B, Le Gurun S, Trovato-Salinaro A, Condorelli DF, Haefliger JA, Willecke K, Meda P. 2001. Cx36 and the function of endocrine pancreas. Cell Adhes Commun. 8: 387-91.

Cason N, White TW, Cheng S, Goodenough DA, Valdimarsson G. 2001. Molecular cloning, expression analysis, and functional characterization of connexin44.1: a zebrafish lens gap junction protein. Dev Dyn. 221: 238-47.

Caveney S. 1985. The role of gap junction in development. Ann. Rev. Physiol. 47: 319-35.

Cha RS, Thilly WG. 1995. Specificity, efficiency, and fidelity of PCR. In: PCR Primer: A laboratory manual. Editor: Dieffenbach CW, Dveksler GS. New York. Cold Spring Harbor Laboratory Press.

Chang Q, Balice-Gordon RJ. 2000. Gap junctional communication between developing and injured motoneurons. Brain Res Brain Res Rev. 32: 242-9.

Chow L, Lye SJ. 1994. Expression of the gap junction protein connexin-43 is increased in the human myometrium toward term and with the onset of labor. Am J Obstet Gynecol. 170: 788-95.

Clairmont A, Tessmann D, Seis H. 1996. Analysis of connexin43 gene expression induced by retinoic acid in F9 teratocarcinoma cells. FEBS Lett. 397: 22-4.

Condorelli DF, Belluardo N, Trovato-Salinaro A, Mudo G. 2000. Expression of Cx36 in mammalian neurons. Brain Res Brain Res Rev. 32: 72-85.

Condorelli DF, Parenti R, Spinella F, Trovato-Salinaro A, Belluardo N, Cardile V, Ciricata F. 1998. Cloning of a new gap junction gene (Cx36) highly expressed in mammalian brain neurons. Eur. J. Neurosci. 10: 1202-8.

Connaughton VP. 2001. Organization of ON- and OFF-pathways in the zebrafish retina: neurotransmitter localization, electrophysiological responses of bipolar cells, and patterns of axon terminal stratification. Prog Brain Res. 131: 161-76.

Connaughton VP, Nelson R. 2000. Axonal stratification patterns and glutamate-gated conductance mechanisms in zebrafish retinal bipolar cells. J Physiol. 524: 135-46.

Dahl E, Winterhager E, Reuss B, Traub O, Butterweck A, Willecke K. 1996. Expression of the gap junction proteins connexin31 and connexin43 correlates with communication compartments in extraembryonic tissues and in the gastrulating mouse embryo, respectively. J Cell Sci. 109: 191-7.

Deans MR, Gibson JR, Sellitto C, Connors BW, Paul DL. 2001. Synchronous activity of inhibitory networks in neocortex requires electrical synapses containing connexin36. Neuron. 31: 477-85.

Deans MR, Paul DL. 2001. Mouse horizontal cells do not express connexin26 or connexin36. Cell Adhes Commun. 8: 361-6

Dermietzel R, Gao Y, Scemes E, Vieira D, Urban, M, Kremer M, Bennet MVL, Spray DC. 2000. Connexin43 null mice reveal that astrocytes express multiple connexins. Brain Res Brain Res Rev. 32: 45-56.

Dermietzel R, Spray DC. 1993. Gap junctions in the brain: where, what type, how many and why? Trends Neurosci. 16: 186-92.

De Sousa PA, Juneja SC, Caveney S, Houghton FD, Davies TC, Reaume AG, Rossant J, Kidder GM. 1997. Normal development of preimplantation mouse embryos deficient in gap junctional coupling. J Cell Sci. 110: 1751-8.

Dooley K, Zon LI. 2000. Zebrafish: a model system for the study of human disease. Curr Opin Genet Dev. 10: 252-6.

Donaldson P, Eckert R, Green C, Kistler J. 1997. Gap junction channels: new roles in disease. Histol Histopathol. 12: 219-31.

Driever W, Fishman MC. 1996. The zebrafish: heritable disorders in transparent embryos. J Clin Invest. 97: 1788-94.

Driever W, Solnica-Krezel L, Schier AF, Neuhauss SC, Malicki J, Stemple DL, Stainier DY, Zwartkruis F, Abdelilah S, Rangini Z, Belak J, Boggs C. 1996. A genetic screen for mutations affecting embryogenesis in zebrafish. Development. 123: 37-46.

Eiberger J, Degen J, Romualdi A, Deutsch U, Willecke K, Söhl G. 2001. Connexin genes in the mouse and human genome. Cell Adhes Commun. 8: 163-5.

Essner JJ, Laing JG, Beyer EC, Johnson RG, Hackett PB Jr. 1996. Expression of zebrafish connexin43.4 in the notochord and tail bud of wild-type and mutant no tail embryos. Dev Biol. 177: 449-62.

Feigenspan A, Teubner B, Willecke K, Weiler R. 2001. Expression of neuronal connexin36 in AII amacrine cells of the mammalian retina. J Neurosci. 21: 230-9.

Fischbach GD. 1972. Synapse formation between dissociated nerve and muscle cells in low density cell cultures. Dev. Biol. 28: 407-29.

Foote C, Zhou L, Zhu X, Nicholson B. 1998. The pattern of disulfide linkages in the extracellular loop regions of connexin32 suggest a model for the docking interface of gap junctions. J. Cell Biol. 140: 1187-97.

Gabriel HD, Strobl B, Hellmann P, Buettner R, Winterhager E. 2001. Organization and regulation of the rat Cx31 gene. Implication for a crucial role of the intron region. Eur J Biochem. 268: 1749-59.

Gilbert SF. 1994. Developmental Biology. 4th ed. Sunderland, Massachusetts. Sinauer Associates, Inc.

Granato M, Nusslein-Volhard C. 1996. Fishing for genes controlling development. Curr Opin Genet Dev. 6: 461-8.

Güldenagel M, Ammermuller J, Feigenspan A, Teubner B, Degen J, Söhl G, Willecke K, Weiler R. 2001. Visual transmission deficits in mice with targeted disruption of the gap junction gene connexin36. J Neurosci. 21: 6036-44.

Güldenagel M, Söhl G, Plum A, Traub O, Teubner B, Weiler R, Willecke K. 2000. Expression patterns of connexin genes in mouse retina. J Comp Neurol. 425: 193-201.

Gulisano M, Parenti R, Spinella F, Circirata F. 2000. Cx36 is dynamically expressed

during early development of mouse brain and nervous system. Dev. Neuroreport. 11: 3823-8.

Guthrie SC, Gilula NB. 1989. Gap junctional communication and development. Trends Neurosci. 12: 12-6.

Haffter P, Granato M, Brand M, Mullins MC, Hammerschmidt M, Kane DA, Odenthal J, van Eeden FJ, Jiang YJ, Heisenberg CP, Kelsh RN, Furutani-Seiki M, Vogelsang E, Beuchle D, Schach U, Fabian C, Nusslein-Volhard C. 1996. The identification of genes with unique and essential functions in the development of the zebrafish, Danio rerio. Development. 123: 1-36

Haubrich S, Schwarz HJ, Bukauskas F, Lichtenberg-Frate H, Traub O, Weingart I, Willecke K. 1996. Incompatibility of connexin 40 and 43 Hemichannels in gap junctions between mammalian cells is determined by intracellular domains. Mol Biol Cell. 7: 1995-2006.

Houghton FD, Barr KJ, Walter G, Gabriel HD, Grummer R, Traub O, Leese HJ, Winterhager E, Kidder GM. 2002. Functional significance of gap junctional coupling in preimplantation development. Biol Reprod. 66: 1403-12.

Huang GY, Cooper ES, Waldo K, Kirby ML, Gilula NB, Lo CW. 1998a. Gap junction-mediated cell-cell communication modulates mouse neural crest migration. J Cell Biol. 143: 1725-34.

Huang RP, Fan Y, Hossain MZ, Peng A, Zeng ZL, Boynton AL. 1998b. Reversion of the neoplastic phenotype of human glioblastoma cells by connexin 43 (cx43). Cancer Res. 58: 5089-96.

Jacob A, Beyer EC. 2001. Mouse connexin 45: genomic cloning and exon usage. DNA Cell Biol. 20: 11-9.

Janssen-Bienhold U, Dermietzel R, Weiler R. 1998. Distribution of connexin43 immunoreactivity in the retinas of different vertebrates. J Comp Neurol. 396: 310-21.

Kelsell DP, Dunlop J, Hodgins MB. 2001. Human diseases: clues to cracking the connexin code? Trends Cell Biol. 11: 2-6.

Kidder GM, Winterhager E. 2001. Intercellular communication in preimplantation development: the role of gap junctions. Front Biosci. 6: D731-6.

Krutovskikh V, Yamasaki H. 2000. Connexin gene mutations in human genetic diseases. Mutat Res. 462: 197-207.

Krutovskikh VA, Yamasaki H, Tsuda H, Asamoto M. 1998. Inhibition of intrinsic gap-junction intercellular communication and enhancement of tumorigenicity of the rat bladder carcinoma cell line BC31 by a dominant-negative connexin 43 mutant. Mol Carcinog. 23: 254-61.

Lampe PD, Lau AF. 2000. Regulation of gap junctions by phosphorylation of connexins. Arch Biochem Biophys. 384: 205-15.

Landisman CE, Long MA, Beierlein M, Deans MR, Paul DL, Connors BW. 2002. Electrical synapses in the thalamic reticular nucleus. J Neurosci. 22: 1002-9.

Lefebvre DL, Piersanti M, Bai XH, Chen ZQ, Lye SJ. 1995. Myometrial transcriptional regulation of the gap junction gene, connexin-43. Reprod Fertil Dev. 7: 603-11.

Li, L. 2001. Zebrafish mutants: behavioral genetic studies of visual system defects. Dev Dyn. 221: 365-72.

Li WE, Waldo K, Linask KL, Chen T, Wessela A, Parmacek MS, Kirby ML, Lo CW. 2002. An essential role for connexin43 gap junctions in mouse coronary artery development. Development. 129: 2031-42.

Lo CW, Gilula NB. 1979. Gap junctional communication in the post-implantation mouse embryo. Cell. 18: 411-22.

Maier N, Güldenagel M, Söhl G, Siegmund H, Willecke K, Draguhn A. 2002. Reduction of high-frequency network oscillations (ripples) and pathological network discharges in hippocampal slices from connexin 36-deficient mice. J Physiol. 541: 521-8.

Malicki J. 1999. Development of the retina. Methods Cell Biol. 59: 273-99.

McLachlan E. 2000. Cloning and preliminary expression analysis of a putative connexin gene in the zebrafish (*Danio rerio*). Honours Thesis. Department of Zoology, University of Manitoba.

McLachlin JR, Caveney S, Kidder GM. 1983. Control of gap junction formation in early mouse embryos. Dev Biol. 98: 155-64.

Meier C, Petrasch-Parwez E, Habbes HW, Teubner B, Güldenagel M, Degen J, Sohl G, Willecke K, Dermietzel R. 2002. Immunohistochemical detection of the neuronal connexin36 in the mouse central nervous system in comparison to connexin36-deficient tissues. Histochem Cell Biol. 117: 461-71.

Mills SL, Massey SC. 1995. Differential properties of two gap junctional pathways made by AII amacrine cells. Nature. 377: 734-7.

Mills SL, Massey SC. 2000. A series of biotinylated tracers distinguishes three types of gap junction in retina. J Neurosci. 20: 8629-36.

Mills SL, O'Brien JJ, Li W, O'Brien J, Massey SC. 2001. Rod pathways in the mammalian retina use connexin 36. J Comp Neurol. 436: 336-50

Mount SM. 1982. A catalogue of splice junction sequences. Nucleic Acids Res. 10: 459-72.

Mullins MC, Nusslein-Volhard C. 1993. Mutational approaches to studying embryonic pattern formation in the zebrafish. Curr Opin Genet Dev. 3: 648-54.

Nadarajah B, Jones AM, Evans WH, Parnavelas JG. 1997. Differential expression of connexins during neocortical development and neuronal circuit formation. J. Neurosci. 17: 3096-111.

Nagy JI, Li X, Rempel J, Stelmack G, Patel D, Staines WA, Yasumura T, Rash JE. 2001. Connexin26 in adult rodent central nervous system: demonstration at astrocytic gap junctions and colocalization with connexin30 and connexin43. J Comp Neurol. 441: 302-23.

Nelson R, Famiglietti EV Jr, Kolb H. 1978. Intracellular staining reveals different levels of stratification for on- and off-center ganglion cells in cat retina. J Neurophysiol. 41: 472-83.

Neuhauss SC, Biehlmaier O, Seeliger MW, Das T, Kohler K, Harris WA, Baier H. 1999. Genetic disorders of vision revealed by a behavioral screen of 400 essential loci in zebrafish. J Neurosci. 19: 8603-15.

Nicholson SM, Gomes D, de Nechaud B, Bruzzone R. 2001. Altered gene expression in Schwann cells of connexin32 knockout animals. J Neurosci Res. 66: 23-36.

O'Brien J, Al-Ubaidi MR, Ripps H. 1996. Connexin35: A Gap junctional protein expressed preferentially in the skate retina. Mol. Biol. Cell. 7: 233-43.

O'Brien J, Bruzzone R, White TW, Al-Ubaidi MR, Ripps H. 1998. Cloning and expression of two related connexins from the perch retina define a distinct subgroup of the connexin family. J. Neurosci. 18: 7625-37.

Oguro K, Jover T, Tanaka H, Lin Y, Kojima T, Oguro N, Grooms SY, Bennett MV, Zukin RS. 2001. Global ischemia-induced increases in the gap junctional proteins connexin 32 (Cx32) and Cx36 in hippocampus and enhanced vulnerability of Cx32 knock-out mice. J Neurosci. 21: 7534-42.

Orsino A, Taylor CV, Lye SJ. 1996. Connexin-26 and connexin-43 are differentially expressed and regulated in the rat myometrium throughout late pregnancy and with the onset of labor. Endocrinology. 137: 1545-53.

Ou CW, Orsina A, Lye SJ. 1997. Expression of connexin-43 and connexin-26 in the rat myometrium during pregnancy and labor is differentially regulated by mechanical and hormonal signals. Endocrinology. 138: 5398-407.

Page RDM. 1996. TREEVIEW: An application to display phylogenetic trees on personal computers. Comput. Appl. Biosci. 12: 357-8.

Parenti R, Campisi A, Vanella A, Cicirata F. 2002. Immunocytochemical and RT-PCR analysis of connexin36 in cultures of mammalian glial cells. Arch Ital Biol. 140: 101-8.

Parenti R, Gulisano M, Zappala A, Circirata F. 2000. Expression of connexin36 mRNA in adult rodent brain. Neuroreport. 11(7): 1497-1502.

Priest CA, Thompson AJ, Keller A. 2001. Gap junction proteins in inhibitory neurons of the adult barrel neocortex. Somatosens Mot Res. 18: 245-52.

Prime G, Horn G, Sutor B. 2000. Time-related changes in connexin mRNA abundance in the rat neocortex during postnatal development. Brain Res Dev Brain Res. 119: 111-25.

Rash JE, Staines WA, Yasumura T, Patel D, Furman CS, Stelmack GL, Nagy JI. 2000. Immunogold evidence that neuronal gap junctions in adult rat brain and spinal cord contain connexin-36 but not connexin-32 or connexin-43. Proc Natl Acad Sci U S A. 97: 7573-8.

Rash JE, Yasumura T, Davidson KG, Furman CS, Dudek FE, Nagy JI. 2001a. Identification of cells expressing Cx43, Cx30, Cx26, Cx32 and Cx36 in gap junctions of rat brain and spinal cord. Cell Adhes Commun. 8: 315-20.

Rash JE, Yasumura T, Dudek FE, Nagy JI. 2001b. Cell-specific expression of connexins and evidence of restricted gap junctional coupling between glial cells and between neurons. J Neurosci. 21: 1983-2000.

Reaume AG, De Sousa PA, Kulkarni S, Langille BL, Zhu D, Davies TC, Juneja SC, Kidder GM, Rossant J. 1995. Cardiac malformation in neonatal mice lacking connexin43. Science. 267: 1831-4.

Reuss B, Hellmann P, Traub O, Butterweck A, Winterhager E. 1997. Expression of connexin31 and connexin43 genes in early rat embryos. Dev Genet. 21: 82-90.

Risek B, Klier FG, Phillips A, Hahn DW, Gilula NB. 1995. Gap junction regulation in the uterus and ovaries of immature rats by estrogen and progesterone. J Cell Sci. 108: 1017-32.

Roerig B, Feller MB. 2000. Neurotransmitters and gap junctions in developing neural circuits. Brain Res Brain Res Rev. 32: 86-114.

Roscoe WA, Barr KJ, Maawi AA, Pomerantz DK, Kidder GM. 2001. Failure of spermatogenesis in mice lacking connexin43. Biol Reprod. 65: 829-38.

Rozental R, Giaume C, Spray DC. 2000a. Gap junctions in the nervous system. Brain Res Brain Res Rev. 32: 11-5.

Rozental R, Srinivas M, Gokhan S, Urban M, Dermietzel R, Kessler JA, Spray DC, Mehler MF. 2000b. Temporal expression of neuronal connexins during hippocampal ontogeny. Brain Res Brain Res Rev. 32: 57-71.

Saez JC, Berthoud VM, Kadle R, Traub O, Nicholson BJ, Bennett MV, Dermietzel R. 1991. Pinealocytes in rats: connexin identification and increase in coupling caused by norepinephrine. Brain Res. 568: 265-75.

Sambrook J, Fritsch EF, Maniatis, T. 1989. Molecular Cloning: a laboratory manual. 2nd ed. New York. Cold Spring Harbor Laboratory Press.

Scherer SS, Bone LJ, Deschenes SM, Abel A, Balice-Gordon RJ, Fischbeck, KH. 1999. The role of the gap junction protein connexin32 in the pathogenesis of X-linked Charcot-Marie-Tooth disease. Novartis Found Symp. 219: 175-87

Serre-Beinier V, Le Gurun S, Belluardo N, Trovato-Salinaro A, Charollais A, Haefliger JA, Condorelli DF, Meda P. 2000. Cx36 preferentially connects beta-cells within pancreatic islets. Diabetes. 49: 727-34.

Söhl G, Degen J, Teubner B, Willecke K. 1998. The murine gap junction gene connexin36 is highly expressed in mouse retina and regulated during brain development. FEBS Letters 428: 27-31.

Söhl G, Güldenagel M, Traub O, Willecke K. 2000. Connexin expression in the retina. Brain Res Brain Res Rev. 32: 138-45.

Solomon IC, Halat TJ, El-Maghrabi MR, O'Neal MH 3rd. 2001. Localization of connexin26 and connexin32 in putative CO(2)-chemosensitive brainstem regions in rat. Respir Physiol. 129: 101-21.

Spray DC, Dermietzel R. 1995. X-linked dominant Charcot-Marie-Tooth disease and other potential gap-junction diseases of the nervous system. Trends Neurosci. 18: 256-62.

Spray DC, Harris AL, Bennett MV. 1981. Equilibrium properties of a voltage-dependent junctional conductance. J Gen Physiol. 77: 77-93.

Srinivas M, Rozental R, Kojima T, Dermietzel R, Mehler M, Condorelli DF, Kessler JA, Spray DC. 1999. Functional properties of channels formed by the neuronal gap junction protein connexin36. J. Neurosci. 19: 9848-55.

Teubner B., Degen J, Söhl G, Güldenagel M, Bukauskas F, Trexler EB, Verselis VK, De Zeeuw CI, Lee CG, Kozak CA, Petrasch-Parwez E, Dermietzel R, Willecke K. 2000. Functional expression of the murine connexin 36 gene coding for a neuron-specific gap junctional protein. J Membr Biol. 176: 249-62.

Teubner B, Odermatt B, Güldenagel M, Sohl G, Degen J, Bukauskas F, Kronengold J, Verselis VK, Jung YT, Kozak CA, Schilling K, Willecke K. 2001. Functional expression of the new gap junction gene connexin47 transcribed in mouse brain and spinal cord neurons. J Neurosci. 21: 1117-26.

Thompson JD, Gibson TJ, Plewniak F, Jeanmougin F, Higgins DG. 1997. The Clustal X windows interface: flexible strategies for multiple sequence alignment aided by quality analysis tools. Nucleic Acids Res. 25: 4876-82.

Turner DL, Weintraub H. 1994. Expression of achaete-scute homolog 3 in Xenopus embryos converts ectodermal cells to a neural fate. Genes Dev. 8: 1434-47.

Unger VM, Kumar NM, Gilula NB, Yeager M. 1997. Projection structure of a gap junction membrane channel at 7 A resolution. Nat Struct Biol. 4: 39-43.

Unger VM, Kumar NM, Gilula NB, Yeager M. 1999. Electron cryo-crystallography of a recombinant cardiac gap junction channel. Novartis Found Symp. 219: 22-30.

Vaney DI. 1999. Neuronal coupling in the central nervous system: lessons from the retina, in: Gap junction-mediated intercellular signaling in health and disease. Novartis Found Symp. 219: 113-33.

Vaney DI, Nelson JC, Pow DV. 1998. Neurotransmitter coupling through gap junctions in the retina. J. Neurosci. 18: 10594-602.

Vaney DI, Weiler R. 2000. Gap junctions in the eye: evidence for heteromeric, heterotypic and mixed-homotypic interactions. Brain Res Brain Res Rev. 32: 115-20.

Weiler R, Pottek M, He S, Vaney DI. 2000. Modulation of coupling between retinal horizontal cells by retinoic acid and endogenous dopamine. Brain Res Brain Res Rev. 32: 121-9.

Westerfield M. 1995. The Zebrafish Book: A guide for the laboratory use of zebrafish. *Brachydanio rerio*. Eugene, OR. University of Oregon Press.

White TW. 2000. Functional analysis of human Cx26 mutations associated with deafness. Brain Res Brain Res Rev. 32: 181-3.

White TW. 2002. Unique and redundant connexin contributions to lens development. Science. 295: 319-20.

White TW, Bruzzone R, Wolfram S, Paul DL, Goodenough DA. 1994. Selective interactions among the multiple connexin proteins expressed in the vertebrate lens: the second extracellular domain is a determinant of compatibility between connexins. J Cell Biol. 125: 879-92.

White TW, Bruzzone R. 1996. Multiple connexin proteins in single intercellular channels: connexin compatibility and functional consequences. J. Bioenerg. Biomembr. 28: 339-73.

White TW, Bruzzone R, Paul DL. 1995. The connexin family of intercellular channel forming proteins. Kidney Int. 48: 1148-57.

White TW, Deans MR, O'Brien J, Al-Ubaidi MR, Goodenough DA, Ripps H, Bruzzone R. 1999. Functional characteristics of skate connexin35, a member of the gamma subfamily of connexins expressed in the vertebrate retina. Eur J Neurosci. 11: 1883-90.

White TW, Paul .L. 1999. Genetic diseases and gene knockouts reveal diverse connexin functions. Annu. Rev. Physiol. 61: 283-310.

Wulliman MF, Rupp B, Reichert H. 1996. Neuroanatomy of the Zebrafish Brain: a topological atlas. Basel, Switzerland. Birkhäuser Verlag.

Yamasaki H, Krutovskikh V, Mesnil M, Tanaka T, Zaidan-Dagli ML, Omori Y. 1999. Role of connexin (gap junction) genes in cell growth control and carcinogenesis. C R Acad Sci III. 322: 151-9.

Yamanaka I, Kuraoka A, Inai T, Iishibashi T, Shibata Y. 2001. Differential expression of major gap junction proteins, connexins 26 and 32, in rat mammary glands during pregnancy and lactation. Histochem Cell Biol. 115: 277-84.

Yeager M, Gilula NB. 1992. Membrane topology and quaternary structure of cardiac gap junction ion channels. J Mol Biol. 223: 929-48

Yuste R, Nelson DA, Rubin WW, Katz LC. 1995. Neuronal domains in developing neocortex: Mechanisms of coactivation. Neuron. 14: 7-17.

Yuste R, Peinado A, Katz LC. 1992. Neuronal domains in developing neocortex. Science. 257: 665-9.

Zhou XW, Pfahnl A, Werner R, Hudder A, Llanes A, Leubke A. Dahl G. 1997. Identification of a pore lining segment in gap junction hemichannels. Biophys J. 72: 1946-53.

Zhang C, Finger TE, Restrepo D. 2000. Mature olfactory receptor neurons express connexin 43. J Comp Neurol. 426: 1-12.

Zhang JT, Nicholson BJ. 1994. The topological structure of connexin 26 and its distribution compared to connexin 32 in hepatic gap junctions. J Membr Biol. 139: 15-29.

Zhang ZQ, Zhang W, Wang NQ, Bani-Yaghoub M, Lin ZX, Naus CC. 1998. Suppression of tumorigenicity of human lung carcinoma cells after transfection with connexin43. Carcinogenesis. 19: 1889-94.

Zoidl G, Meier C, Petrasch-Parwez E, Zoidl C, Habbes HW, Kremer M, Srinivas M, Spray DC, Dermietzel R. 2002. Evidence for a role of the N-terminal domain in subcellular localization of the neuronal connexin36 (Cx36). J Neurosci Res. 69: 448-65.